Íris Cláudia Felisberto Guerreiro
Licenciada em Biologia

Exploring new therapeutic targets and novel therapies for resistant colorectal cancer subtypes

Dissertação para obtenção do Grau de Mestre em
Genética Molecular e Biomedicina

Orientador: Dra. Maria Cristina Mantas Albuquerque Valeroso, Investigadora, Unidade de Investigação em Patobiologia Molecular (UIPM), Instituto Português de Oncologia de Lisboa Francisco Gentil, EPE (IPOLFG)

Júri:

Presidente: Doutora Paula Maria Theriaga Mendes Bernardes Gonçalves, Professora Associada da Faculdade de Ciências e Tecnologia da Universidade Nova de Lisboa;

Arguente: Doutora Maria Cristina Mantas Albuquerque Valeroso, Investigadora do Instituto Português de Oncologia de Lisboa Francisco Gentil;

Vogal: Doutora Maria Luísa Santos de Sousa Cyrne, Professora Auxiliar com Agregação da Faculdade de Ciências da Universidade de Lisboa.

FACULDADE DE CIÊNCIAS E TECNOLOGIA
UNIVERSIDADE NOVA DE LISBOA

Julho 2019

Aos meus pais

AGRADECIMENTOS

Gostaria, em primeiro lugar, de manifestar o meu agradecimento a todos aqueles que de forma direta ou indireta contribuíram para a concretização deste trabalho e me apoiaram ao longo desta jornada.

Começo por agradecer à Dra. Cristina Albuquerque, pela oportunidade que me concedeu de desenvolver este projeto sob sua orientação, por todo o apoio, aconselhamento e transmissão de valiosos conhecimentos nas mais diversas áreas. Um muito obrigado por toda a disponibilidade e compreensão que demonstrou para comigo ao longo deste tempo, o seu apoio foi sem dúvida essencial para o meu crescimento como profissional e pessoal.

À Mestre Inês Francisco e Doutoranda Patrícia Silva, agradeço toda a ajuda prestada na revisão desta dissertação, todo o conhecimento transmitido e apoio na realização do trabalho prático e esclarecimento de dúvidas.

Ao Dr. Bruno Filipe, estou grata por toda a ajuda prestada em laboratório, por toda a disponibilidade no esclarecimento de dúvidas e pela constante simpatia e boa disposição.

Á Mestre Lucília Pereira, um obrigado pela sua indispensável ajuda ao longo deste projeto, pelos conhecimentos valiosos que me transmitiu, por me ter dado sempre força para avançar e pelo contributo e ajuda na revisão desta dissertação.

À Doutora Branca Cavaco, Coordenadora da Unidade de Investigação em Patobiologia Molecular, do Instituto Português de Oncologia, Lisboa, Francisco Gentil, E.P.E, por me ter concedido a oportunidade de integrar este projeto.

A todos os restantes membros da Unidade de Investigação em Patobiologia Molecular, por toda a simpatia, em especial à Dra. Sofia Fragoso, Dra. Patrícia Machado e Dra. Sidónia Santos, por toda a simpatia, energia positiva e boa disposição no laboratório.

Às minhas colegas Mariana Santos e Patrícia Valentim, que me acompanharam ao longo de todo o percurso e o tornaram, sem dúvida, mais fácil com a sua amizade, boa disposição e companheirismo.

À Mestre Marlene Duarte, pelo incansável apoio, amizade e ajuda que me prestou durante todo o tempo como colega de laboratório. À Mestre Teresa Duarte e Mestre Ana Magalhães, por toda a amizade, entreajuda e ainda, por todos os momentos de boa disposição.

Ao Yuval, pelo incansável apoio que me deu em todos os momentos, fossem eles melhores ou piores, por toda a paciência para ouvir os meus desabafos, enfim, por tantas e tantas coisas que não haveria espaço para as enumerar. O meu profundo obrigada por estares sempre presente.

Às minhas amigas Ana Sofia Morais e Vanessa Ribeiro, muito obrigada pela vossa amizade incondicional e por todo o apoio ao longo deste percurso. À minha querida Tina, um obrigado especial por ser a pessoa maravilhosa que é e por ser uma grande fonte de inspiração e energia positiva.

Por fim, a toda a minha família. Em especial a vocês, mãe pai e mano por todo o vosso apoio e amor incondicionais, por me apoiarem e incentivarem sempre e por todos os valores que me transmitiram ao longo da vida, que me permitiram chegar onde cheguei e, acima de tudo, ser quem sou. Um obrigada muito especial à minha mãe, pelo enorme exemplo de força, coragem e determinação que representa para mim e por ser a prova viva que estejamos quão em baixo estivermos, teremos sempre força suficiente para nos levantar. Muito obrigada.

RESUMO

O cancro do cólon e recto (CCR) representa a quarta principal causa de morte por cancro a nível mundial. O tratamento com CRC é determinado de acordo com o estadio da doença. O 5-fluoruracil (5-FU), a oxaliplatina e o irinotecano são os principais compostos utilizados no tratamento do CCR em diferentes estratégias terapêuticas. No entanto, em formas mais agressivas de CRCs, as células desenvolvem frequentemente, mecanismos de resistência que levam à ineficácia dessas terapias. Assim, é de grande importância a melhor compreensão dos mecanismos moleculares subjacentes ao CRC, a fim de encontrar novos alvos terapêuticos e novas estratégias terapêuticas para o tratamento de CRC avançado e resistente.

A desregulação das vias de sinalização Wnt β-catenina e Sonic hedgehog/Gli (Shh / Gli), entre muitas outras, têm sido implicadas na carcinogénese e metastização do CCR. A activação excessiva da sinalização Wnt/β-catenina estimula o desenvolvimento da CRC através da activação de alvos relacionados com o cancro, a jusante. O gene *TCF7L2*, que codifica o principal ativador da transcrição desta via, origina diferentes isoformas de *TCF7L2* que foram implicadas no CRC. Além disso, a regulação defeituosa da via Shh/Gli tem sido destacada pelo seu papel significativo na progressão do CCR, afetando a regulação de uma diversidade de processos celulares envolvidos na carcinogénese do CCR. Durante a metastização, as células desenvolvem características mesenquimais, através do processo de transição epitélio-mesenquimal (EMT). Além disso, existe uma ligação estabelecida entre as células estaminais de cancro (CSCs) e as metástases.

Portanto, o objetivo deste projeto foi explorar novos alvos terapêuticos e novas terapias para os subtipos de CCR resistente.

Ao estudar a expressão do gene TCF7L2 em uma coorte de 38 pacientes com CCR e linhas celulares representativas de CCR, identificamos expressão diferencial de isoformas específicas de *TCF7L2*, variando na inclusão de exões entre os exões 1-5 e exões 11-17, que parecem diferir entre as amostras de doentes com CCR e entre tecido normal e tumoral. Portanto, isso abre a porta para uma investigação mais aprofundada sobre a expressão diferencial das isoformas do *TCF7L2* e sua relação com a tumorigénese do CCR e, eventualmente, com o risco de CCR.

Numa segunda fase do projeto, analisámos um painel de 10 compostos diferentes (drogas citostáticas usadas no tratamento convencional de CCR, moduladores epigenéticos, terapias direcionadas de vias de sinalização específicas e nutracêuticos) e as combinações mais promissoras entre eles, em termos de efeitos anti-proliferativo e anti-migratório, em duas linhas celulares de CCR representativas de tumores mucinosos resistentes à terapia (HT-29 e LS174T). As combinações mais promissoras foram avaliadas quanto ao seu efeito na expressão de marcadores genéticos envolvidos no ciclo celular, na estaminalidade do CRC, na transição epitelial-mesenquimal e nas vias de sinalização Wnt/β-catenina e Shh/Gli. Com esse trabalho, identificamos combinações de terapia promissoras para o tratamento de subtipos de CCR resistentes e exploramos o potencial de novos compostos como complemento da terapia convencional no tratamento de formas agressivas de CCR.

Termos-chave: cancro colorectal, metástases, *TCF7L2*, moduladores das vias de sinalização, nutracêuticos

ABSTRACT

Colorectal cancer (CRC) represents the fourth leading cause of death by cancer in the world. CRC treatment is determined according to disease stage. 5-fluoruracil (5-FU), oxaliplatin and Irinotecan are the main chemotherapeutic compounds used in CRC treatment in different therapeutic strategies. However, in most aggressive CRCs, cells often develop resistance mechanisms leading to ineffectiveness of these therapies. Thus, it is of great importance the better understanding of molecular mechanisms underlying CRC in order to find new therapeutic targets and novel therapeutic strategies for treating advanced and resistant CRC.

Deregulation of Wnt/β-catenin and Sonic hedgehog/Gli (Shh/Gli) signaling pathways, among many others, has been implicated in CRC carcinogenesis and metastasis. Excessive activation of Wnt/β-catenin signaling stimulates CRC development through activation of downstream cancer-related targets. *TCF7L2* gene, encoding the main transcriptional activator of this pathway, originates different *TCF7L2* isoforms that have been implicated in CRC. Moreover, defective regulation of Shh/Gli pathway have been denoted for its significant role in CRC progression, affecting the regulation of a diversity of cell processes involved in CRC carcinogenesis. During metastasis, cells develop mesenchymal characteristics, through the epithelial-to-mesenchymal transition (EMT) process. Furthermore, there is an established link between cancer stem cells (CSCs) and metastasis.

Therefore, the aim of this project was to explore new therapeutic targets and novel therapies for resistant colorectal cancer subtypes.

By studying *TCF7L2* gene expression in a cohort of 38 CRC patients and CRC representative cell lines, we identified differential expression of specific *TCF7L2* isoforms, varying in exon inclusion within exons 1-5 and exons 11-17, that appear to differ among CRC patients' samples and between normal and tumor tissues. Therefore, this opens the door for further investigation on differential expression of *TCF7L2* isoforms and its relation to CRC tumorigenesis and eventually to CRC risk.

In a second phase of the project we tested a panel of 10 different compounds (cytostatic drugs used in conventional CRC treatment, epigenetic modulators, targeted therapies of specific signaling pathways and nutraceuticals) and the most promising combinations between them, for anti-proliferative and anti-migratory activities, in two CRC cell lines representative of mucinous tumors resistant to therapy (HT-29 and LS174T). The most promising combinations were evaluated for their effect in the expression of gene markers involved in cell-cycle, CRC stemness, epithelial-mesenchymal transition and Wnt/β-catenin and Sonic hedgehog/Gli (Shh/Gli) signaling pathways. With this work we were able to identify promising therapy combinations for the treatment of resistant CRC subtypes and explore the potential of new compounds as complement for conventional therapy in treatment of aggressive forms of CRC.

Key-words: colorectal cancer, metastasis, *TCF7L2*, signaling pathway modulators, nutraceuticals

TABLE OF CONTENTS

FIGURE INDEX

TABLE INDEX

ACRONYMS

2D – Two-dimensional
3D – Tri-dimensional
5-FU – 5-Fluorouracil
ABCB1 – ATP binding cassette subfamily B member 1
AC – Amsterdam criteria
AFAP – Attenuated familial adenomatous polyposis
APC - Adenomatous polyposis coli
BC – Bethesda criteria
BMI – Body mass index
BMPR1A – Bone morphogenetic protein receptor type 1A
CBD-BD – β-catenin binding domain-binding protein
CCNA2 – CyclinA2
CDH1 – E-cadherin
CDKN1A – Cyclin-dependent kinase inhibitor 1 or CDK-interacting protein 1
cDNA – Complementary DNA
CIMP - CpG island methylator phenotype
CIN - Chromosomal instability
CMS – Consensus molecular subtypes
CRC – Colorectal cancer
CSCs – Cancer stem cells
CtBP – Carboxyl-terminal binding protein
CTNNB1 – catenin beta 1
ddNTP – Dideoxynucleoside triphosphate
DMSO – Dimethyl Sulfoxide
dNTP – Deoxynucleotide triphosphate
EC – Endometrial cancer
EDTA – Ethylenediamine tetraacetic acid
EMT – Epithelial-mesenchymal transition
EPCAM – Epithelial cell adhesion molecule
FAP – Familial adenomatous polyposis
FCCTX – Familial colorectal cancer type X
FJP – Familial juvenile polyposis
GAPDH – Glyceraldehyde-3-phosphate dehydrogenase
GI – Gastro-intestinal
GLI1 – GLI family zinc finger 1
HDAC – Histone deacetylases
HH – Hedgehog
HIP – Hedgehog interacting protein
HMG – High motility group
HNPCC - Hereditary nonpolyposis colorectal cancer
IBD - Inflammatory bowel disease
IHC – Immunohistochemistry
ISCs – Intestinal stem cells
JPS – Juvenile polyposis syndrome
KRAS – Kirsten Ras
LGR5 – Leucine-rich repeat-containing G-protein coupled receptor 5
LOH - Loss of heterozygosity
LS – Lynch syndrome
MAP – *MUTYH*-associated polyposis
MAPK – Mitogen-activated protein kinase
MLH – MutL Homolog
MMP – Matrix metalloproteinase
MMP7 – Matrix metallopeptidase 7
MMR – Mismatch repair
MSH – *MutS Homolog*
MSI – Microsatellite Instability
MSS – Microsatellite stable
mTOR – Mechanistic target of rapamycin
MUTYH – mutY DNA glycosylase
NES – Nuclear export sequences
NGS – Next generation sequencing
NLS – Nuclear signaling domain
PCR – Polymerase chain reaction
PDX – Patient-derived xenographts
PJS – Peutz-Jeghers syndrome
PMS – PMS1 Homolog

PROM1 – Prominin 1

PTCH1 – Patched 1

qPCR – Quantitative PCR

RT – Reverse transcription

SFN – Sulforaphane

Shh – Sonic Hedgehog

Smo – Smoothened

SNAI1 – Snail family transcriptional repressor 1

SP – Serrated polyposis

TCF – T-cell factor

TCF7L2 – Transcription factor 7 like 2

TEM – Transição epitelial-mesenquimal

TGFB1 – Transforming growth factor beta 1

TM – Melting temperature

TP53 – Tumor protein p53

TS – Thymidylate synthase

v/v – volume/volume

VAX2 – Ventral anterior homeobox 2

VIM – Vimentin

w/v – weight/volume

Wt – Wild type

ZEB1 – Zinc finger E-box binding homeobox 1

1. INTRODUCTION

1.1 Colorectal cancer

Globally, colorectal cancer (CRC) represents the third most commonly diagnosed cancer in men (10.0% of the total cancer cases), second in women (9.2% of the total cancer cases) and the fourth leading cause of death by cancer in the world. According to GLOBOCAN, about 1.4 million new cases and near 700.000 deaths occurred in 2012, accounting for higher incidence (about 55% of the cases) in more developed regions and higher mortality (52% of total deaths) in less developed countries, reflecting the poor survival in these regions (Ferlay *et al.*, 2015).

This malignancy occurs in response to several associated non-modifiable risk factors such as the individual age, inflammatory bowel disease (IBD) and hereditary factors, and a series of environmental and lifestyle associated factors, including body mass index (BMI), drinking alcohol, smoking cigarettes and red meat consumption (Haggar *et al.*, 2009; Johnson *et al.*, 2013). The lifetime risk of CRC in an individual above the age of 50 with no personal or family history of CRC has a chance of 5%–6% of developing this medical condition. However, the involvement of first and/or second-degree relatives with CRC increases this risk up to 20%, reaching 80%-100% in hereditary CRC syndromes, namely in hereditary nonpolyposis colorectal cancer (HNPCC) and familial adenomatous polyposis (FAP), respectively (Rustgi, 2007).

Traditionally, CRCs are classified into sporadic and familial or hereditary. The first resulting of successive spontaneous somatic mutations and representing near 70% of all CRC cases, while the latter, standing for the remaining 30% of the cases, results from inherited germline mutations. However, only nearly 5% of the hereditary cases can be included into any of the currently recognized syndromes, whereas the other 25% of the patients do not present a Mendelian inheritance but simply a familial predisposition to develop cancer and therefore are not included in any of the familiar syndromes (Zambirinis *et al.*, 2009; Jasperson *et al.*, 2010; Yamagishi *et al.*, 2016).

1.2 Genomic instability and colorectal carcinogenesis

CRC is a very heterogeneous disease both from molecular carcinogenesis and morphological perspectives. Three genomic instability pathways have been described as associated to the early steps of malignant transformation from adenoma into carcinoma process in colorectal carcinogenesis: the chromosomal instability pathway (CIN), microsatellite instability pathway (MSI) and the CpG island methylator phenotype pathway (CIMP) (Bae *et al.*, 2016; Linnekamp *et al.*, 2018).

1.2.1 Chromosomal instability pathway

CIN is the most common pathway among CRCs, implicated in about 85% of sporadic CRCs (Conteduca *et al.*, 2013). This pathway is characterized by an imbalance in the number (aneuploidy) and structure of chromosomes, associated genetic mutations of proto-oncogenes and tumor suppressor

genes and a high frequency of loss of heterozygosity (LOH) (Pino and Chung, 2010; Pancione *et al.*, 2012).

The steps involved in this process follow the traditional adenoma-carcinoma sequence, first described in 1990 as a multistep model for tumorigenesis, by Fearon and Vogelstein (Fearon and Vogelstein, 1990). The authors described this model as an accumulation of genetic and epigenetic alterations which are directly responsible for specific events contributing to the initiation step, characterized by the transition of healthy colon epithelium to an adenoma and/or determining the progression step, culminating in carcinoma (Figure 1.1) (Fearon and Vogelstein, 1990; Colussi *et al.*, 2013).

According to this linear model, the tumorigenesis starts with the adenoma development from the healthy colon epithelium by the inactivation of a tumor suppressor gene located on the long arm of human chromosome 5 (5q), involved in the APC/β-catenin/TCF signaling pathway: the adenomatous polyposis coli (APC), either by LOH or mutation. APC protein inactivation results in the non-effective phosphorylation of β-catenin therefore leading to its accumulation in the cytoplasm and posterior translocation to the nucleus, causing an excessive induction of TCF targets, implicated in cell proliferation, differentiation, migration and adhesion (Colussi *et al.*, 2013). Following adenoma formation, mutations in *KRAS* gene, a proto-oncogene located on the short arm of human chromosome 12 (12p), causing its constitutive activation, provides cell the capacity of avoiding apoptosis and LOH in *SMAD4* gene, in the long arm of human chromosome 18 (18q) lead to differentiation of adenoma and consequently to the progression step. The crucial event mediating the adenoma-carcinoma transition in CRC is the deregulation of proliferative activity by loss of cell cycle and apoptosis control capacity, result of the biallelic inactivation or LOH of *TP53* gene, located in the long arm of human chromosome 17 (17q) (Pancione *et al.*, 2012; Colussi *et al.*, 2013).

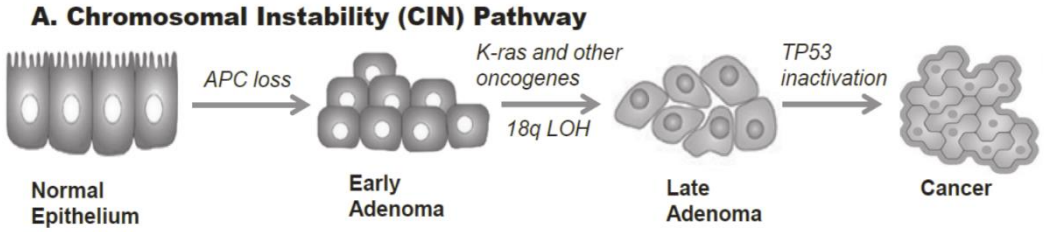

Figure 1.1 – Chromosomal instability pathway – main molecular events (Adapted from: Mundade, R. et al., 2014).

1.2.2 Microsatellite instability pathway

The MSI pathway (Figure 1.2) represents about 15% of CRC sporadic cases and more than 95% of Lynch syndrome. Tumor initiation following this pathway is mainly related to the impairment of the DNA mismatch repair (MMR), caused by mutation on any of several genes participating in this system (Cunningham *et al.*, 1998; Armaghany *et al.*, 2012). Later CRC progression following the MSI pathway

is associated with loss of function of several genes encoding regulators of cell proliferation (such as *TGFβR2)* and the cell cycle/apoptosis (such as *BAX*) (Mundade *et al.*, 2014).

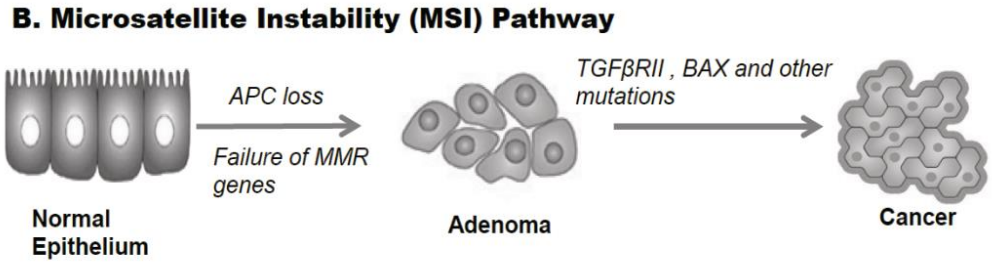

Figure 1.2 – Microsatellite instability pathway – main molecular events (Adapted from: Mundade *et al.*, 2014).

The MMR system (Figure 1.3) is crucial in the repair of DNA sequence mismatches during DNA replication, in which four main proteins (MLH1, MSH2, MSH6 and PMS2) interact together to detect and cut mismatches, allowing DNA polymerase and DNA ligase to correctly resynthesize and bind the DNA strand (Vilar and Gruber, 2010; Gelsomino *et al.*, 2016). Inactivation of the MMR proteins occur either through aberrant CpG islands methylation of the promoter of *MLH1* gene, which explains most of the sporadic cases, or via mutations in a member of the MMR family, generally associated to Lynch syndrome cases (Armaghany *et al.*, 2012; Mundade *et al.*, 2014).

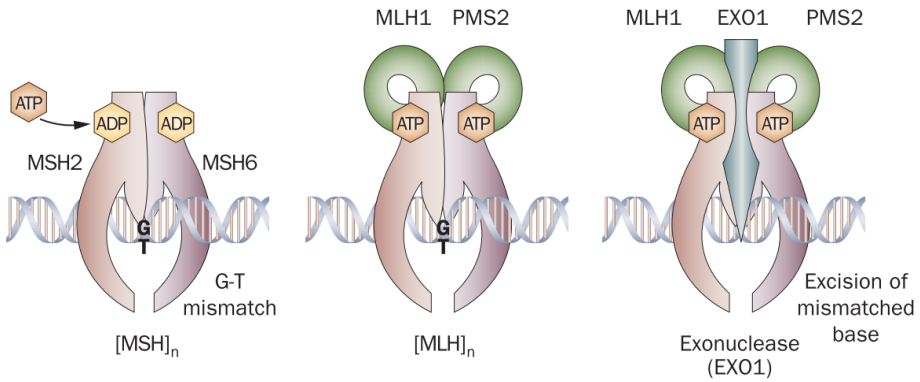

Figure 1.3 – Model of mismatch repair proteins mechanism. After mismatch detection, MSH2 associates with either MSH6 or MSH3, and MLH1 couples with PMS2, PMS1 or MLH3, forming the MSH and a MLH complexes that allow the recognition and further excision of the mismatch by exonuclease1 (EXO1) (Adapted from: Vilar and Gruber, 2010).

A defective MMR system leads to the presence of either longer or shorter microsatellites throughout the genome, making MSI a good somatic marker for the loss of DNA MMR activity. Regarding this, MSI can be defined as high (MSI-H) upon the presence of instability in >30% of the microsatellite markers analysed, low (MSI-L) if instability is present in 10%-29% of microsatellite markers, and microsatellite stable (MSS) when none of the analysed markers are unstable (Armaghany *et al.*, 2012).

Microsatellites are short DNA repeats of 1–6 bases, abundant throughout the genome, located in coding and non-coding regions. These repeats are polymorphic among individuals but unique and

uniform in length in every tissue of each particular individual. Due to the repeated structure, microsatellites are very susceptible to replication errors that are generally repaired by the MMR system. The disruption of MMR system by loss of function of any of the intervenient proteins leads to error accumulation in microsatellites, resulting in genetic instability, which may acquire oncogenic potential if occurring in coding regions for genes involved in essential cell functions and pathways (Boland and Goel, 2010; Gelsomino *et al.*, 2016).

1.2.3 CpG islands methylator phenotype pathway

The CIMP pathway, also known as serrated pathway due to the morphological serrated appearance of the precursor lesions, is represented in 20%-30% of CRCs. This pathway is mainly characterized by the atypical hypermethylation of CpG dinucleotide sequences in the promoter regions, leading to the inactivation of several genes involved in cell cycle regulation, apoptosis, angiogenesis, DNA repair, invasion and adhesion (Figure 1.4). Based on the methylation status of a systematic screen of CpG sites, representing CIMP-defining loci, CIMP phenotype can be defined as high (CIMP-H) or low (CIMP-L) (Pancione *et al.*, 2012; Colussi *et al.*, 2013; Hagland *et al.*, 2013).

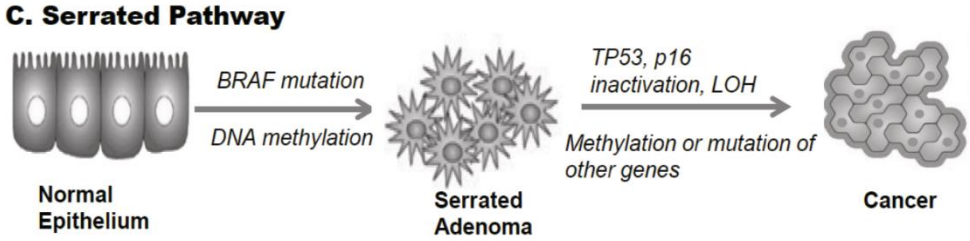

Figure 1.4 – CpG islands methylator phenotype pathway – main molecular events (Adapted from: Mundade *et al*., 2014).

CIMP-L CRCs have been associated with *KRAS* mutations and DNA hypermethylation of a reduced number of CIMP-defining loci and appears to be independent of MSI status (Hinoue *et al.*, 2012). On the other hand, CIMP-H CRCs are highlighted by two main features: the very high frequency epigenetic silencing, by promoter DNA hypermethylation of genes that are involved in cell differentiation, DNA repair, and cell-cycle control, including the tumor suppressor gene *p16* and the MMR gene *MLH1* and presence of *BRAF* (p.V600E) mutation (Al-Sohaily *et al.*, 2012; Hinoue *et al.*, 2012; Mundade *et al.*, 2014). BRAF is a serine/threonine-specific protein kinase that plays a crucial role in regulating the MAPKs/ERKs (mitogen-activated protein kinases/extracellular signal-regulated kinases) signaling pathway, involved in cell division, differentiation, and secretion. The point mutation in *BRAF* (p.V600E) leads to its constitutive activation, increasing its negative feedback mechanism and consequently the enhancement of MAPK/ERK signaling. The overactivation of this cascade causes downstream effectors to induce uncontrolled cell proliferation, evasion of immune response, angiogenesis, tissue invasion, and metastasis, as well as resistance to apoptosis (Mundade *et al.*, 2014).

1.3 Hereditary colorectal syndromes

As mention before, about 20-30% of CRC cases have familial or hereditary origin. From these, about 5-10% are related to an established familial genetic syndrome. The hereditary CRCs are broadly divided into nonpolyposis and polyposis syndromes. Individuals with hereditary CRC syndromes are at risk for earlier development of cancer, increased risk of metachronous cancers, and extracolonic manifestations. As such, identification of these individuals is critical for prevention and early detection and treatment of associated malignancies to reduce associated morbidity and mortality (Jasperson *et al.*, 2010; Wells and Wise, 2017).

1.3.1 Polyposis associated CRC syndromes

1.3.1.1 Familial adenomatous and attenuated adenomatous polyposis

FAP represents approximately 0,5-1% of all CRC cases and is the most common gastrointestinal polyposis syndrome. It is characterized by the early onset of hundreds to thousands of adenomatous colonic polyps beginning in the second decade of life. This condition carries a 100% percent risk of CRC, is transmitted in an autosomal dominant fashion and exhibits 100% penetrance among affected individuals. However, enhanced awareness of the disease and more aggressive strategies for screening and surveillance have substantially decreased the incidence of CRC and associated mortality. Patients with FAP develop colon cancer at the medium age of 40 years, or 10 to 15 years after the initial development of polyposis. Attenuated FAP (AFAP) is a milder form that is characterized by fewer adenomas, a later age of adenoma development and cancer diagnosis (Half *et al.*, 2009; Jasperson *et al.*, 2010; Wells and Wise, 2017).

FAP and AFAP result from germline mutations in the *APC* gene and is associated to the CIN tumorigenesis pathway. Most FAP patients have a family history of colorectal polyps and cancer, however, 25-30% of them are "de novo", without clinical or genetic evidence of FAP in family members. The latter cases can be partially explained as being the result of germline mosaicism (Albuquerque *et al.*, 2002; Jasperson *et al.*, 2010).

1.3.1.2 *MUTYH*-associated polyposis

MUTYH-associated polyposis (MAP) was the first described autosomal recessive colon cancer syndrome, with an estimate account of 0,5-1% of all CRC cases. This condition is caused by bi-allelic mutation in the mutY Homolog (*MUTYH*) gene, encoding a DNA glycosylase involved in base excision repair, which deficiency results in genetic instability of the *APC* gene among others, including *KRAS* and *TP53*. MAP shares clinical features with FAP/AFAP such that 10-20% of patients with suspected FAP/AFAP without an identified *APC* mutation exhibit a mutation in *MUTYH*. However, a family history of polyposis is rarely evident because of its inheritance pattern (Gala and Chung, 2011; Wells and Wise, 2017).

1.3.1.3 Hamartomatous polyposis

Hamartomatous polyposis syndromes are characterized by an overgrowth of cells native to the area in which they normally occur and is implicated in less than 0.5% of all CRC cases. This syndrome includes three Peutz-Jeghers Syndrome (PJS), Juvenile Polyposis Syndrome (JPS) and Cowden syndrome, being the first two associated to an increased risk for CRC (Gala and Chung, 2011; Carballal *et al.*, 2014; Stoffel and Kastrinos, 2014).

Peutz-Jeghers Syndrome is an autosomal dominant disorder, characterized by moderate–large sized, but few intestinal hamartomatous polyps, muco-cutaneous pigmentation, and a high lifetime risk of gastrointestinal, pancreatic, and breast cancers. Germline mutations in the serine threonine kinase 11 (*STK-11*) tumor suppressor gene, involved in the mTOR pathway, are found in 50-70% of the patients with PJS. However, not all families with PJS are linked to this locus, suggesting that additional genes are involved in its pathogenesis (Carballal *et al.*, 2014; Stoffel and Kastrinos, 2014).

Familial Juvenile Polyposis (FJP) is also a rare autosomal dominant disorder in which 10 or more juvenile polyps are observed in the GI tract associated with certain congenital abnormalities, including cardiac valvular disease and/or atrial and ventricular septal defects, in some affected families. FJP is associated with increased risk of gastric, colorectal and pancreatic cancers. Approximately 50% of the individuals with a clinical diagnosis of JPS present mutations in SMAD family member 4 (*SMAD4*) and bone morphogenetic protein receptor type IA (*BMPR1a*) genes, encoding proteins involved in the transforming growth factor beta (TGFβ) signaling pathway (Al-Sohaily *et al.*, 2012; Carballal *et al.*, 2014).

Cowden syndrome has an autosomal dominant mode of transmission characterized by the presence of polyps of a diverse nature: juvenile, lipomas, lymphoid, ganglioneuromas, and inflammatory, throughout the GI tract. The vast majority of the patients diagnosed with this disorder present muco-cutaneous lesions, cranial abnormalities and the mucosa of the esophagus is characterized by its nodular appearance. This syndrome is caused by mutations the phosphatase and tensin homolog (*PTEN*) gene which confers increased risk for several types of extra-GI cancers, most commonly breast, thyroid, and endometrial. In addition, there are recent studies suggesting an increased risk for CRC (Al-Sohaily *et al.*, 2012; Carballal *et al.*, 2014).

1.3.1.4 Serrated polyposis

Serrated polyposis (SP) is characterized by the presence of multiple colorectal epithelial polyps with a serrated architecture, accompanied with an increased predisposition to CRC. Serrated polyps are represented by different subtypes of lesions (hyperplastic, sessile serrated polyps/adenomas and traditional serrated adenomas) with a common histological feature: the ‘saw-tooth’ appearance in the crypt epithelium. Despite no gene mutation has been linked to SP, reports of familial aggregation of SPs, multiplicity of lesions and increased risk of CRC among first-degree relatives of patients with SP suggests a possible hereditary cause. Moreover, since both autosomal and recessive patterns of inheritance have been described, genetic heterogeneity is likely among SPs. Regarding its origin, it has been proposed that this syndrome arises through the serrated pathway rather than through the classic adenoma-carcinoma sequence pathway. The serrated pathway is an epigenetically mediated

mechanism whereby hypermethylation of CpG islands occurs in the promoter region of tumor suppressor genes, resulting in the silencing of the tumor promoter region, ultimately leading to MSI. Tumors arising via this pathway are CIMP-high, a feature that can be found in 15% to 20% of sporadic colon carcinomas (Carballal *et al.*, 2014; Silva *et al.*, 2016; Wells and Wise, 2017).

1.3.2 Nonpolyposis associated CRC syndromes

Hereditary nonpolyposis CRC (HNPCC) is the most common hereditary CRC syndrome, accounting for at least 2% to 3%of all CRCs. These syndromes follow an autosomal-dominant inheritance pattern and is characterized by the significantly increased risks for colon cancer as well as for cancers of the endometrium, stomach, small intestine, hepatobiliary system, kidney, ureter and ovary (Lindor, 2009; Wells and Wise, 2017).

Establishing the Amsterdam criteria (AC) was an essential step to define HNPCC, allowing the uniform classification based on family history. These criteria were the first diagnostic guidelines to be developed, and the aim of these was to determine whether a family should be classified as having HNPCC. In 1991 the International Collaborative Group on hereditary nonpolyposis CRC had established the AC-I (table 1.1). However, these guidelines turn out to be too strict and could exclude small families or those presenting HNPCC-associated tumors, also quite common in HNPCC, leading to the establishment of the extended AC-II criteria in 1999 (table1.1) (Mothersill and Seymour, 2004; Llor *et al.*, 2005).

Table 1.1 – Amsterdam criteria I and II (Adapted from: Vasen *et al.* 1999).

Amsterdam criteria I (1991)	**There should be at least 3 relatives with CRC, plus all the following**:
	One affected patient should be a first-degree relative of the other 2;
	At least 2 successive generations should be affected;
	At least 1 CRC should be diagnosed before the age of 50 years;
	Familial adenomatous polyposis should be excluded.
Amsterdam Criteria II (1999)	**There should be at least 3 relatives with an HNPCC-associated cancer (CRC, cancer of the endometrium, small bowel, ureter, or renal pelvis), plus all the following:**
	One affected patient should be a first-degree relative of the other 2;
	At least 2 successive generations should be affected;
	Cancer in one or more affected relatives should be diagnosed before the age of 50 years;
	Familial adenomatous polyposis should be excluded in any cases of CRC.

Although the use of the AC achieves the original purpose, their limited sensitivity does not allow decisions about choosing which patients should undergo genetic analysis. The Bethesda criteria (BC) (Table 1.2) were therefore developed aiming to improve diagnosis criteria for CRC and aid in the decision whether individuals that do not fulfil the AC I/II should undergo genetic testing. The fulfilment of one of the BC implicates the study of the tumor by immunohistochemistry and/or MSI testing.

Immunohistochemistry (IHC), using antibodies to the MMR proteins MLH1, MSH2, MSH6, and PMS2, allows the evaluation for the loss of MMR protein expression. For MSI testing, the original microsatellite panel included two mononucleotide microsatellite markers, BAT25 (4q12) and BAT26 (2p21), and three dinucleotide microsatellite markers D2S123 (2p16), D5S346 (5q22-23) and D17S250 (17q12) (Mothersill and Seymour, 2004; Umar *et al.*, 2004).

Table 1.2 – Revised Bethesda criteria (Adapted from Umar *et al.* 2004).

	Tumors from individuals should be tested for MSI in the following situations:
Bethesda criteria	**1.** CRC diagnosed before the age of 50 years;
	2. Presence of synchronous or metachronous CRC or other HNPCC-associated tumors (colorectal, endometrium, stomach, ovary, pancreas, ureter, renal pelvis, biliary tract, brain, small bowel, sebaceous glands, and kerotoacanthomas), regardless of age.
	3. CRC with MSI-high pathologic-associated features (Crohn-like lymphocytic reaction, mucinous/signet cell differentiation, or medullary growth pattern) diagnosed before the age of 60 years.
	4. CRC diagnosed in one or more first-degree relatives with an HNPCC-related tumor, with one of the cancers being diagnosed before the age of 50 years.
	5. CRC diagnosed in two or more first- or second-degree relatives with HNPCC-related tumors, regardless of age.

The application of these criteria is decisive in the diagnosis of HNPCC (Figure 1.5), in which families fall into 2 categories: Lynch syndrome (LS), associated with hereditary defects in DNA MMR genes, and familial colorectal cancer type X (FCCTX), with no detectable mutation in DNA MMR genes (Umar *et al.*, 2004; Shiovitz *et al.*, 2014).

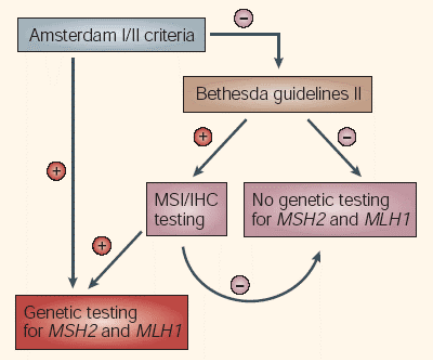

Figure 1.5 - Schematic representation of the use of Amsterdam and Bethesda criteria in the diagnosis of HNPCC (Adapted from: Umar *et al.*, 2004).

1.3.2.1 Lynch syndrome

Lynch syndrome (LS) represents the most common hereditary CRC syndrome, accounting for 1–3% of all CRC cases. LS is an autosomal dominant condition caused by a defect in one of the MMR genes. It is characterized by a predisposition to develop colorectal and endometrial cancer (EC), among other less frequent tumors at an early age (Carballal *et al.*, 2014).

LS arises from a germline mutation in the class of genes involved in DNA MMR, including MSH2, *MLH1*, *MSH6*, and *hPMS2*, already described in section 1.2.2. Mutations in *MSH2* and *hMLH1* account for the up to 90% of LS cases, while mutations in *MSH6* account for approximately 10% and mutations in *PMS2* are detected on rare occasions. Additionally, germline deletions in the *EPCAM* gene*, encoding* epithelial cell adhesion molecule (EpCAM), were found in a subset of families with LS. These LS families were subsequently found to have germline deletions in the 3′ region of *EPCAM*, which resulted in EpCAM-MSH2 fusion transcripts (Jasperson *et al.*, 2010).

Individuals with LS carry a heterozygous germline MMR mutation and, for malignancy to occur, a second copy of the affected MMR gene must be somatically inactivated. Loss of function of the MMR system may lead to DNA replication errors, especially in microsatellites, which can occur in tumor suppressor genes or proto-oncogenes leading to carcinogenesis. DNA replication errors are propagated through daughter cells, leading to errors in microsatellites, making them unstable (MSI-H) (Carballal *et al.*, 2014; Wells and Wise, 2017).

1.3.2.2 Familial colorectal cancer type X

In 2005, Lindor *et al.* promoted the use of the term “Familial Colorectal Cancer Type X” to distinguish HNPCC families in which no DNA MMR defect was evident, from the LS families. Therefore, FCCTX represents the cases of CRC that meet clinical AC-I, whose tumours do not show alterations regarding the DNA MMR system after assessment by tumour IHC and/or MSI testing (Lindor *et al.*, 2005; Shiovitz *et al.*, 2014).

FCCTX follows an autosomal dominant inheritance pattern, but the genetic basis remains unknown, and may constitute more than one genetic aetiology (Shiovitz *et al.*, 2014). Compared to LS, FCCTX is associated to lower CRC risks, absence of increased risks for other tumours and older age at diagnosis and a higher adenoma/carcinoma ratio with tendency towards more adenomas, suggesting a slower progression of adenomas to carcinomas. In addition, tumours characterised by a functional MMR system are frequently observed at the distal of the colon, whereas LS tumors occur most frequently at the proximal side (Lindor, 2009).

Several linkage studies, next generation sequencing (NGS) and association studies, have been conducted to discover predisposing genes behind FCCTX. A germline mutation in ribosomal protein RPS20 (*RPS20*) gene (c.147dupA), encoding a ribosomal RNA maturation protein has been identified in a FCCTX family. The product of *RPS20* is required during the late steps of 18S ribosomal RNA formation, and has been associated to *TP53* stabilization. Conversely, the constant activation of *TP53* consecutive to ribosomal stress induced by *RPS20* mutation could favour, in the long run, the selection of cells that escape regulation by *TP53* (Nieminen *et al.*, 2014). Three different missense mutations (p.Val78Met, p.Gly484Ala and p.Ser326Phe) in the semaphorin 4A (*SEMA4A*) gene were also identified in three FCCX families, where the p.Val78Met variant demonstrated significantly increased MAPK/Erk and PI3K/Akt signalling activation as well as cell cycle progression in HCT-116 CRC cell line (Schulz *et al.*, 2014). However, the importance of this gene and its involvement in FCCTX seems to be controversial since another study failed to find evidences to support variations in SEMA4A as a determinant of FCCTX risk (Kinnersley *et al.*, 2016). Other than these, also two variants of the *BMPR1A*

gene (p.Gludel88 and c.68-10_68+14del) and a variant in the DNA polymerase delta 1 (*POLD1)* gene (p.Pro300Leu) have been reported in FCCTX families (Nieminen *et al.*, 2011; Duarte, 2015).

1.4 Consensus molecular subtypes of CRC

Although the three different molecular tumorigenic pathways provide an insight into the carcinogenesis process, they still do not fully explain the whole extension of CRC complexity and heterogeneity among tumours. Therefore, the need to achieve a more complete understanding into CRCs complexity arose and led to the establishment and validation of categories representing biologically distinct molecular subtypes based on gene expression. In the past years, several studies have been independently carried out aiming to find the called consensus molecular subtypes (CMS). Nevertheless, different expression–based CRC classifications were reported, showing considerable inconsistencies among them (Guinney *et al.*, 2015; Linnekamp *et al.*, 2018).

In 2015, Guinney and colleagues generated an international consortium, dedicated to large-scale data sharing and analytics across expert groups, in order to resolve inconsistencies among the reported gene expression–based CRC classifications and facilitate clinical translation. From this consortium, upon evaluation of results from six independent CRC subtyping algorithms, resulted in four CMSs: CMS1 (MSI immune), CMS2 (canonical), CMS3 (metabolic) and CMS4 (mesenchymal) (Figure 1.6). CMS1 represents most of MSI tumours that display immune activation. CMS2 reflects the classical subtype, containing WNT/MYC-driven tumours with epithelial characteristics, whereas CMS3 is enriched for *KRAS*-mutated tumours with activation of metabolic pathways. Finally, CMS4 has mesenchymal features, shows a high stromal content and activation of TGFβ and VEGFR pathways (Guinney *et al.*, 2015; Linnekamp *et al.*, 2018). Recently, all of these CMSs were identified in different *in vitro* and *in vivo* models, such as CRC cell lines, primary cultures and patient-derived xenografts (PDX) models (Figure 1.6) (Linnekamp *et al.*, 2018).

CMS1 MSI immune	CMS2 Canonical	CMS3 Metabolic	CMS4 Mesenchymal
MSI, CIMP high, hypermutation	SCNA high	Mixed MSI status, SCNA low, CIMP low	SCNA high
BRAF mutations		*KRAS* mutations	
Immune infiltration and activation	WNT and MYC activation	Metabolic deregulation	Stromal infiltration, TGF-β activation, angiogenesis
Worse survival after relapse			Worse relapse-free and overall survival

Figure 1.6 – Four CMS from the consortium and main characteristics of each subgroup (Adapted from: Guinney *et al.*, 2015). SCNA - Somatic copy number alterations.

In addition to molecular signatures, the four groups diverge in their association to different clinicopathological features and prognosis. CMS1 tumors were frequently diagnosed in females with right-sided lesions and presented with higher histopathological grade. Conversely, CMS2 and CMS4 tumors were mainly left- sided and CMS4 tumors tended to be diagnosed at more advanced stages (III and IV). Additionally, CMS4 tumors associate to worse overall survival and worse relapse-free survival,

whereas CMS2 are related to superior survival rates after relapse and long-term survival. Notably, the CMS1 population had a very poor survival rate after relapse, in agreement with recent studies showing worse prognosis of patients with MSI and BRAF-mutated CRCs that recur (Figure 1.6) (Guinney *et al.*, 2015; Lee *et al.*, 2017a).

1.5 Wnt/β-Catenin signaling pathway in CRC

Wnt/β signaling pathway is involved in the regulation of a variety of cell processes, which make it one of the major players in the establishment of tissue architecture during embryogenesis and in homeostasis of several tissues. The hallmark of this pathway is the accumulation and translocation of β-catenin into the nucleus (Figure 1.7).

Upon the inactive state of Wnt signaling, cytoplasmic β-catenin is degraded by a β-catenin destruction complex, which includes Axin, APC, protein phosphatase 2A (PP2A), glycogen synthase kinase 3 (GSK3) and casein kinase 1α (CK1α). Wnt proteins are secreted glycoproteins that bind to Frizzled and/or LRP transmembrane receptors, activating a signal transduction cascade, in which the cytoplasmic protein Disheveled is activated and leads to inactivation of the degradation complex. β-catenin is then able to enter the nucleus and associate with TCF/LEF transcription factors, thus inducing transcriptional regulation of Wnt target genes (Fevr *et al.*, 2007; Komiya and Habas, 2008).

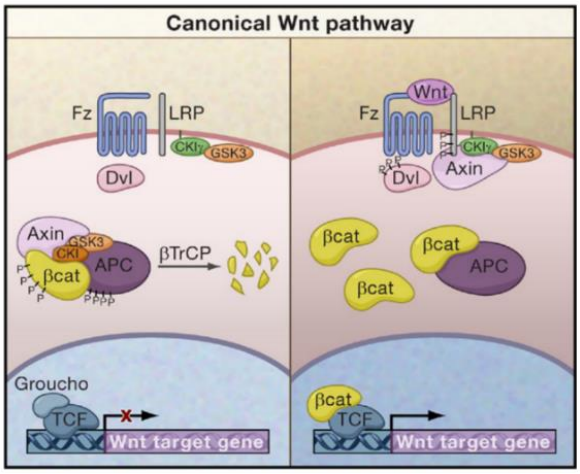

Figure 1.7 – WNT/βcatenin signaling pathway. Main intervenient proteins and processes upon inactive (left) or active (right) pathway (Adapted from: Clevers, 2006).

Many of β-catenin target genes have been implicated in regulating innumerable cellular processes, including proliferation (e.g., *MYC*, *CCND1*, *PPARD*), stem cell fate (*ASCL2*, *LGR5*), survival (*ABCB1*, *BIRC5*), differentiation (*ID2*, *ITF2*, *ENC1*), migration (*MMP7*, *MMP14*), and angiogenesis (*VEGF*). As mentioned above, processes play an important role in embryonic development and tissue homeostasis, however, its faulty regulation contributes to the initiation and progression of colon cancer. Wnt signaling represents the primary process behind intestinal epithelium homeostasis, through the regulation of stem cell proliferation and pluripotency. Loss of function of effectors such Tcf4 (*TCF7L2*) or β-catenin (*CTNNB1*) lead to the collapse of intestinal crypts, while aberrant activation of the Wnt pathway increases the number of stem cells, either way causing disruption of intestinal architecture (Herbst *et*

al., 2014; Krausova and Korinek, 2014). Moreover, the need of WNT-TCF activity in CRC is supported by the finding that a crypt/adenoma displays TCF-dependent gene expression signature (e.g. *SOX4, LGR5, AXIN2, cMYC*) (Leung *et al.*, 2002; Varnat *et al.*, 2010). and that this signature and tumour cell proliferation are abrogated *in vitro* by the inhibition of TCF function through the expression of dominant-negative TCF (dnTCF7L2) (Van de Wetering *et al.*, 2002; Varnat *et al.*, 2010).

The tight regulation of Wnt signaling cascade is the key to avoid tumor initiation by abnormal proliferation of intestinal stem cells (ISCs). This regulation is modulated by co-operative activity of the Hedgehog and bone morphogenic protein (BMP) cascades (van Dop *et al.*, 2009; Krausova and Korinek, 2014). As the progenitor cells further decline from the crypt base, the Hedgehog-induced, mesenchyme-to-epithelium BMP signaling promotes differentiation, restraining proliferation, while colon ISCs are protected from the pro-differentiation BMP signals by BMP antagonists (Krausova and Korinek, 2014). As mentioned above, human hereditary and sporadic colon cancers usually develop from the earliest aberrant crypt foci to larger adenomas, which will progress to carcinoma and invasive adenocarcinomas. Genetic or epigenetic changes of Wnt pathway components are frequently found in most colon cancer cases which lead to aberrant Wnt/b-catenin signaling (Figure 1.8) (Song *et al.*, 2015).

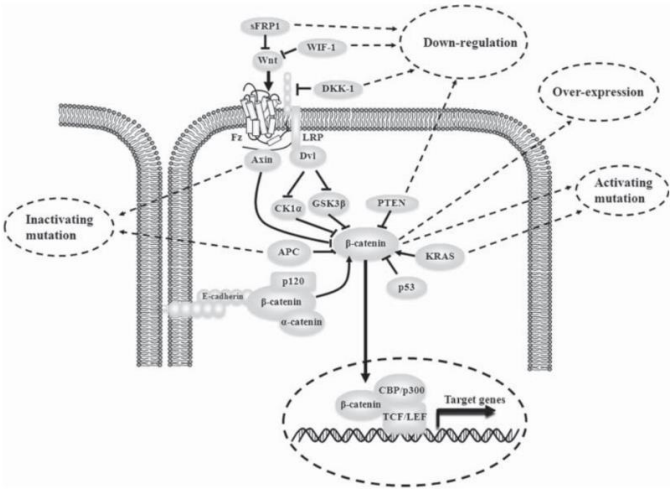

Figure 1.8 - . Mechanism leading to aberrant Wnt/β-catenin signaling in colon cancer. There include genetic like inactivating and activating mutations or epigenetic changes like DNA hypermethylation of Wnt pathway components (Adapted from: Song *et al.*, 2015).

Found in about 80% of colon tumors, APC mutations usually occur in a mutation cluster region that is important for binding to Axin and lead to produce truncated form of APC as well as the stabilization of β-catenin. In addition, truncated APC, lacking both nuclear export sequences (NES), is incompetent for β-catenin shuttling between cell nucleus and cytoplasm. Among the 10% of colon cancer cases that contain wildtype APC, β-catenin is mutated by point or in frame deletion of serine and threonine residues. These mutations render β-catenin difficult for ubiquitination and degradation by cellular proteasomes. Moreover, Axin mutation is found in some MSI colon tumor cases. Axin is an important component of destruction complex and its inactive mutations could disturb the process of b-catenin degradation. Components of Wnt/ β-catenin signaling, acting as Wnt inhibitors, such as sFRP1, WIF-1 and DKK1, are silenced by hypermethylation, also leading to aberrant Wnt/b-catenin signaling in colon cancer.

While colorectal adenomas progressing to invasive carcinoma, further genetic changes in oncogenes or tumor suppressors, such as KRAS, p53, PTEN, are found to aggravate the activation of Wnt/b-catenin signaling. Excessive activation of Wnt/β-catenin signaling stimulates colon cancer development through its downstream cancer-related targets such as c-myc, Cyclin D1, Cox-2, MMPs, uPAR, VEGF, etc. (MacDonald *et al.*, 2009; Krausova and Korinek, 2014; Song *et al.*, 2015).

1.5.1 *TCF7L2* in CRC

T-cell factors (TCF) represent a vast family of conserved DNA-binding proteins and transcriptional regulators containing a high motility group (HMG)-box. Nowadays, TCFs are most studied as nuclear effectors of Wnt growth factor signalling, a context where this factors act as assembly platforms for multifactorial transcription complexes, acting either to repress or stimulate the expression of Wnt target genes (Weise *et al.*, 2009).

Wnt/β-catenin pathway activation and the input of β-catenin into the nucleus allows the formation of β-catenin/TCF complexes and ultimately to the switch of Wnt/β-catenin target genes from inactive to active states. However, this gene expression control is achieved in a highly context dependent manner, as the type of response may vary according to the tissue or even time points. Although the mechanisms under this differential response ability are still largely unknown, TCFs are likely to be crucial in the process of target gene selection, therefore modulating Wnt effects. Structural diversity among TCF proteins due to dual promoter usage and extensive alternative splicing is most likely the cause of functional differences following WNT signaling activation (Weise *et al.*, 2009).

TCF7L2 acts as repressor in the absence of *CTNNB1* gene, and as activator of the pathway in its presence. Among the TCF/LEF family members, *TCF7L2* the highest expression in normal intestine and colon tissue, and is highly expressed in CRC-human derived cells. Mutations causing a loss-of-function of this gene were found in sporadic CRC, associated to increased cell growth, which further confirms that apart from its physiological role in healthy intestine and colon, TCF7L2 status is important for initiation and/or progression of CRC disease (Tang *et al.*, 2008; Hrckulak *et al.*, 2016). Furthermore, studies using *TCF7L2* RNAi-targeted CRC cell lines demonstrated an increase in cell growth potential, also suggesting a tumor suppressor role for *TCF7L2* in CRC (Angus-Hill *et al.*, 2011).

TCF7L2 protein presents several domains: the interaction domain to β-catenin, at the N-terminal region; interaction domain to Groucho related gene (*GRG*) and Carboxy-terminal binding protein (CtBP); HMG interaction domain to DNA; nuclear signaling domain (NLS); CRARF domain – amino acid signature motifs within the C-clamp – also known as C-clamp domain, which participates in the interaction of the protein with the DNA (Duval et al., 2000; Weise et al., 2009).

1.5.2 *TCF7L2* isoforms

TCF7L2 gene, encoding TCF7L2, also known as TCF4, comprises 17 exons, however, protein structure may differ due to its various sites of alternative splicing, which originate different isoforms containing different variations of its functional regions (Figure 1.9a). These isoforms can be distinguished in three classes, according to the exons involved in the splicing and the resulting protein,

leading to distinct termination sites in exon 17: long size isoforms (E), medium size isoforms (M) and short size isoforms (S) (Figure 1.9b).

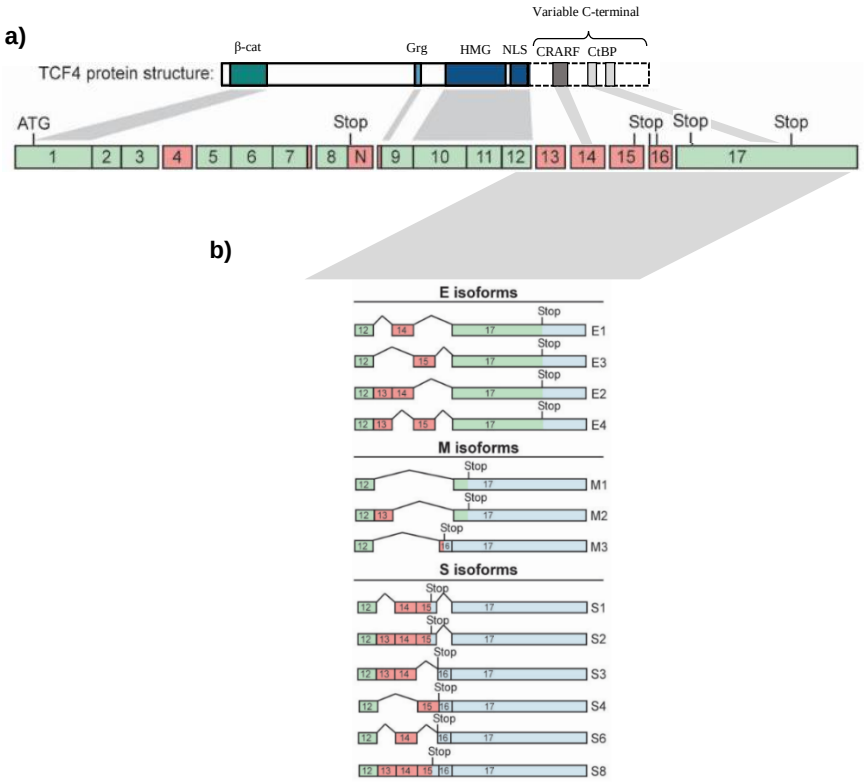

Figure 1.9 – TCF4 protein structure with representation of the three alternative splicing regions (a) and main C-terminal splice variants (b). In red are represented alternatively spliced exons. Green exons are constitutively incorporated. Blue areas represent untranslated regions (Adapted from: Weise *et al.*, 2009).

The alternative splicing in this gene mainly occurs in three identified regions: the exon 4, a 23 amino acid region whose function remains unknown; the splice donor region at the 3'-end of exon 8 which, if skipped, gives rise to isoforms that include the N-terminal region of TCF7L2, where the β-catenin binding domain is present, but lack the HMG-box and all other elements beyond it – TCF7L2N variants, which likely function as dominant negative factors in Wnt signalling; alternative splicing of exons 13, 14, 15 and 16 in numerous combinations, generating TCF7L2E, TCF7L2M and TCF7L2S isoforms with highly diverging C-termini (Figure 1.9b). TCF7L2E variants harbour a complete C-clamp region and contain two binding motifs for the transcriptional repressor Carboxy-terminal Binding Protein (CtBP). All other TCF7L2 isoforms lack the CtBP-binding sites and possess either no C-clamp (TCF7L2M) or only an incomplete version of it (TCF7L2S) (Atcha *et al.*, 2007; Weise *et al.*, 2009; He *et al.*, 2015).

1.6 Hedgehog/Gli signaling pathway in CRC

Hedgehog (Hh) proteins are secreted glycoproteins that activate a membrane receptor complex, formed by Patched (PTCH) and Smoothened (SMO), to drive a cytoplasmic signal transduction that activates Gli zinc-finger transcription factors. From the three hedgehog reported molecules (sonic-,

indian- and desert-hedgehog), sonic hedgehog (Shh) is the most widely expressed in this pathway and most frequently associated to tumor development. There are three main Gli proteins that have both activator and repressor functions: Gli1 is a strong transcriptional activator; Gli2 has both activator and repressor functions; and Gli3 is mostly a repressor (Ruiz i Altaba *et al.*, 2002; Ruiz i Altaba, 2007; Lee *et al.*, 2017b). In addition to hh ligands, PTCH, SMO and GLIs, several other proteins including fused (FU), Costal 2 (COS2), and suppressor of fused (SuFu) are involved in this pathway (Papadopoulos *et al.*, 2016; Lee *et al.*, 2017b). During inactive state of Shh/Gli signaling, where no hh ligand is present and SMO is inactivated by PTCH, Gli1 factor is transcriptionally silent, while Gli2 and Gli3 remain expressed in order to maintain HH-Gli targets silenced, due to their repressive nature (Figure 1.10). Activation of this pathway is subject to a tight regulation by many inhibitors at different levels. Hh ligands bind and inactivate PTCH in the membrane receptor complex, leading to activation of SMO, therefore, of Gli activity. Gli activation leads to transcriptional activation of Gli1 and a switch on the activity of Gli2 and Gli3 from repressor to activator (Figure 1.10). The active state of this pathway is subject to a precise regulation by the timing of ligand action as well as by positive and negative feedback mechanisms. Gli1 has a positive auto-regulatory role, extending the duration and possibly strength of signaling. However, this is counteracted by higher levels of feedback inhibitors also induced by Gli1, such as PTCH and hedgehog-interacting protein 1 (HIP1) (Ruiz i Altaba *et al.*, 2002; Papadopoulos *et al.*, 2016).

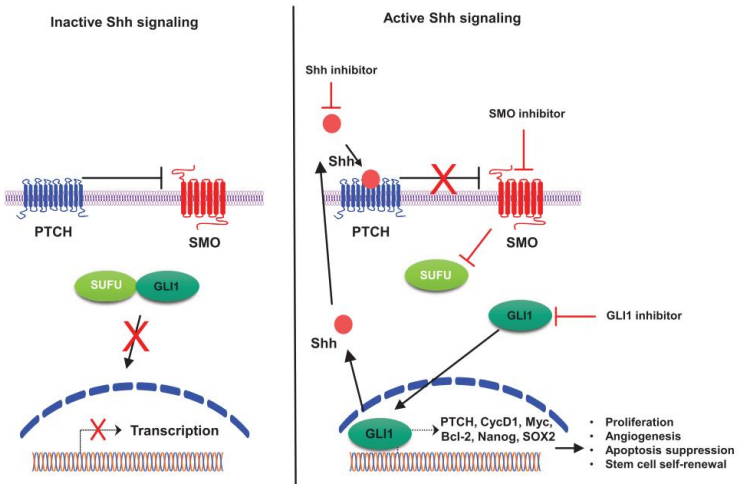

Figure 1.10 – Hedgehog signaling pathway (Adapted from: Lee *et al.*, 2017b).

In addition to the route described above, the canonical route, Shh/Gli pathway can also be regulated multiple oncogenes and tumor suppressors such as p53, KRAS, BRAF and PTEN, following therefore non-canonical signaling routes (Song *et al.*, 2015; Regan *et al.*, 2017).

Shh/Gli is crucial in several cellular processes during embryogenesis, with a well-established role as an important morphogenetic signal in the gastrointestinal patterning, however it remains essential in the maintenance of homeostasis of the gastrointestinal tract in the adult. A defective regulation of this pathway have been shown to affect a diversity of processes, including cell proliferation, cell survival, epithelial-to-mesenchymal transition (EMT) and stem cell regeneration (Papadopoulos *et al.*, 2016; Lee *et al.*, 2017b). It has been suggested that aberrant Hedgehog/Gli signaling plays a crucial role in colon cancer progression. The persistent activation of Shh/Gli signaling in colon cancer is driven in a ligand-

dependent manner, which is mediated through either canonical or non-canonical signaling routes. Shh/Gli signaling related components, Shh, PTCH1, SMO and Gli, are observed to be over-expressed in colon tumor, suggesting a positive correlation between tumor progression and expression levels of Shh, PTCH1 or SMO (Figure 1.11). In non-canonical signaling routes, increased Gli function is regulated by multiple oncogenes and tumor suppressors, which consequently leads to aberrant Hedgehog signaling during colon carcinogenesis (Song *et al.*, 2015; Regan *et al.*, 2017).

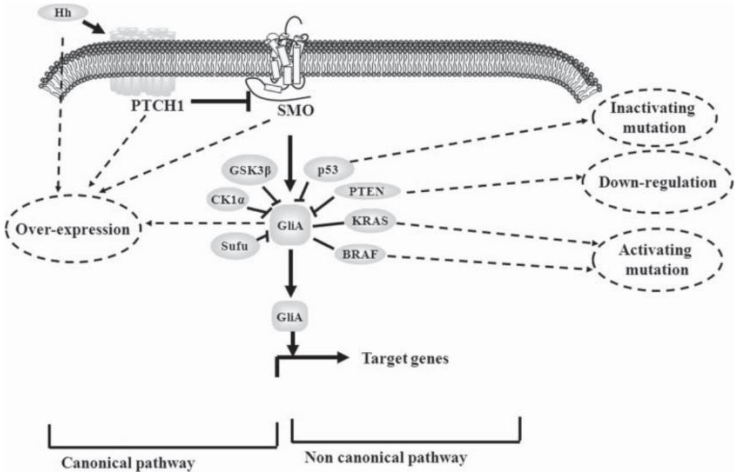

Figure 1.11 - Mechanism leading to aberrant Shh/Gli signaling in colon cancer. Canonical routes involve in the over-expression of Hh ligand, PTCH1, SMO and Gli. Non-canonical signaling routes include genetic or expression changes of multiple oncogenes and tumor suppressors such as p53, KRAS, BRAF and PTEN (Adapted from: Song *et al.*, 2015).

1.7 Wnt/β-catenin and Hedgehog/Gli signaling pathways interaction in CRC

While Wnt/β-catenin and Shh/Gli signaling pathways are crucially involved in CRC processes, crosstalk between them has been identified to be important in recurrence, invasion and metastasis. The molecular crosstalk between these two signaling pathways follows two different routes. Firstly, both Wnt/β-catenin and Shh/Gli signaling pathways are regulated by molecules such as GSK3b, CK1a, Sufu, p53, PTEN, SMO and KRAS, which leads to an indirect crosstalk in the regulation of these pathways. Two protein kinases GSK3b and CK1a negatively regulate both β-catenin and Gli1. Sufu, as a suppressor of the Fused kinase, which interacts with Gli1 but also binds to β-catenin as a negative regulator. In addition, inactive mutation of p53 or loss of PTEN in CRC could stimulate both pathways by activating β-catenin and Gli1. It has been reported that high levels of functional p53 could lead to a reduction of the amount and transcriptional activity of β-catenin. PTEN knockdown can increase the stabilization of β-catenin through activating PI3K/AKT pathway. Regarding Shh/Gli signaling, knockdown of p53 increases Gli1 activity whereas overexpression of p53 inhibits Gli1 activity in CRC cells. Either enhanced levels of PTEN or inhibition of downstream AKT could disturb Gli1 activity. SMO is an upstream active factor of Gli1 in Shh/Gli signaling and studies have shown an inhibition of SMO could reduce protein levels of active β-catenin and induce its nuclear exclusion, independent on the effect of Gli. Activated KRAS could stimulate the action of 2 pathways in colon cancer, since KRAS

mutation up-regulates β-catenin through the inhibition of GSK-3b mediated by PI3K/AKT signaling and overexpression of both KRAS mutants and the downstream component AKT enhance Gli1 activity in colon cancer cells (Varnat *et al.*, 2010; Song *et al.*, 2015; Ma *et al.*, 2015).

Secondly, a direct interaction between pathways, in which β-catenin interacts with Gli1 by Gli3R and each downstream target. In colon cancer, Gli3R displays mutual antagonism with β-catenin and Gli1: Gli3R inhibits β-catenin activity by antagonizing its active forms; over-expression of Gli1 decreases the mRNA levels of Gli3R, and the transcription of Gli1 is also repressed by the enhanced Gli3R expression. Thus, β-catenin and Gli1 could regulate each other through Gli3R. In addition, β-catenin could regulate Gli1 by inducing the expression of downstream targets, such as β-catenin binding domain–binding protein (CBD-BP), which binds to the coding region of Gli1 mRNA and stabilizes it, or c-myc, whose enhanced expression induces elevate Gli1 mRNA levels and could repress Gli3, forming Gli3R and then exert mutual antagonism with Gli1. Gli1 also regulates β-catenin through its targets: Snail, Wnt, Shh and sFRP1. Snail interacts with β-catenin and stimulates its transcriptional activity. Several Wnt ligands, have been shown to be target proteins of Gli1, while they are the upstream ligands of Wnt/β-catenin signaling. Another target protein, sFRP1, is an antagonist of Wnt ligands which indirectly inhibits the activity of downstream β-catenin. In addition, Gli1 could up-regulate Shh expression, which is secreted and acts on stromal cells. Stromal cells responding to Shh enhance *Foxf1* and *Foxf2* expression, which inhibits mesenchymal expression of Wnt5a and leads to suppression of β-catenin. Finally, β-catenin and Gli1 have antagonistic roles in regulating TCF and downstream target genes in metastatic colon cancer. Even if β-catenin is still highly expressed in metastatic colon cancer, TCF's targets are decreased in contrast to that in non-metastatic stage. In addition, studies have suggested enhanced Gli1 could attenuate TCF activity and its downstream targets in colon cancer cells (Varnat *et al.*, 2010; Song *et al.*, 2015; Ma *et al.*, 2015).

1.8 Epithelial-to-mesenchymal transition and the metastasizing process

Metastasis is the major cause of death in cancer patients. The metastatic process involves detachment of tumor cells from the primary tumor, invasion, intravasation, survival within the circulation, extravasation and colonization at the secondary site (Pantel and Brakenhoff, 2004). In this process, tumor cells develop mesenchymal characteristics that facilitate tumor detachment and acquisition of a migratory ability (Chambers et al., 2002; Zhang et al., 2016). Metastasizing process is very complex and a great variety of signaling pathways, including TGFβ, Notch, Hedgehog, Wnt, NF-κB, PI3K/Akt and RAS (Huber et al., 2005; Larue and Bellacosa, 2005).

EMT denotes a process in which cells change their phenotype between epithelial and mesenchymal states and is involved in the metastatic cascade, as it leads to the molecular reprogramming and phenotypic changes that characterize this conversion. A variety of factors, including cadherins, Snail, β-catenin, TGFβ and MMPs regulate the metastatic process through different mechanisms. For instance, these factors lead to several phenotypic alterations, such as changes in cell-cell adhesion, apical-basal polarity and tissue architecture (Liu et al., 2015). As a critical regulator of multiple signaling pathways leading to EMT, the expression of *Snail* is closely associated with cancer metastasis (Wang et al., 2013). As an early event in EMT, cells undergo a cadherin switch, associated

with increased motility and invasiveness, expressing N-cadherin (*CDH2*) instead of E-cadherin (*CDH1*), meaning *CDH1* expression decreases as cell go through EMT (Kroepil et al., 2012). Over-expression of vimentin was detected in several cancer types of cancer cells, including CRC, which correlated well with increased migration and invasive potentials (Satelli and Li, 2011). The expression of vimentin intermediate filaments in epithelial cells, which normally express only keratin, was also reported during EMT process. Its overexpression was reported in various tumor cell lines, including CRC cell lines, which has led vimentin to acquire importance as a marker of EMT in cancer cells. Accordingly, during the reverse process of EMT, mesenchymal-epithelial transition (MET), the cells start acquiring epithelial phenotype and show a decreased vimentin expression with lower motility rates.(Thiery, 2002; Chaffer et al., 2006) Zeb1 is another marker that has been associated to EMT, since its overexpression in cancer is related to repression of epithelial genes, such as E-cadherin and activation of mesenchymal genes, including vimentin (Peinado *et al.*, 2007; Chen *et al.*, 2017).

Wnt signaling pathway plays a crucial role on EMT by activating the transcription of several genes involved in migration, invasiveness and tumor aggressiveness, including, among others, E-cadherin and MMP7 (Brabletz et al., 2002; Thiery, 2002). The loss of E-cadherin, the main cell-cell adhesion molecule, represents a crucial event on EMT process and can be achieved through the presence of inactivating mutations or transcriptional repression (Kang and Massagué, 2004). Studies have reported the role of Snail in repressing E-cadherin and inducing the expression of mesenchymal markers such as Vimentin, fibronectin and MMP2 (Yokoyama et al., 2003; Vega et al., 2004).

1.9 Stem cells and colorectal carcinogenesis

Heterogeneity in solid cancer cells represents a very complex matter, however, two general models were proposed in order to highlight different phenotypes among cells on the same tumor cell population (Figure 1.12). The first model refers that cancer cells with different phenotypes have the potential of developing a tumor (Figure 1.12 a). The second, the CSCs model, predicts a hierarchical structure within the same tumor, in which cells harbouring stemness properties and self-renewal ability, are responsible for tumor growth (Figure 1.12 b). This latter model explains heterogeneity inside the tumor being originated by one cell and also that maintenance in the tumor is due to the presence of a stem-like niche (Reya et al., 2001; Burrell et al., 2013).

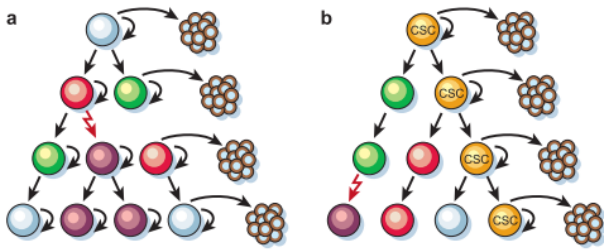

Figure 1.12 – Representative models of carcinogenesis. Cancer cells with different phenotypes have the potential of developing a tumor (a); Cells harbouring stemness properties and self-renewal ability, are responsible for tumor development (b) (Adapted from: Reya *et al.*, 2001).

Isolation and evaluation of the tumorigenic ability of a subset of cells in colorectal tumors, compared to the original tumor has proven that CSCs are in fact the cells that promote tumor growth (Dalerba et al., 2007). Specific cell clusters with stemness properties, based on acknowledged markers, such as CD44, CD133, Lgr5 and EpCAM, has also proven the link between CSC and the origin of metastasis (Du et al., 2008; Chu et al., 2009; Ma and Allan, 2011; Aguilar-Gallardo and Simón, 2013; Wahab et al., 2017).

CD133 is a transmembrane cell-surface protein, encoded by *PROM1*, localized to the plasma membrane and it was found to be expressed in cancer progenitor cells in the colon, among several other organs (O'Brien *et al.*, 2007). Additionally, recent studies have shown that *PROM1* can serve as an essential marker for detecting and enriching several types of CSCs and that *PROM1* expression levels are correlated with CSC tumor-promoting capacity (Yin *et al.*, 2007; Tang *et al.*, 2012). CD44 is a ubiquitously expressed cell adhesion molecule and also a potential cell surface marker on colon CSCs and was reported to be involved in altering the directional motility/migration of human colon cancer cells (Subramaniam *et al.*, 2007; Saigusa *et al.*, 2012a). Moreover, in the presence of CD133, CD44+/EPCAM-high/ALDH+ phenotype increased tumor growth compared to the isolated CD133+ cell niche (Dalerba et al., 2007). *LGR5*, has been reported as an intestinal stem cell marker and recent studies showed that *LGR5* was associated with carcinogenesis and tumor invasion in CRC. Nevertheless, recent data observed increased expression of this marker in the upper region of the colonic crypt during dysplasia, confirming it as an invasive cell population. *LGR5* overexpression has been associated with early stages of tumorigenesis, invasiveness and metastasis, thus considered as a potential CSC marker (Uchida et al., 2010; Baker et al., 2015).

1.10 Conventional therapeutics in CRC

CRC treatment is determined according to disease stage (Appendix A). Surgery is the main treatment for CRC cure, however, in cases with ganglionar involvement (stage III), the administration of adjuvant chemotherapy is the treatment of choice for optimizing the chances of healing. The treatment of choice in stage III is the scheme that combines oxaliplatin with 5-FU and Leucovorin – FOLFOX. The use of adjuvant chemotherapy in stage II CRC is more controversial, however there is a subgroup of patients at this stage with increased risk of recurrence [T4, inadequate nodal surgery (< 12 nodes removed), lympho-vascular invasion, visceral peritoneum affectation, bowel obstruction or poorly differentiated histology] in which the use of adjuvant chemotherapy using FOLFOX can be considered (Carrato, 2008).

In metastatic disease (stage IV), CRC therapeutic approach is complex and involves the combination of loco-regional treatment of metastases with systemic treatment to obtain disease resectability. Regarding chemotherapy in these patients, it can be used as adjuvant treatment, a complement to metastases potentially curative by surgery, as neo-adjuvant treatment to achieve resectability of initially unresectable disease, or as palliative therapy. As adjuvant treatment, the administration of FOLFOX is currently considered first choice. Regarding neo-adjuvant treatment for potentially resectable disease, FOLFOX and FOLFIRI have exhibited similar response rates, however, the combination of oxaliplatin, irinotecan and 5-FU (FOLFOXIRI) exhibit higher reported response rates

(66%), achieving a higher rate of resectability than FOLFIRI or FOLFOX individually. Palliative therapy with chemotherapy increases survival, can reduce the symptomatology and can improve quality of life. The treatment length may be 6 months or until disease progression, mainly depending on toxicity. The choice of both first-line and subsequent treatments depends on previous treatments, the administration and toxicity profiles as well as the objectives to be achieved with the treatment. The use of 5-FU results in approximately 12-months survival being equivalent to Capecitabine treatment. FOLFOX and FOLFIRI exhibit similar survival outcomes in first-line metastatic disease, with 15 months OS, being also equivalent in oxaliplatin schemes the substitution of 5-FU by capecitabine (Binefa *et al.*, 2014; Marques *et al.*, 2017). Marques and his colleagues showed that in patients with unresectable metastatic CRC, first-line triplet chemotherapy (FOLFOXIRI) leads to improved survival and efficacy outcomes in comparison to doublet chemotherapy backbone (FOLFIRI or FOLFOX), though at the expense of additional toxicity leading to adverse event-related withdrawal and a higher risk of grade ≥3 adverse events, notably neurotoxicity (including peripheral neuropathy), non-febrile neutropenia, and diarrhea (Marques *et al.*, 2017).

Prognostic markers, such as the presence of MSI-H in the tumor should be taken into account when assessing the use of adjuvant chemotherapy disease because there are studies reporting little benefit or even a negative impact of 5-FU adjuvant chemotherapy without Oxaliplatin in these cases (Binefa *et al.*, 2014). Regarding these cases, targeted therapy, with monoclonal antibodies binding to either the epidermal growth factor receptor (EGFR), or the VEGF inhibitor Bevacizumab, is currently considered to be standard of care for first-line treatment of metastatic CRC (Marques *et al.*, 2017).

1.10.1 Mechanism of action of conventional therapeutic agents

5-FU is an analogue of uracil with a fluorine atom at the C-5 position in place of hydrogen. It rapidly enters the cell using the same facilitated transport mechanism as uracil and is converted intracellularly to several active metabolites: fluorodeoxyuridine monophosphate (FdUMP), fluorodeoxyuridine triphosphate (FdUTP) and fluorouridine triphosphate (FUTP). These active metabolites disrupt RNA synthesis and the action of thymidylate synthase (TS), responsible for catalysing the reductive methylation of deoxyuridine monophosphate (dUMP) to deoxythymidine monophosphate (dTMP), essential for DNA replication and repair. The rate-limiting enzyme in 5-FU catabolism is dihydropyrimidine dehydrogenase (DPD), which converts 5-FU to its degraded form - dihydrofluorouracil (DHFU). More than 80% of administered 5-FU is normally catabolized primarily in the liver, where DPD is abundantly expressed (Longley *et al.*, 2003).

Irinotecan is a potent chemotherapeutic agent which, upon administration, is converted by carboxylesterase in the liver and in plasma to an active metabolite (SN-38). SN-38 is a potent inhibitor of topoisomerase I (Topo-1), as it binds to DNA-Topo-I complex, generates a gap in DNA structure and therefore prevents DNA replication and ultimately leads to cell death (Cunningham *et al.*, 2001; Keyvani-Ghamsari *et al.*, 2017).

Finally, oxaliplatin acts as a DNA interacting agent, it mainly forms intra-strand adducts between two adjacent guanine residues or guanine and adenine, disrupting DNA replication and transcription (Gherman *et al.*, 2012).

1.11 Other compounds in CRC therapy

1.11.1 DNA methyltransferase and HDAC inhibitors

Epigenetic alterations including aberrant DNA methylation, abnormal histone modifications or altered expression levels of various non-coding RNAs, are predominant in CRC and must be taken into account in terms of therapeutic drugs choice. Therapies including DNA-demethylating agents and histone deacetylases (HDAC) inhibitors have been studied as possible options for CRC treatment improvement. 5-Azacitidine (Azacytidine) and Vorinostat are, respectively, examples of these types of therapeutic agents (Sarkar *et al.*, 2013; Wilson *et al.*, 2013; Deming *et al.*, 2014; Kim *et al.*, 2014). Azacytidine is a cytosine analogue that incorporates into replicating DNA in place of cytosine and trap DNMTs, resulting in proteasome degradation and heritable global demethylation as cells divide, inducing DNA demethylation across all genomic features. This drug has been approved for the treatment of myelodysplastic syndrome, a pre-leukemic disorder. More recently, clinical trials have been initiated to investigate the possibility of extending their utilization to solid tumors, such as ovarian and lung cancers, either alone or in combination with other. Transient exposure to low doses of DNA demethylating agents can exert durable antitumor effects in solid tumors and long-term stability of demethylation of promoter CpG islands has been shown to have anticancer effects (Sarkar *et al.*, 2013; Kim *et al.*, 2014; Yang *et al.*, 2014). Vorinostat is a small molecule inhibitor of class I and II HDAC enzymes and is currently approved for use in refractory cutaneous T-cell lymphoma and is under clinical studies for other pathologies (Wilson *et al.*, 2013; Deming *et al.*, 2014).

1.11.2 Specific signaling pathway modulators

As mentioned in section 1.6, Shh/Gli signaling pathway aberrant activation is closely involved in carcinogenesis (Ruiz i Altaba *et al.*, 2002; Song *et al.*, 2015). GANT61 is a hexahydropyrimidine derivative and represents a Gli1 and Gli2 inhibitor (Lauth *et al.*, 2007; Mazumdar *et al.*, 2011c). This agent acts in the nucleus by blocking Gli function through inhibition of Gli1- and Gli2-mediated transcription, with a high degree of selectivity for HH/Gli signaling (Mazumdar *et al.*, 2011c). In 2013, Fu and colleagues have demonstrated that GANT-61 modulates CSC proliferation, EMT, and apoptosis in pancreatic cancer cells. Furthermore, the compound blocked CSC tumor growth through inhibition of Gli1, Gli2, Bcl-2, CCND2 and Zeb1, and induction of death receptors DR4 and DR5 (Fu *et al.*, 2013). Moreover previous studies showed reduced GLI1, GLI2 and PTCH1 mRNA expression, significantly modulated complementary DNA (cDNA) microarray gene expression profiles downstream of Gli1/Gli2 function and cell cycle arrest in S-phase, in human colon carcinoma cell lines after treatment with GANT61 (Shi *et al.*, 2010; Mazumdar *et al.*, 2011a).

Hepatocyte growth factor (HGF) and its receptor cMET are the main intervenient on the HGF/cMET signaling pathway and have been previously reported to be involved in a series of malignant tumors. HGF/cMET is known to prevent apoptosis through Akt activation and a great number of studies have correlated the overexpression of HGF and cMet to cancer invasion, metastasis and also poor prognosis in various cancers. cMet is the cell surface receptor and the only known functional receptor for HGF and

is closely associated to invasion and metastatic progression of cancers, including CRC (Otte *et al.*, 2000; Saigusa *et al.*, 2012b; Xiang *et al.*, 2017). Significant overexpression of cMet mRNA and protein have been previously reported in CRC tumors in comparison to adjacent normal colon mucosa (Zeng *et al.*, 2004; Safaie Qamsari *et al.*, 2017). Capmatinib represents a cMet inhibitor, thus bearing the potential to counteract the role of this pathway in cancer (Sartore-Bianchi *et al.*, 2016).

1.11.3 Nutraceuticals

Sulforaphane (SFN) is a member of the isothiocyanate family present in cruciferous vegetables such as broccoli and broccoli sprouts. SFN has numerous molecular targets, that vary according to cancer stage and target tissue (Clarke *et al.*, 2008). Several studies have shown that SFN can modulate many steps involved in cancer development, including cell proliferation, apoptosis, angiogenesis, and metastasis (Fimognari and Hrelia, 2007; Pereira *et al.*, 2017; Tafakh *et al.*, 2018). Moreover, SFN has previously been shown to induce cell cycle arrest, correlated to increased expression of cyclins A and B, followed by apoptotic cell death in HT-29 CRC cells (Gamet-Payrastre *et al.*, 2000). Figure 1.13 depicts the main molecular targets of SFN regarding the mentioned processes.

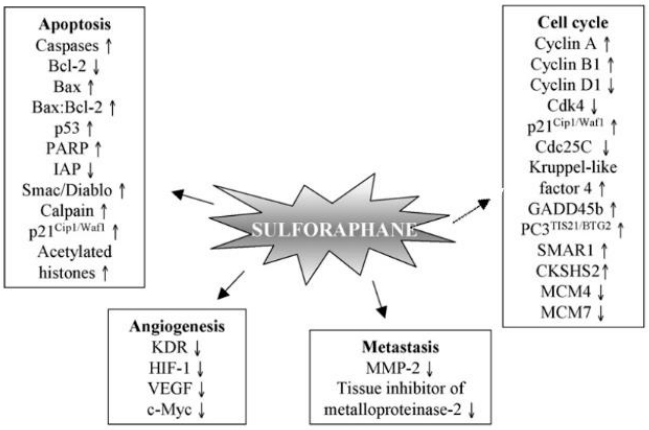

Figure 1.13 – Molecular targets of SFN involved in cell cycle, apoptosis, angiogenesis and metastasis (Adapted from: Fimognari and Hrelia, 2007).

Plant belonging to the *Scutellaria* genus have been widely used in herbal medicine. Biologically active flavonoids, including apigenin, baicalein, baicalin, chrysin, scutellarein, and wogonin are found in leafs and roots of several *Scutellaria* species. Several studies have reported anti-inflammatory, ant-oxidative, anxiolytic, antiviral and anti-cancer activity associated to these flavonoid compounds (Ma, 2005; Parajuli *et al.*, 2009; Kim *et al.*, 2012). In fact, in 2008, Kim and colleagues have shown baicalein to actively induce apoptosis via Akt activation in a p53-dependent manner in HT-29 colon cancer cells, suggesting its use as a chemopreventive or therapeutic agent for HT-29 colon cancer. Other studies have shown the potential of Chrysin, baicalein and scutellarein to inhibit the proliferation of malignant glioma and breast carcinoma cells without affecting primary or non-malignant cells (Androutsopoulos *et al.*, 2009; Parajuli *et al.*, 2009).

Another flavonoid compound, tangeretin (4′,5,6,7,8-pentamethoxyflavon), represents one of the most effective citrus flavonoids at inhibition of human cancer cell proliferation (Manthey and Guthrie,

2002). This agent has been presented as a potential chemopreventive agent through several studies showing its potent anti-inflammatory, anti-proliferative, and anti-carcinogenic activities (Lin *et al.*, 2003; Chen *et al.*, 2007; Ting *et al.*, 2015). Moreover, tangeretin was shown to reduce inflammation-related cyclooxygenase (Cox2) expression in human lung epithelial carcinoma cells (Chen *et al.*, 2007) and induce G1 and S phase cell cycle arrest in breast and colon carcinoma cells, respectively, 24h after treatment (Pan *et al.*, 2002; Morley *et al.*, 2007).

2. AIMS

PART I

Study of the expression of specific *TCF7L2* isoforms for the identification of novel therapeutic targets/biomarkers

Considering the great gap on the understanding of the molecular mechanisms leading to tumor initiation and progression in CRC, as a first line, this study aimed to explore the involvement of variable expression of *TCF7L2* isoforms in colorectal tumorigenesis. We therefore aimed to study *TCF7L2* isoforms, varying in the inclusion of exons within exons 1-5 and 12-17 of the gene, in a panel of blood leucocyte samples from CRC patients (fulfilling the Bethesda guidelines or FCCTX patients) and representative CRC cell lines and further analyse differential expression among samples. This study should provide essential information for future investigation on the potential correlation between the expression of different isoforms and tumor specific features. Thus, promoting a better understanding of the molecular mechanisms involved in tumorigenesis and metastasizing process in CRC and possibly identify new biomarkers, molecular targets and therapeutics.

PART II

Explore novel therapies for resistant colorectal cancer subtypes

In view of the great need for development of directed and effective therapies in CRC, this work aimed to explore novel therapies for resistant colorectal cancer subtypes, using conventional pharmacological compounds, new targeted therapies and nutraceuticals, either isolated or in combination, in 2D and 3D CRC cell models representative of resistant tumor subtypes. To achieve this goal, we aimed to assess the effect of isolated compounds or in combination on cell viability, migratory ability and in the expression of a series of key markers implicated in main tumorigenesis and metastasizing processes. The potential of these alternative treatment approaches in targeting the more aggressive CRC phenotypes, are the first step for further investigation and development of novel therapeutic strategies.

3. MATERIALS AND METHODS

3.1 Biological samples

A total of 38 RNA samples, from peripheral blood were used in this study. The samples were obtained from patients registered in IPOLFG, EPE (*Instituto Português de Oncologia de Lisboa, Francisco Gentil*) and used for research purposes upon their informed written consent. These samples belong to FCCTX, no germline mutations identified and BC patients.

The human CRC cell lines HT-29, LS174T, SW48, SW480, SW620, LoVo and HCT116 used in this study, were gently provided by Dr Riccardo Fodde, from the pathology department at ERASMUS University Medical Center, in Rotterdam. The main characteristics of these cell lines are listed on appendix B, table B.1.

HT-29 and LS174T were the cell lines used in cell-based assays. The HT-29 cell line was originally established in 1964 from the primary tumor 44-year-old caucasian woman with colorectal adenocarcinoma (Martínez-Maqueda *et al.*, 2015). The LS174T cell line is a trypsinized variant of the original LS-180 cell line, established in 1974 from a moderately well-differentiated colon adenocarcinoma, with spread to pericolonic adipose tissue, removed from a 58-year-old caucasian woman.(Tom *et al.*, 1976) Both cell lines present epithelial morphology and adherent growth profile, under standard culture conditions (Tom *et al.*, 1976; Martínez-Maqueda *et al.*, 2015). The molecular characteristics of these cell lines differ in terms of oncogene expression, relevant mutations and microsatellite stability, as illustrated in Appendix B, tables B.1 and B.2, respectively.

3.2 Nucleic acid isolation

3.2.1 RNA isolation from peripheral blood samples

RNA isolation from peripheral blood was performed according to the method described for TRI Reagent® Solution (Ambion, Life Techonologies). The final RNA concentration was assessed using Nanodrop2000 (Thermo Scientific). Purity and integrity of the isolated RNA was assessed by electrophoresis, in which 1µL of isolated RNA is added to 9µL of Orange G 1x (loading dye) and then subjected to a 0,8% (w/v) agarose gel, in TBE 1x (Tris-Borate-EDTA buffer solution) stained with ethidium bromide, for 45 minutes, at 140V. Lambda/HindIII DNA Ladder (Fermentas) was used as molecular weight marker. The results were analysed by visualization of the gel using a UV transilluminator. RNA samples were stored at -80°C until further use. All the solutions used for agarose gel preparation and electrophoresis are described in appendix B.

3.2.2 RNA isolation from CRC cell lines

RNA was obtained from CRC cell lines lysates using RNeasy® Mini Kit (QIAGEN), according to the manufacturer's instructions. RNA concentration, obtained after isolation, was assessed using Nanodrop2000 (Thermo Scientific). Samples were then stored at -80°C until further use.

3.3 Polymerase chain reaction

Polymerase chain reaction (PCR) is a molecular biology technique, used to create multiple copies of a specific segment of DNA in a mixture of DNA molecules, based on the enzymatic activity of DNA polymerase. This amplification reaction requires the presence of several key components: a) two previously designed short DNA sequences (primers) flanking the DNA target region; b) deoxynucleotide triphosphates (dNTP's), the substrates for DNA synthesis that are incorporated in the new DNA fragments; c) DNA polymerase enzyme, to catalyse the synthesis of new fragments; d) bivalent cation, usually magnesium (Mg^{2+}) as the cofactor for DNA polymerase; e) buffer solution to provide the chemical environment for optimum activity and stability of the DNA polymerase.

The PCR amplification reaction is achieved using a thermocycler, a device capable of raising and lower temperature in different pre-programmed steps. For PCR, three consecutive steps are repeated in a series of 30 to 40 cycles. The first step in the PCR reaction allows the denaturation of the double-stranded DNA molecules in the mixture, by heating the samples to proximately 94ºC. The second step involves the annealing of the primers to complementary strands of DNA, in which the samples are cooled to a temperature that is calculated accordingly to the primers sequence. The third step, occurs at the optimal DNA polymerase temperature and allows the formation of the new DNA strands through the binding of the enzyme and further elongation of the DNA strand by base complementarity to the template strand. The determination of the number of cycles follows the principle that PCR products are generated in an exponential pattern (2^n, being n the cycle number) and reaches a plateau after the point when most reagents have been consumed.

3.3.1 PCR primers design

Primer appropriate design is a crucial step for successful DNA/cDNA amplification. In this study, PCR primers were designed accordingly to a series of requirements.

Small sequences containing 18 to 23 nucleotides, flanking the region of interest were chosen from the reference gene sequence (Built GRCh38, NCBI: https://www.ncbi.nlm.nih.gov/) of the gene of interest. *In silico* analysis of the primers was performed using the software NetPrimer (PREMIER Biosoft: http://www.premierbiosoft.com/netprimer), a tool that allows the selection of an optimal primer pair, since all primers are analysed for theoretical secondary structures including hairpins, repeats, self and cross dimers and the stability of this structures. It also calculates primer melting temperature (Tm) and GC content (the number of G's and C's in the primer as a percentage of the total bases). Therefore, the suitable pair of primers was chosen avoiding, as much as possible, the formation of secondary structures and to have a GC content between 40 and 55%, that should be similar between the pair, as well as melting temperatures.

After obtaining a primer pair that fulfilled these requirements, the size of the fragment obtained, as well as the specificity of the primers within the human genome (to ensure that the primers were only annealing with the desired sequence), were accessed using the software Primer-Blast (NCBI: https://www.ncbi.nlm.nih.gov/tools/primer-blast).

3.3.2 PCR optimization

PCR optimization was performed for each DNA fragment amplified in this study, in order to determine the optimal reaction conditions (annealing temperature, Mg^{2+} concentration and DNA polymerase kit) for the amplification of each specific target.

The theoretical annealing temperature for each primer was determined using equation 1, which takes into account the number of adenines (A), thymines (T), guanosines (G) and cytosines (C) in each primer sequence.

$$Primer\ annealing\ temperature\ (°C) = 2 \times (A + T) + 4 \times (G + C)$$

Equation 1

The starting annealing temperature was determined by equation 2, which takes into account the specific pair of primers used in the reaction (primers forward (Fw) and reverse (Rv)).

$$Annealing\ temperature\ (°C) = \frac{(Annealing\ temperature)_{Primer\ Fw} + (Annealing\ temperature)_{Primer\ Rv}}{2} - 2$$

Equation 2

This temperature was increased if nonspecific PCR product were observed, or decreased in the cases where there was no, or very low, amplification product.

Furthermore, the optimum Mg^{2+} concentration to obtain a specific PCR product was determined for each target fragment through titration of a solution containing Mg^{2+} ions. Mg^{2+} concentration was raised if no, or very low amplification product was observed and decreased upon the presence nonspecific PCR products.

3.3.3 cDNA amplification by PCR

Fragment amplification using enzymatic Biotaq™ kit (Bioline) was achieved using a reaction mixture containing 1µL of gDNA/cDNA template, 0.3µL of each primer (Fw and Rv) at a working concentration of 10pmol/µL, the appropriate volume to the previously optimized concentration of the $MgCl_2$ solution, 1µL of dNTPs (200 mM, Illustra™, GE Healthcare), 1.25µL of reaction solution buffer, 0.08µL of the DNA polymerase (5U/µL), and ddH_2O to make up the final reaction volume of 12.5µL. The reaction buffer solution, $MgCl_2$ solution and DNA polymerase were provided by each specific kit. PCR reactions were performed in UNO96 thermocycler (VWR), using the conditions and PCR programs described in Appendices C and D, respectively.

3.4 Agarose gel electrophoresis

Agarose gel electrophoresis allows the qualitative analysis of nucleic acid fragments, based on separation according to their size. In this method, an electric field is applied, allowing the movement of the negatively charged nucleic acids, through an agarose gel matrix, towards a positive electrode. Because DNA has a uniform mass/charge ratio, the approximate length of a nucleic acid fragment can

be determined following the principle that the log of the molecular weight is inversely proportional to migration rate through a gel matrix. The use of a fluorescent intercalating agent, such as ethidium bromide, allows the visualization of DNA after migration along the gel, by exposition to ultraviolet (UV) light.

During a PCR optimization process (described in section 3.3.2), the reaction efficiency was evaluated by loading to the gel the total volume of amplification product combined with 3µL of Orange G 5x. For already optimized PCR reactions, efficiency was assessed using 3µL of the amplified product combined with 7µL of Orange G 1x.

For fragments with an expected molecular weight below 1000bp, electrophoresis was performed in a 2% (w/v) agarose gel, stained with ethidium bromide, followed by separation at 140V for 30 minutes in TBE 1x, using 6.5µL of the molecular marker GeneRuler 50bp DNA Ladder (Thermofisher Scientific). The same electrophoresis conditions were used for fragments with a predicted molecular weight around 1500bp electrophoresis, with an extra molecular weight marker - 1 kb DNA Ladder (Promega). For higher molecular weight fragments (≥ 2000bp) electrophoresis was carried out in a 1.2% agarose gel (w/v), stained with ethidium bromide, run at 140V for around 1 to 2 hours, using, as molecular weight marker, 6.5µL of both 1 kb DNA Ladder (Promega) and Lambda DNA/HindIII Marker (Thermo Scientific). After electrophoresis process, the gel was exposed to UV light in a transilluminator (Biometra) for DNA/RNA fragments visualization.

Preparation of agarose gel and solutions for use in electrophoretic analysis are detailed in Appendix C.

3.5 Sanger sequencing

Sanger sequencing, also known as chain-termination sequencing or dideoxy sequencing has been the powerhouse of DNA sequencing since its invention in the 1970s. The process is based on the detection of labelled chain-terminating nucleotides that are incorporated by a DNA polymerase during the replication of a template. Dideoxy sequencing is based on synthesis of DNA strands that are complementary to a template DNA strand. The sequencing reaction uses normal dNTPs and modified dideoxynucleoside triphosphates (ddNTPs) for strand elongation. The ddNTPs lack a 3′- OH group that is required for the formation of a phosphodiester bond between two nucleotides, causing DNA polymerase to stop DNA extension whenever a ddNTP is incorporated. The resulting DNA fragments are subjected to capillary electrophoresis, where the fragments flow through a gel-like matrix at different speeds according to their size. Because each ddNTP is labelled with a different fluorescent dye (each of which fluoresces at a different wavelength), the sequencing can be done as a single reaction. As the DNA fragments exit the capillary electrophoresis gel, the dyes are excited by a laser and the emitted light is detected. The result is an electrophoretogram where bases are represented by a sequence of coloured peaks (Watson et al. 2012).

3.5.1 Agarose band excision and purification

For each PCR product, different molecular weight bands, corresponding to distinct isoforms of the gene of interest in this study (*TCF7L2*), were excised from the agarose gel in order to isolate and identify the different expressed isoforms. After electrophoresis, the agarose gel was exposed to UV light in a trans-illuminator in order to visually identify the bands of interest, which were carefully isolated and excised using a scalpel.

Excised bands were then subject to purification process in order to isolate the DNA and obtain a final sample containing agarose-free DNA. This process was carried out using QIAquick® Gel Extraction Kit (QIAGEN), according to manufacturer's instructions. Purified DNA samples were stored at -20°C until further use.

3.5.2 Sequencing reaction

For each amplified fragment to be sequenced, a reactional mixture was made, containing: 2 µL of the forward or reverse primer (1,6pmol/µL); 2µL of buffer sequencing 5x, BigDye® Terminator v1.1 (Applied Biosystems), to maintain a constant pH; a variable amount of BigDye™ Terminator v1.1 Cycle (Applied Biosystems), depending on the size of the fragment to be sequenced; a variable amount of the purified DNA, which varies according to size of the fragment to be analysed and the intensity of the excised band; and ddH2O to make up a final 20µl volume. Sequencing reaction was performed on a Veriti® Thermal Cycler (Applied Biosystems) using the conditions described in the Appendix D. The products obtained by the sequencing reaction were stored at 4°C for a maximum of 24 hours until DNA precipitation and purification.

3.5.3 DNA precipitation and purification

After sequencing reaction, the method used for DNA precipitation and purification is based on a salting out reaction recommended for the BigDye™ Terminator kit v1.1 Cycle Sequencing Kit (Applied Biosystems). This process aims to obtain a purified DNA pellet free of contaminants that could interfere with capillary electrophoresis and comprises the use of three reagents: absolute ethanol, sodium acetate and EDTA (Ethylenediaminetetraacetic acid). Absolute ethanol and sodium acetate promote DNA precipitation by neutralizing nucleic acids charges and reducing their solubility. EDTA is a chelator of magnesium ions, therefore inhibiting the enzyme used in the sequencing reaction. Ethanol 70% (v/v) was used to wash the DNA pellet, which was dried at 37°C. DNA pellet was stored at 4°C until capillary electrophoresis was performed. The detailed protocol and solutions used in this procedure are described in Appendix F.

3.5.4 Capillary electrophoresis

After precipitation and purification of the sequencing reaction, DNA pellets were resuspended in 17µL of HI-DI formamide (Applied Biosystems), used as a capillary injection solvent. Samples were then homogenized in a vortex and the total volume was transferred to a 96-well plate (Platemax, Axygen) suitable for the automatic sequencer. The plate was sealed and placed in thermocycler at 95°C for 5

minutes, in order to denature all samples and then incubated on ice for 1-2 minutes, followed by a centrifugation of 2 minutes at 1200 rpm, allowing sample deposition and removal of possible air bubbles. The seal was then removed and the sample plate was placed on a ABI Prism™ 3130 Genetic Analyzer (Applied Biosystems) sequencing instrument, where the capillary electrophoresis was run at 50°C and 15 kV.

3.5.5 Result analysis

Capillary electrophoresis results were obtained in the form of an electrophoretogram generated by the Sequencing Analysis software 3.4.1 (Applied Biosystems). The sequence was manually compared to the reference sequence of the target gene, withdrawal from of the Ensembl database (Built GRCh38).

3.6 cDNA synthesis by reverse transcription

Reverse transcription (RT) reaction is used to synthetize DNA from a single-stranded RNA template, obtaining cDNA. This process follows the principle that reverse transcriptase enzymes can direct the synthesis of a strand of cDNA using an RNA template and a short primer complementary to the 3' end of the RNA. The first cDNA strand can then be used as template for a PCR.

cDNA synthesis is achieved in a two-step reaction, with two different reaction mixtures. The first mixture contained a variable volume of RNA, containing 1µg of RNA, whenever possible, or the maximal amount within a maximum of 7.25µL, 0.5µL of random hexamer primer solution (3 µg/µL, Roche), which consists in a mixture of oligonucleotides that will recognize and bind the 3' end (poli-A tail) of a variety of single-stranded RNA templates in the sample, and diethylpyrocarbonate-treated (DEPC-treated) (MERK) ddH_2O, used in order to inactivate possible RNase in the sample, for a final volume of 7.75µL. This first reaction was incubated at 70ºC for 10min in a T3 Thermocycler (Biometra®) and further subjected to a second reaction mixture containing 4µL of First Strand Buffer 5x (Invitrogen); 4µL of dNTPs (200 Mm, Illustra™ GE Healthcare); 2µL of dithiothreitol (DTT) (0.1M, Invitrogen), an enzymatic stabilizer; 0.75µL of RnaseOut™ Recombinant Ribonuclease Inhibitor (40 U/µL, Invitrogen), an RNase inactivator; 1µL of Superscript® II Reverse Transcriptase (200 U/µL, Invitrogen), and 0.5µL of DEPC-treated ddH2O (MERK) to make up the final volume of 12.25µL, which added to the first reaction make the final volume of 20µL. The samples are then placed in the same thermocycler to continue and finish the synthesis reaction (Appendix E). cDNA samples were then stored at -20ºC until further use.

3.7 Quantitative polymerase chain reaction

The quantitative polymerase chain reaction (qPCR), is a molecular biology technique based on the conventional PCR, used to detect and quantify nucleic acids in a sample in real-time. This technique has numerous applications, yet, is commonly combined with RT (described in section 3.6) – RT-qPCR, with the purpose of quantifying gene expression.

This technique allows the accumulation of amplified product to be directly detected and measured along the reaction progress, in real-time, making possible the accurate quantification of the product after each cycle. This real-time procedure is made possible by adding to the reaction fluorescent molecules

that are incorporated in the new DNA double strands during the PCR and emit a fluorescent signal, proportional to the amount of DNA at each moment. DNA binding dyes (e.g. SYBR® Green) and fluorescently labelled sequence specific primers or probes (e.g. TaqMan® probe) are the fluorescent molecules most commonly used in qPCR. Regarding this, qPCR is performed in specialized thermal cyclers equipped with fluorescence detectors.

By plotting the fluorescent signal against the number of cycles, the instrument generates an amplification curve in real time (Figure 3.1), representing the accumulation of product over the duration of the PCR reaction. This amplification curve typically presents three different phases: initiation phase, exponential phase and a plateau phase. During the PCR reaction, besides the emitted florescence, there is also background fluorescence which is defined as a baseline and needs to be overcome in order to obtain meaningful information from the signal. The point at which the amount of fluorescent signal overcomes the baseline and is therefore distinguishable from the background, defines the threshold level. Regarding this, the first stage of the amplification curve, the initiation phase, occurs during the first PCR cycles, where the emitted fluorescence cannot be distinguished from the baseline. The exponential phase starts as soon as the emitted signal can be distinguished from the background and is represented by the exponential increase in fluorescence until the reagents are exhausted and the reaction enters plateau phase, where no increase in fluorescence is observed.

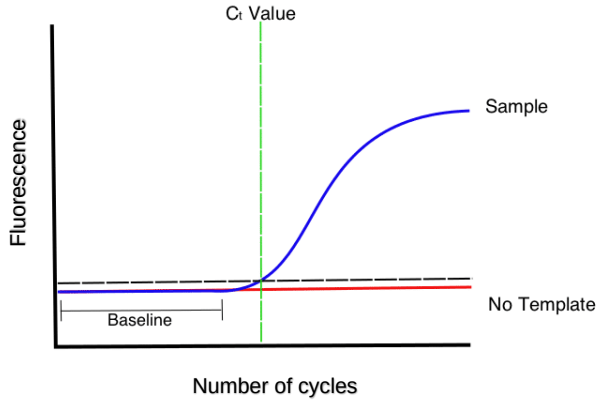

Figure 3.1 – Graphic representation of a qPCR amplification plot (Adapted from: Porterfield, Andrew; "What is a C_t value?", available at: *https://bitesizebio.com/24581/what-is-a-ct-value/*; visited on April 24th 2018).

During exponential phase, the cycle number at which the fluorescence signal reaches the threshold level, is called the threshold cycle (C_t) and can be used to calculate the amount of template present in the original sample. These values can vary, depending on the defined baseline and the amount of template present at the start of the reaction, meaning that the higher amount of initial template, the few amplification cycles are required to produce enough product to emit fluorescent signal, therefore resulting in lower C_t value. Thus, the obtained C_t values are inversely related to the initial amount of target in the reaction.

Quantification of gene expression by qPCR can be achieved either by absolute or relative quantification. The first method is based on a standard curve, prepared from samples of known template concentration, therefore the absolute number of copies on any unknown sample can be determined by

interpolation of its C_t into this standard curve. On the other hand, the relative quantification determines fold changes in expression, by comparing the levels in gene expression between a test sample and a control sample (e.g. drug-treated vs untreated), using a reference gene for normalization – the $\Delta\Delta C_t$ method. Here, the calibration curve result for the gene of interest in each sample is normalized to that of a reference gene, according to equation 3:

$$\Delta Ct = Ct_{(target\ gene)} - Ct_{(reference\ gene)}$$

Equation 3

The normalized values are then compared between samples to obtain the expression ratio in both test and control samples and thus, determine the fold change in expression, applying the following equations (Equation 4 and 5):

$$\Delta\Delta Ct = \Delta Ct_{(test)} - \Delta Ct_{(control)}$$

Equation 4

$$2^{-\Delta\Delta Ct} = Normalized\ expression\ ratio$$

Equation 5

The reference gene must be expressed in constant levels across all the samples and this expression must not be affected by experimental conditions (e.g. GAPDH (glyceraldehyde-3- phosphate dehydrogenase), β-actin, etc.).

3.7.1 Optimization of qPCR conditions and qPCR reaction

The calculations applied on the $\Delta\Delta C_t$ method assume that both reference and target genes are amplified with efficiencies around 100%. For this reason, as for any qPCR assay, it is crucial to determine the amplification efficiency of reference and target genes before using the method.

To assess the amplification efficiencies for each gene, serial dilutions of a reference cDNA sample were performed, for final concentrations of 20, 10, 5, 2.5 and 1.25ng/µL. The reactions were performed in duplicate using 96 well plates (Axygen™ 96-well PCR Microplates), for a final volume of 15µL, containing: 4µL or 3.5µL of ddH2O, for Power SYBR® Green PCR Master Mix (Applied Biosystems) or KAPA SYBR® FAST qPCR Kit Master Mix Universal (KapaBiosystems), respectively; 0.75µL of each primer (forward and reverse) either at 3.5, 5 or 7.5 pmol/µL – to access optimal primer concentration; 7.5µL of either Power SYBR® Green PCR Master Mix (Applied Biosystems) or KAPA SYBR® FAST qPCR Kit Master Mix Universal (KapaBiosystems) – to assess the most suitable master mix; and 2µL of cDNA (from the serial dilutions), except for negative control where the cDNA volume was replaced by ddH2O, using the ABI PRISM 7900HT Sequence Detection System (Applied Biosystems) and SDS 2.4 software (Applied Biosystems), for further result analysis.

A standard curve was then created by plotting the starting template concentration (20, 10, 5, 2.5 and 1.25ng/µL) against the average of the two C_t values obtained during the amplification of each

dilution. This curve allowed the withdrawal of an equation from the linear regression line and the determination of amplification efficiency after application of equation 6.

$$Efficiency\ (E) = 10^{-1/m}$$

Equation 6

After optimization, qPCR reactions were performed to a final volume of 15µL, as described above, in triplicates, using each primer pair and cDNA at the optimized concentration.

The C_t values acquired by the software were imported into an Excel spreadsheet and the relative expression analysis was performed according to the $2^{-\Delta\Delta Ct}$ method (described in section 3.7). Statistical analysis was performed using GraphPad Prism software (version 7.03), using the mean and standard deviation (SD) of the triplicates of each experiment.

3.8 Cell culture and maintenance

Both, HT-29 and LS174T cell lines, were cultured in 25 and 75 cm^2 (T-25 and T-75 t-flasks, respectively) cell culture flasks (Sarstedt and VWR) in Dulbecco's Modified Eagle Medium 1x (DMEM; Gibco), supplemented with 10% (v/v) of heat-inactivated fetal bovine serum (FBS; Merk), 1% (v/v) penicillin and streptomycin 100x (PenStrep; Gibco) and 1% (v/v) L-glutamine 200mM (Gibco). The culture flasks were maintained in controlled humidified atmosphere at 37ºC and 5% (v/v) CO_2 in a CO_2 air-jacketed incubator (NUAIRE™). Cells were monitored every other day using an Olympus CK2 inverted microscope.

3.8.1 Cell subcultivation

Cell subcultivation was performed at least twice a week, using the same trypsinization method for both cell lines, in the adequate ratios, depending on culture T-flask (T-25 or T-75) and cell based assays planning. After discarding the medium, cells were washed with pre-warmed Dulbecco's Phosphate Buffered Saline 1x (DPBS; Lonza), followed by incubation with 0,1% (v/v) Trypsin (Gibco) in DPBS, at 37°C for 5 to 7 minutes. Trypsin inactivation was achieved by adding complete medium, and the sub-cultivation in the appropriate ratio was accomplished by adding medium to the suitable cell suspension volume in the flask. All the volumes used for cell splitting are summarized in table 3.1. The remaining cell suspension was either discarded or kept in a falcon tube, for lysate collection, cryopreservation or direct use in cell-based assays.

Table 3.1 – Cell subcultivation - ratios and volumes

T-FLASK	SUBCULTIVATION RATIO (v/v)	DPBS WASH (mL)	0,1% TRYPSIN (mL)	MEDIUM (INACTIVATION) (mL)	CELL SUSPENSION (mL)	MEDIUM (mL)	FINAL VOLUME (mL)
T-25	1 : 5 1 : 3,5	3	1	4	1 1,5	4 3,5	5
T-75	1 : 6,5 1 : 5 1 : 4	5	3	7	1,5 2 2,5	8,5 8 7,5	10

3.8.2 Cell cryopreservation and thawing

The process of cell cryopreservation was achieved using the remaining cell suspension from the cell sub-cultivation process (described in section 3.9.1). In this method, the collected cell suspension was centrifuged at 125g for 8min. After discarding the supernatant, the pellet of cells was resuspended in a solution containing 90% (v/v) FBS (Merk), important to avoid starvation of nutrients upon thawing, and 10% (v/v) DMSO (Sigma), which prevents formation of ice crystals ant therefore prevents cell lysis during thawing. This suspension of cells was then placed in cryovials (1ml/cryovial ABDOS). Cryovials were stored at -80°C for 24h and then in liquid nitrogen until further use.

Thawing process was carried out at 37°C, in a water-bath. The cell suspension in the cryovial was then placed in a 15mL falcon tube (Sarstedt) containing 9mL of complete medium and centrifuged at 125g for 8min. After discarding the supernatant, in order to remove as much DMSO containing medium as possible, the pellet of cells was resuspended in 1mL of complete medium and placed in a T25 flask containing 4mL of complete medium (previously placed in controlled humidified atmosphere at 37ºC and 5% (v/v) CO_2).

Cell culture flasks were kept in culture, as further described in section 3.9.

3.8.3 Cell counting

Cell counting was crucial to achieve the appropriate cell density in each cell-based assay. The method used to determine the number of viable cells present in the cell suspension was the trypan blue exclusion assay, based on the principle that viable cells have intact cell membranes and therefore exclude certain dyes, such as trypan blue, while dead cells do not. Moreover, the cell counting was performed using the Neubauer-Improved chamber.

Cell suspensions were properly diluted in trypan blue (Gibco) and loaded into both chambers of the hemocytometer. The counting was performed in the 4 quadrants of each chamber and the cell density was determined by equation 7:

$$Cell\ density\ (cells/mL) = \frac{\sum Cells\ per\ quadrant}{8} \times Dilution\ factor \times 10^4$$

Equation 7

3.9 Cell-based assays

In this study, all the cell-based assays were performed regarding the effect of cytotoxic, DNA methyltransferase and histone deacetylase (HDAC) inhibitors specific signaling pathway modulators and nutraceutical compounds, at different levels, in HT-29 and LS174T CRC cell lines. Cytostatic and nutraceutical compounds were kindly provided by the pharmacy service of IPOLFG, E.P.E. and the Nutraceuticals & Controlled Delivery Laboratory - iBET, respectively. All the compounds herein used are described in table 3.2.

Table 3.2 – Therapeutic compounds used in this study and respective specifications.

	Compound	Stock [ ] (mM)	Solvent	Mechanism of action
Cytostatic	5-Fluorouracil (Teva)	50 mM	H_2O	Thymidylate synthase (TS) inhibitor (Longley *et al.*, 2003)
	Oxaliplatin (Fresenius Kabi)	12,5 mM	H_2O	inhibition of DNA synthesis (Gherman *et al.*, 2012)
	Irinotecan (HIKMA)	34 mM	H_2O	Topoisomerase I inhibitor (Cunningham *et al.*, 2001)
DNA methyltransferase and HDAC inhibitors	Azacitidine (Sigma)	5mM	H_2O + DMSO	DNA methyltransferase inhibitor (Gang *et al.*, 2014)
	Vorinostat	6mM	DMSO	Histone deacetylases (HDAC) inhibitor (Richon, 2006)
Specific signaling pathway modulators	GANT61 (Selleckchem)	5mM	ETOH	Gli transcription factor inhibitor (Mazumdar *et al.*, 2011c)
	Capmatinib (Selleckchem)	2,5 mM	DMSO	c-Met inhibitor (Liu *et al.*, 2011)
Nutraceuticals	SFN (LKT laboratories)	10 mM	DMSO	Antiproliferative, antiangiogenic, and antimetastatic (Tafakh *et al.*, 2018)
	Scutellarein tetramethylether (Extrasynthese)	29,21 mM	DMSO	Anti-inflammatory, ant-oxidative, anxiolytic, antiviral and anti-cancer activity (Ma, 2005; Parajuli *et al.*, 2009; Kim *et al.*, 2012)
	Tangeretin (Extrasynthese)	8 mM	DMSO	Anti-inflammatory, anti-proliferative, and anti-carcinogenic (Lin *et al.*, 2003; Chen *et al.*, 2007; Ting *et al.*, 2015)

3.9.1 Viability assay

The antiproliferative effect of cytotoxic, DNA methyltransferase and HDAC inhibitors, specific signaling pathway modulators and nutraceutical compounds was assessed in HT-29 and LS174T cell lines, using the same method for both. All the compounds used in this assay, and respective experimental conditions, are listed in table 3.3. Cells were seeded in 96-well plates in a density of $1x10^4$ cells/well ($1x10^5$ cells/mL). At 24h post-seeding, medium was discarded and cells were incubated with the appropriate compounds, diluted in complete medium for a maximum concentration, which was the starting point of eight serial dilutions in a 1:2 proportion (Table 3.3). For testing combination of compounds, the dilutions were performed to five, instead of eight, serial concentrations and were added the volume of either irinotecan or GANT61 in order to obtain a final concentration of 50µM and 15µM of these compounds, respectively (Table 3.4). Two controls were obtained by incubating cells with complete medium and with solvent or combination of solvents, diluted in complete medium in a percentage (v/v) corresponding to that in the maximum concentration used for each compound (Tables 3.3 and 3.4). At 24h post-treatment, cells were washed with 100µL DPBS and incubated with 100µL WST-1 reagent (Roche) diluted in a proportion of 1:20 in culture medium, for 3h at 37ºC, 5% CO_2. In this step, three empty wells were used as reagent control, allowing the subtraction of background absorbances for each individual plate reading.

The WST-1 colorimetric assay is based in the bioreduction of tetrazolium salt into a soluble formazan by a cellular mechanism dependent on the glycolytic production of NAD(P)H in viable cells. Hence, the amount of formazan dye formed is directly correlated to the number of metabolically active cells in the culture.

Table 3.3 – Isolated compounds and conditions used in viability assay.

	Compound	Stock [ ]	Max. [ ] – Min. [ ] in assay	Solvent [ ] (% $_{(v/v)}$)
Cytostatic	5-Fluorouracil	50 mM	800µM – 6.25µM	1.6% H_2O
	Oxaliplatin	12.5 mM	800µM – 6.25µM	6.53% H_2O
	Irinotecan	34 mM	800µM – 6.25µM	2.35% H_2O
DNA methyltransferase and HDAC inhibitors	Azacitidine	5mM	200µM – 1.6µM	3.7% H_2O
				0.3% DMSO
	Vorinostat	6mM	50µM – 0.4µM	0,83% DMSO
Specific signaling pathway modulators	GANT61	5mM	200µM – 1.6µM	4% ETOH
	Capmatinib	2,5 mM	25µM – 0.2µM	1% DMSO
Nutraceuticals	SFN	10mM	100µM – 0.8µM	1% DMSO
	Scutellarein tetramethylether	21.29mM	50µM – 0.4µM	0.2% DMSO
	Tangeretin	8mM	25µM – 0.15µM	0.6% DMSO

Table 3.4 –Combinations of compounds and conditions used in viability assay.

Category	Compound	Stock [ ]	[ ] used in the assay	Solvent [ ] (% $_{(v/v)}$)
Cytostatic	Irinotecan	34 mM	50µM	2.35% H_2O
Specific signaling pathway modulator	GANT61	5mM	15µM	4% ETOH
Nutraceuticals	Sulforaphane (SFN)	10mM	25µM	1% DMSO
	Tangeretin	8mM	25µM	0.6% DMSO
Cytostatic + Cytostatic	Irinotecan + Oxaliplatin *	34 / 12,5 mM	50µM + 100µM	2.35% H_2O + 6.53% H_2O
Cytostatic + Nutraceuticals	Irinotecan + Sulforaphane	34 / 10 mM	50µM + 25 µM	2.35% H_2O + 1% DMSO
	Irinotecan + Tangeretin	34 / 8 mM	50µM + 25µM	2.35% H_2O + 0.6% DMSO
Specific signaling pathway modulator + Cytostatic	GANT61 + Oxaliplatin	5 / 12,5 mM	15µM + 100µM	4% ETOH +
Specific signaling pathway modulator + Nutraceuticals	Gant61 + Sulforaphane	5 / 10 mM	15µM + 25µM	4% ETOH + 0.6% DMSO

Considering this, cell viability was assessed by absorbance reading, at 450 and 750nm, using an iMark microplate absorbance reader (BioRad), and the background absorbances are subtracted, following equation 8:

$$Sample\ absorbace = \ absorbance\ at\ 450\ nm - Absorbance\ at\ 750\ nm$$

Equation 8

The percentage of viable cells in each test sample (treated cells) was assessed relatively to the control samples (non-treated cells), through the application of equation 9 (after subtracting to all readings the average of the background absorbance of the control of WST-1 diluted in medium):

$$\text{Cell viability (\%)} = \frac{Absorbance_{(test\ sample)}}{Absorbance_{(control\ samples)}} \times 100$$

Equation 9

The concentration required to reduce cell viability in 50% (IC_{50} value) for each compound or combination of compounds, was obtained using GraphPad Prism 6 software (GraphPad Software, Inc., La Jolla, CA). All the experiments were performed in triplicates, in at least 2 independent experiments.

3.9.2 Migration assay – Wound healing

The effect of cytotoxic, DNA methyltransferase and HDAC inhibitors signaling pathway modulators and nutraceutical compounds in migration ability of HT-29 cells was measured through wound-healing assay. The compounds used in this assay are listed in table 3.4. Cells were seeded in 12 well plates in a density of $2x10^5$ cells/well and grown to 90-95% confluence. After reaching the desired confluence, the growth medium was replaced by starvation medium (DMEM supplemented with 0,5% FBS, 1% penicillin and streptomycin and 1% (v/v) L-glutamine 200mM) and left at 37ºC, 5% (v/v) CO_2 for 24h. A 100µl sterile tip was then used to create an open gap across the cell monolayer in each well. Following the scratch, cells were washed twice with DPBS 1x and incubated with the desired compounds, diluted in starvation medium in, at least, two different concentrations (Table 3.4). As controls, cells were either incubated with starvation media or with the solvent of each compound, diluted in starvation medium at a percentage (v/v) corresponding to that of the maximum concentration used for each compound (Table 3.4). Wound closure was monitored at 0h, after scratch and treatment, and at 24 and 48h after a wash with DPBS and addition of starvation medium, using an inverted microscope (Olympus IX53). Regarding the compound GANT61, the monitoring was performed at 0, 24, 48 and 72h. At least two images, at two different positions, were obtained for each well during monitoring at all the time points. The determination of wound areas, at each time point, was assessed ImageJ software and the MRI wound healing tool plugin (Baecker, 2012). The percentage of wound closure for each time point (24, 48, 72h) was assessed by comparison to the area of the original wound (0h) The percentage of migration was hence determined through the application of equation 10:

$$\%\ of\ migration = [1 - \left(\frac{Wound\ area_{(time\ point)}}{Wound\ area_{0h}} \right)] \times 100$$

Equation 10

Wound healing assay was performed in triplicates, in at least two independent experiments. In a monolayer model, LS174T cells grow as tightly packed islands of cells, causing the detachment of a considerable number of cells upon scratch, making wound healing assay unfeasible to perform in this cell line.

Table 3.5 – Compounds and conditions used in the migration assay.

Category	Compound	Stock [ ]	[ ] range used in assay	Maximum Solvent [ ] (% (v/v))
Cytotoxic	5-FU	50 mM	25µM ; 50µM	0.1% H_2O
	Irinotecan	34 mM	25µM ; 50µM	0.1% H_2O
DNA methyltransferase and HDAC inhibitors	Azacitidine	5mM	10 µM ; 25µM ; 40µM	0.7% H_2O
				0.06% DMSO
Specific signaling pathway modulators	GANT61	5mM	10µM – 15µM	0.3% ETOH
Nutraceuticals	SFN	10 mM	7,5µM ; 10µM ;15µM	0.2% DMSO

3.9.3 Gene expression assay using 2D and 3D cell models

The effect of cytotoxic, specific signaling pathway modulators and nutraceutical compounds in the expression of specific cancer markers in 2D (Monolayer) and 3D (Aggregate) cell models, was assessed by RT-q-PCR, as described in section 3.7. This assay was performed regarding the expression analysis of markers (listed on Table 3.6) of cell cycle/proliferation, EMT, cancer stemness and specific players of Wnt and Shh signaling pathways. Cells were seeded in 24 well plates, at a density of $1x10^5$ cells/well ($2x10^5$ cells/mL) in 2D cell models. For 3D cell model, HT-29 cells were seeded under the same conditions, however, each well in the plate was previously coated with 300µL of an agarose solution, 0,6% (w/v) in H_2O, allowing to maintain cells in suspension and promote the formation of cellular aggregates. After 24h, (2D model) or 48h (3D model), either isolated or combined compounds were added to each well, at defined concentration to test (table 3.7 and 3.8). As control, cells were treated with the maximal solvent concentration for each isolated or combined compound in test. The treatment was prepared in a 6x more concentrated solution since the volume was added to the medium already in the well. Thus, 100µL were carefully added to each well in a drop-by-drop method, to a final volume of 600µL/well. At 24h post-treatment, cells (2 wells) and aggregates (3 wells) were collected, using 600µL of RLT buffer (Qiagen), containing 1% β-mercaptoethanol (Sigma) and stored at -80ºC until RNA isolation. Treatments and conditions are listed in table 3.6. RNA isolation and RT-qPCR analysis were performed under the conditions previously described in sections 3.2.2 and 3.6/3.7, respectively.

Table 3.6 – Tumorigenesis and metastasizing process markers used for expression analysis on HT-29 monolayer and aggregate cell models.

Category	Gene	Protein
Cell cycle/ Proliferation	*CDKN1A*	P21
	CCNA2	Cyclin-A2
EMT	*SNAI1*	Snail
	VIM	Vimentin
	CDH1	E-cadherin
	ZEB1	Zeb1
Stemness	*LGR5*	LGR5
	PROM1	CD133
	CD44	CD44
	EPCAM	EpCAM
Wnt signaling pathway	*TCF7L2*	TCF7L2
	TCF7L2 [1-6]	TCF7L2[1-6]
	CTNNB1	β-catenin
	AXIN2	Axin-2
	ABCB1	ABCB1
	MMP7	MMP7
Shh signaling pathway	*GLI1*	Gli1
	VAX2	Vax2
	TGFB1	TGFβ1
	PTCH1	PTCH1
Endogenous control	*GAPDH*	GAPDH
	ACTB	β-actin

Table 3-7 – Characteristics of treatments used in the expression analysis of tumorigenesis and metastasizing process markers on HT-29 monolayer and aggregate cell models. *Tested only in 2D cell model.

Category	Compound	Stock [ ]	[ ] used in the assay	Solvent [ ] (% $_{(v/v)}$)
Cytotoxic	Irinotecan	34 mM	50µM	2.35% H_2O
Specific signaling pathway modulator	GANT61	5mM	15µM	4% ETOH
Nutraceuticals	Sulforaphane (SFN)	10mM	25µM	1% DMSO
	Tangeretin	8mM	25µM	0.6% DMSO
Cytotoxic + Cytotoxic	Irinotecan + Oxaliplatin *	34 / 12,5 mM	50µM + 100µM	2.35% H_2O + 6.53% H_2O
Cytotoxic + Nutraceuticals	Irinotecan + SFN	34 / 10 mM	50µM + 25 µM	2.35% H_2O + 1% DMSO
	Irinotecan + Tangeretin	34 / 8 mM	50µM + 25µM	2.35% H_2O + 0.6% DMSO
Specific signaling pathway modulator + Cytotoxic	GANT61 + Oxaliplatin	5 / 12,5 mM	15µM + 100µM	4% ETOH +
Specific signaling pathway modulator + Nutraceuticals	GANT61 + SFN	5 / 10 mM	15µM + 25µM	4% ETOH + 0.6% DMSO

3.10 Statistical analysis

Statistical analysis concerning cell-based assays was performed using GraphPad Prism 6 software (GraphPad Software, Inc., La Jolla, CA). Comparisons between samples were made by One-way ANOVA analysis, whereas comparisons with more than two variables were performed by a Two-way ANOVA analysis. Values of $p<0.05$ were considered as statistically significant.

3.11 Identification of *TCF7L2* isoforms in 38 CRC patient samples and CRC cell lines

Different transcripts from two different fragments of *TCF7L2* (fragments 1-5 and 12-17) were identified during this study. RNA samples were obtained from patient peripheral blood samples and cell lysates, as described in sections 3.2.1 and 3.2.2, respectively. cDNA was then synthetized, as described in section 3.6 and used as template for PCR reaction (described in section 3.3.3). PCR products were then analysed by electrophoresis, under the conditions described in section 3.4 and subject to Sanger sequencing under the conditions described in section 3.5 and respective subsections.

3.12 Selection and analysis of promising compounds for treatment of the HT-29 CRC cell line

HT-29 and LS174T cells viability was assed, as described in section 3.9.1, after exposure to a panel of ten compounds, listed on table 3.3. Five of the initial compounds, listed on table 3.4, were selected for treating HT-29 cells and perform a migration assay, as detailed in section 3.9.2. In light of the obtained results, expression assays were performed on HT-29-treated cells, as described in section 3.11. Selected combinations of compounds were subject to viability assay, in order to define specific promising low dose combinations, as described in section 3.9.1. Expression of markers implicated in CRC tumorigenesis and metastasizing process was assessed in HT-29 2D and 3D cell models, according to section 3.9.3.

4.1 Expression analysis of *TCF7L2* isoforms

In order to study the variation of the expression of *TCF7L2* isoforms in CRC patients and tumors and evaluate a possible contribution for increased CRC risk and malignancy, the expression of *TCF7L2* alternative transcripts was evaluated in a cohort of 38 CRC patients with features associated to increased CRC risk and/or familial history of CRC, 6 CRC representative cell lines (HT29, LS174T, SW48, SW480, SW620, LoVo and HCT116) and a normal colon representative cell line (CCD 841 CoN). Aiming to analyse the expression of transcripts originating from two different *TCF7L2* described splicing regions (exon 4 and exons 13 to 17), we used cDNA isolated from total RNA from all samples to amplify two specific fragments of this gene: the first from exon 1 to exon 5 (1-5) with an expected total size of 458bp; the second from exon 12 to exon 17 (12-17) with an expected size of 751bp.

After PCR amplification of the fragment [1-5] of *TCF7L2,* all patient leukocytes and CRC cell line samples revealed the expression of three different fragments, with the exception of HT-29 that presented additional fragments, (Figure 4.1a and b). After Sanger sequencing analysis, two of the three common fragments were successfully identified as corresponding to the wild type (wt) isoform and to the isoform lacking the entire exon 4 (Δ-exon4) (Figure 4.2a)).

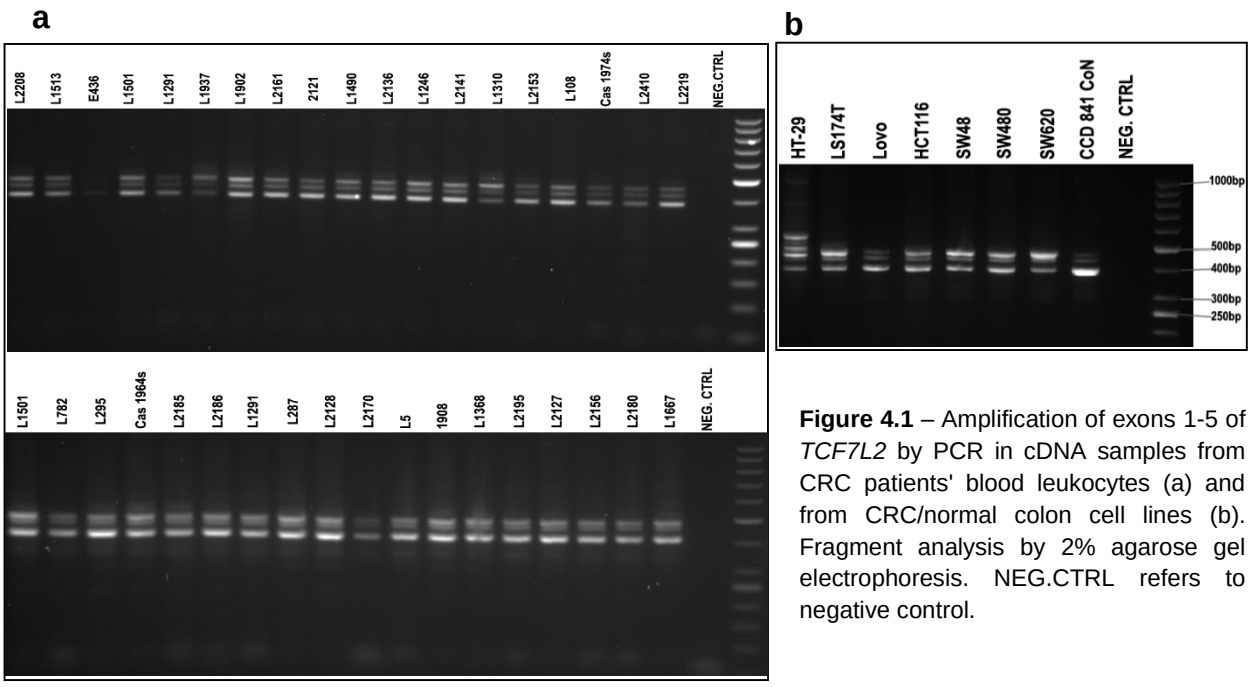

Figure 4.1 – Amplification of exons 1-5 of *TCF7L2* by PCR in cDNA samples from CRC patients' blood leukocytes (a) and from CRC/normal colon cell lines (b). Fragment analysis by 2% agarose gel electrophoresis. NEG.CTRL refers to negative control.

Unfortunately, we were not able to identify the third band (from now on referred as x-isoform) by sanger sequencing, however, we were interested in the fact that this X-isoform and the wt isoform appear to exhibit differential expression among patients and among cell lines. For instance, Ls174t, HCT116, Sw48, Sw480 and Sw620 cell lines seem to have increased expression of the wt isoform compared to the x-isoform while HT-29 cell line appears to have higher x-isoform expression than wt, and lastly, Lovo and CCD841CoN cell lines appear to express equal amounts of both isoforms. This fact may suggest that the increased expression of one isoform or the other can be related to the type of

tumor. However, these band pattern allows a qualitative comparison of the expression. A more precise quantification by qPCR of these isoforms among patients, and the identification of x-isoform would be crucial to analyse a possible correlation between *TCF7L2* isoforms and different types of tumors. Previous studies have found significant correlation between different TCF4 isoforms with divergent properties and different malignant phenotypes (Shiina *et al.*, 2003; Tomimaru *et al.*, 2013). For instance, loss of exon 4 in *TCF7L2* isoforms was previously associated to increased tumorigenicity in hepatocellular carcinoma, having influence on these cells phenotype by functioning as transcription activators or repressors (Tsedensodnom *et al.*, 2011).

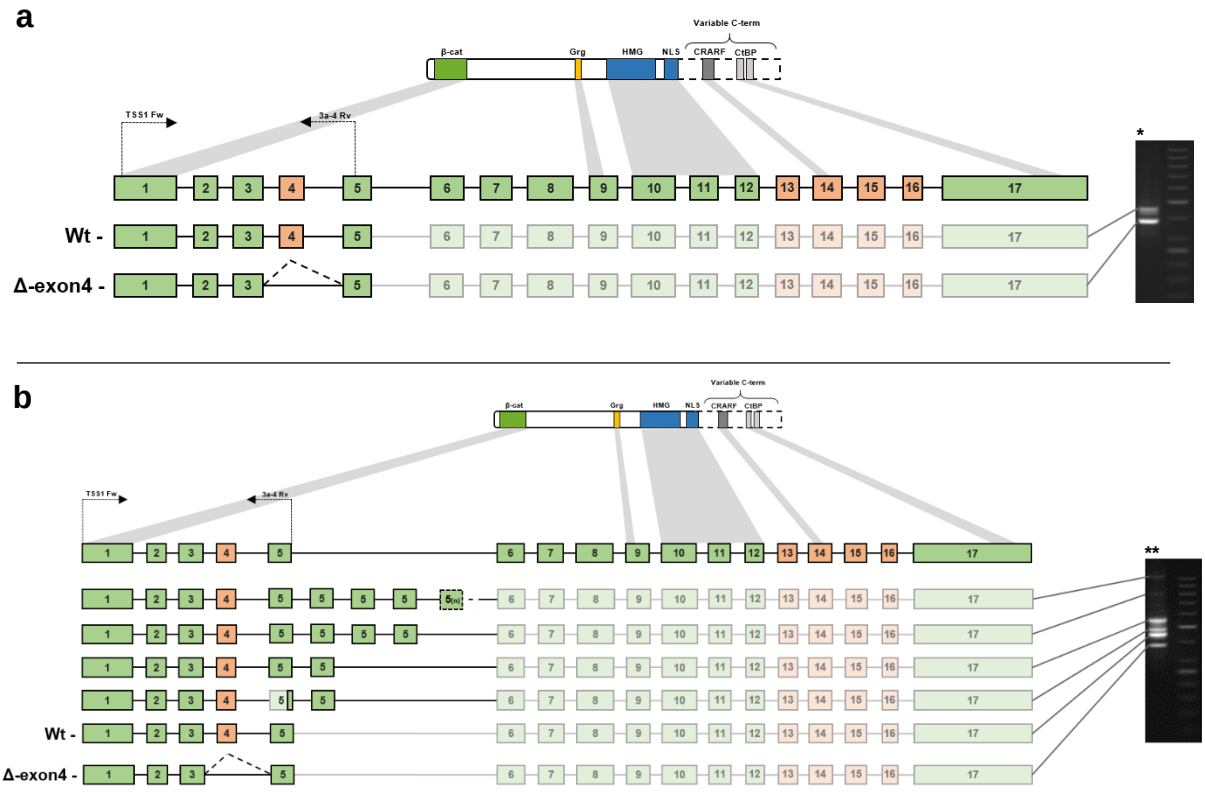

Figure 4.2 – Schematic representation of *TC7L2* isoforms identified after Sanger sequencing of the DNA extracted from the agarose gel bands obtained following the amplification of exons 1-5 of *TCF7L2* gene, using cDNA from CRC patients' blood leukocytes (a) and from the HT-29 CRC cell line (b). Black arrows represent the primers used in the PCR amplification, as well as their location in the *TCF7L2* gene. Green represents known exons; orange represents alternative exons. * Representative amplification pattern of exons1-5 of *TCF7L2* gene using cDNA from a CRC patient (2121); ** Representative amplification pattern of exons 1-5 of *TCF7L2* gene using cDNA from HT-29 CRC cell line.

Previous work in the Gastroenterology group revealed that, in addition to the above mentioned isoforms, HT-29 cell line revealed expression of 4 different isoforms (Figure 4.1b). Sanger sequencing analysis performed in the present project revealed their correspondence to four isoforms containing either partial or full length repetitions of exon 5: one comprising a portion of 33bp of exon 5, immediately after exon 4, followed by a full length exon 5; two isoforms containing 2 and 4 repetitions of exon 5, respectively; finally, an isoform comprising an undetermined number of repetitions of exon 5, for which the exact number of repetitions could not be confirmed by sequencing, however, its ≈1kb size suggests that this isoform comprises around 10 repetitions of exon 5 (Figure 4.2 b). The expression pattern of

TCF7L2 isoforms on HT-29 CRC cell line, in particular the duplication of exon 5, suggests the presence of specific DNA or RNA alterations in the vicinity of exon 5 or eventually the duplication of exon 5 at the DNA level. Moreover, the repetition of this "duplication" led us to hypothesise the existence of circular RNA expression associated to these *TCF7L2* exons in this cell line. Other studies in the group have confirmed this hypothesis using two different approaches: 1) digesting RNA with RNase R (circular RNA is not digested); 2) amplification of the fragment using specific circular RNA primers. Thus, this pilot analysis points out the relevance of further investigation regarding this fragment, not only for the differential expression among samples and cell lines, but also for the presence of additional isoforms expressed on HT-29 cell line.

Amplification of fragment 12-17 of *TCF7L2* revealed the expression of a variable number of isoforms (Figure 4.3 a-b). Sanger sequencing allowed the identification of five different isoforms, common among patient samples. These are represented in figure 4.4 and include an isoform containing exons 11,12 and 17, with approximately 181bp; a second isoform containing exons 11,12,15 and 17, with approximately 254bp; an isoform containing exons 11, 12, 13 and 17 with approximately 232bp; finally, two distinct isoforms with the same approximate size of 305bp, containing exons 11,12,13,14/15 and 17. The latter two isoforms were shown, after Sanger sequencing, to differ by the expression of either exon 14 or exon 15, which have the exact same size (73bp), leading to a single band in the agarose gel. These isoforms appear to be differentially expressed among blood leukocyte samples and especially regarding representative cell lines, which appear to express a reduced panel of these isoforms. For instance, none of the CRC cell lines seems to express the [11-12-13-17] isoform, which is expressed in the normal colon cell line and in blood leukocytes. The inclusion of exon 13 may be relevant considering it results in the expression of E and M isoforms and, its known that the expression of different types of isoforms (E, M and S) are associated to different phenotypes (Weise *et al.*, 2009). Therefore, the differential expression of these isoforms should be explored in future studies in order to understand their role in CRC risk and eventually tumor progression

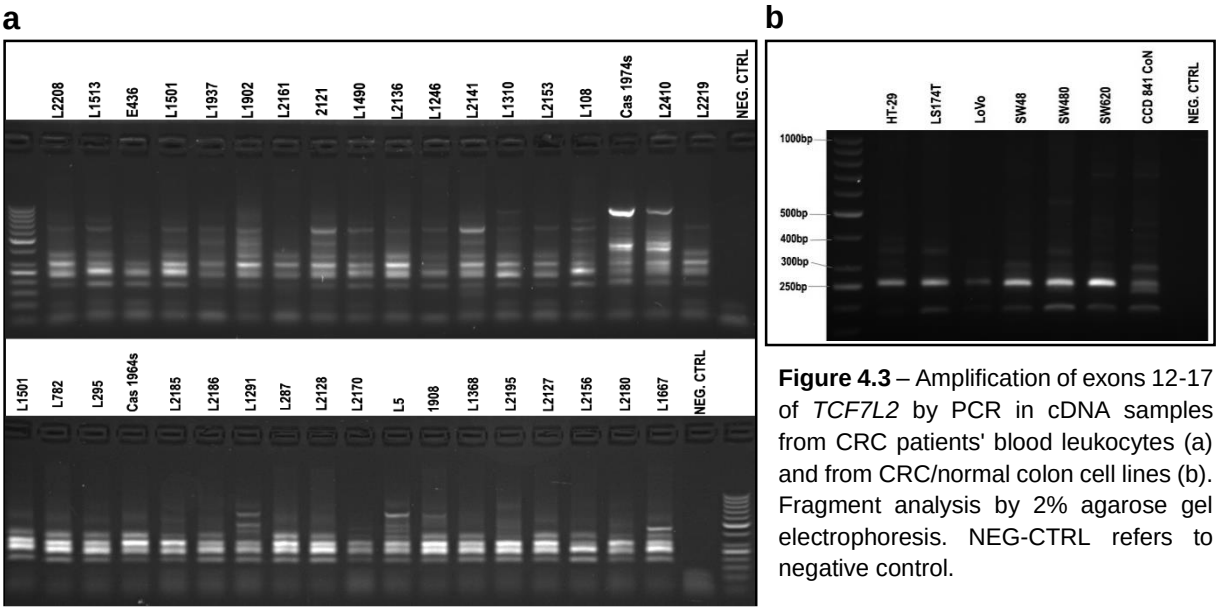

Figure 4.3 – Amplification of exons 12-17 of *TCF7L2* by PCR in cDNA samples from CRC patients' blood leukocytes (a) and from CRC/normal colon cell lines (b). Fragment analysis by 2% agarose gel electrophoresis. NEG-CTRL refers to negative control.

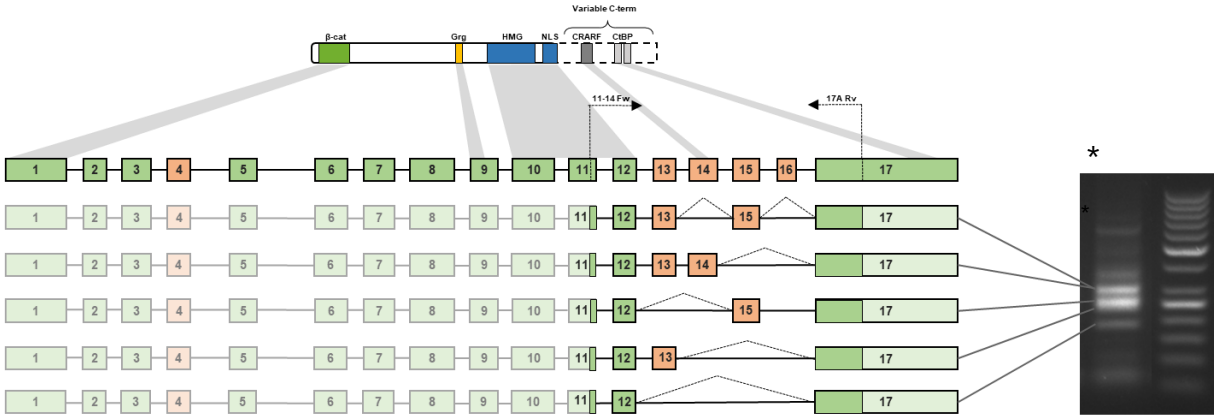

Figure 4.4 – Schematic representation of *TC7L2* isoforms identified after Sanger sequencing of the DNA extracted from the agarose gel bands obtained following the amplification of exons 12-17 of *TCF7L2* gene, using cDNA from CRC patients' blood leukocytes (a) and from the HT-29 CRC cell line (b). Black arrows represent the primers used in the PCR amplification, as well as their location in the *TCF7L2* gene. Green represents known exons; orange represents alternative exons. * Representative amplification pattern of exons 12-17 of *TCF7L2* gene using cDNA from a CRC patient (1501);

4.2 Antiproliferative effect of a panel of isolated compounds on HT-29 and LS174T cell lines

The effectiveness of a selection of pharmaceutical and nutraceutical compounds (table 3.2) in preventing cell proliferation was first assessed using monolayer (2D) cell models of HT-29 and LS174T CRC cell lines. With this we aimed to select the more promising compounds in inducing anti-proliferative activity for further studies in these cell lines. In addition, we also selected a compound having a weak anti-proliferative activity for comparison, namely in gene expression patterns.

Regarding cytostatic agents, we tested the three main compounds used in conventional CRC chemotherapy (5-FU, irinotecan and oxaliplatin). The results demonstrated that irinotecan has potential to inhibit cell proliferation in a dose-dependent manner, in both cell lines (Figure 4.5 a). The IC_{50} doses for this compound were estimated in 89.1±8.3µM and 155.2±10.2µM in HT-29 and LS174T, respectively, therefore with higher sensitivity exhibited by HT-29. These doses were tested using CCD 841 CoN cell line, in a monolayer cell model, and were shown to have low anti-proliferative effect in this cell line (≈20%) (Appendix FG– Figure 1-a). Proliferation of HT-29 cells was reduced by oxaliplatin in a dose-dependent manner (Figure 4.5-b), with an estimated IC_{50} of 522.2±142 µM, a dose which severely inhibit proliferation in CCD 841 CoN cells (≥80%) (Appendix G – Figure 1-a)). Interestingly, in response to oxaliplatin, HT-29 cells' viability decreased until a specific dose and, after this point, increasing doses led to a viability recover, then, at the highest tested dose, viability decreased again. This effect is probably due to cellular efflux mechanisms associated to Oxaliplatin (Martinez-Balibrea *et al.*, 2015). Conversely, this compound revealed higher potential to inhibit proliferation in LS174T cells (Figure 4.5 b), with an estimated IC_{50} of 22.1±2µM, a dose causing no or very low anti-proliferative effect in CCD 841 CoN cells (Appendix G – Figure 1-a)). 5-FU, did not show significant potential to inhibit cell proliferation in either HT-29 or LS174T cell lines (Figure 4.5 c).

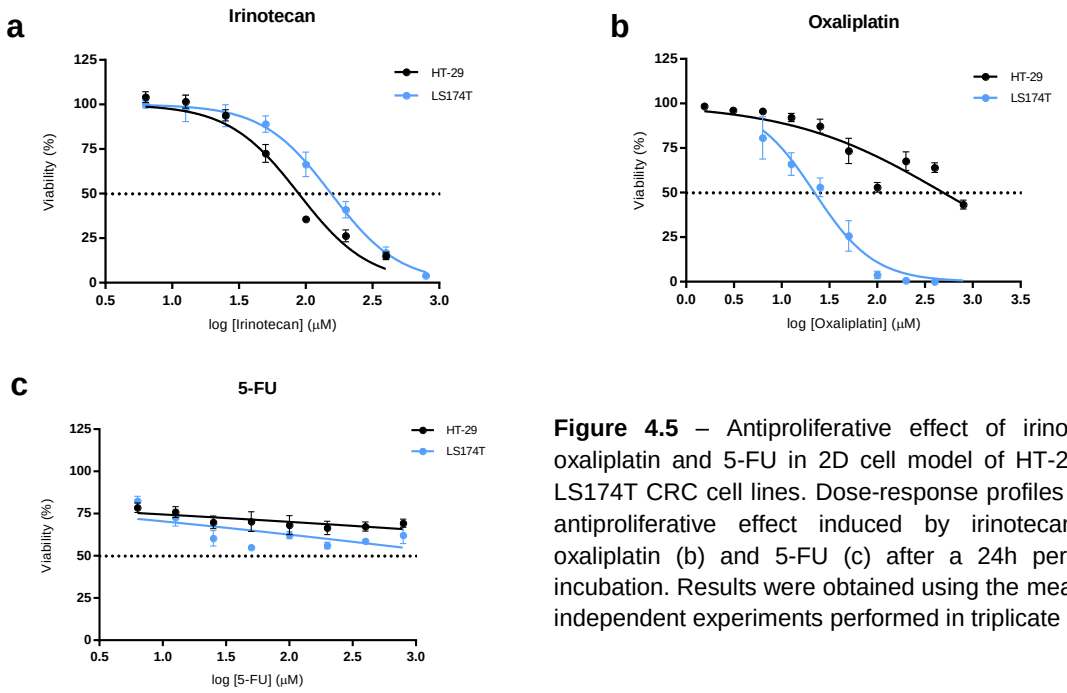

Figure 4.5 – Antiproliferative effect of irinotecan, oxaliplatin and 5-FU in 2D cell model of HT-29 and LS174T CRC cell lines. Dose-response profiles of the antiproliferative effect induced by irinotecan (a), oxaliplatin (b) and 5-FU (c) after a 24h period of incubation. Results were obtained using the mean of 2 independent experiments performed in triplicate ± SD.

HT-29 cells proliferation was not significantly affected by either of the DNA methyltransferase and HDAC inhibitors tested (Figure 4.6 a-b) at the maximal tested doses. Contrarily, both azacitidine and vorinostat seem to affect proliferation in LS174T cells in a dose-dependent manner (Figure 4.6 a-b), at estimated IC_{50} doses of 27.8±5.4µM and 19.4±4.5µM, respectively. These doses were shown to have no or very low effect on CCD841CoN cell proliferation (≤20%) (Appendix G Figure 1 b).

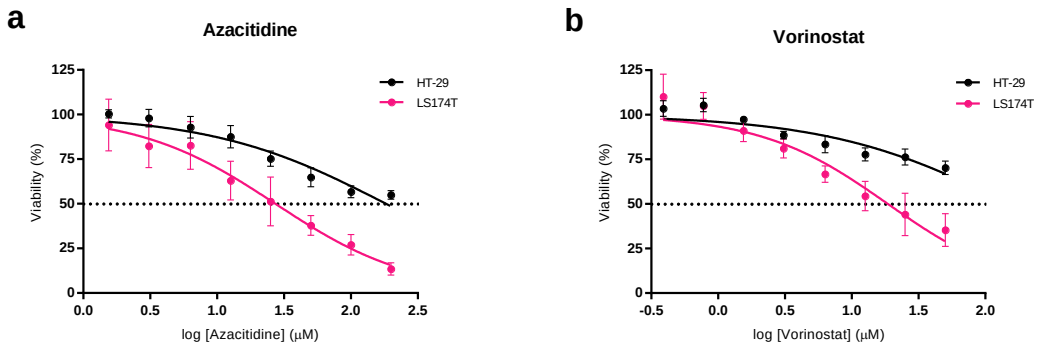

Figure 4.6 – Antiproliferative effect of azacitidine and vorinostat in 2D cell model of HT-29 and LS174T CRC cell lines. Dose-response profiles of the antiproliferative effect induced by azacitidine (a), vorinostat (b) after a 24h period of incubation. Results were obtained using the mean of 2 independent experiments performed in triplicate ± SD.

In the context of Shh/Gli and HGF/Met signaling pathways modulators, our results show that proliferation ability of HT-29 and LS174T cell lines was not affected after treatment with Capmatinib (Figure 4.7 a). GANT61 appears to affect viability of both HT-29 and LS174T cell lines (Figure 4.7 b), at respective estimated IC_{50} doses of 37.1±4.4µM and 26.9±2.4µM. These doses were shown to affect proliferation of CCD 841 CoN cells in ≥80% rates (Appendix G Figure 1-c), thus being highly cytotoxic for normal colonic cells.

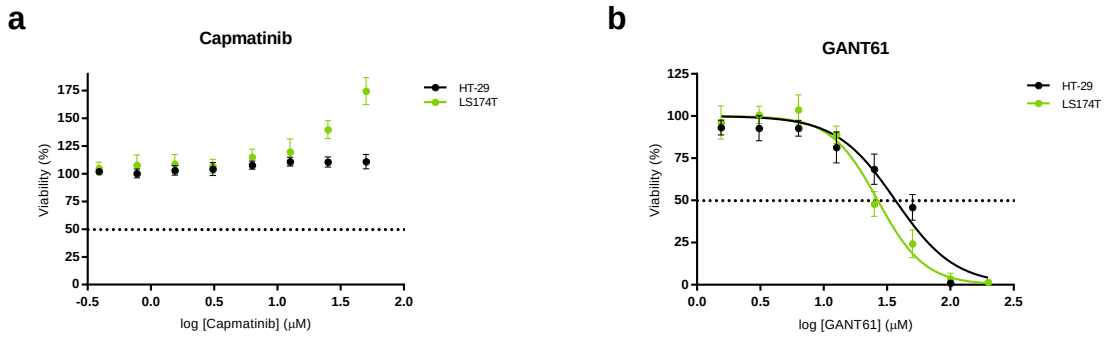

Figure 4.7 – Antiproliferative effect of Capmatinib and GANT 61 in 2D cell model of HT-29 and LS174T CRC cell lines. Dose-response profiles of the antiproliferative effect induced by capmatinib (a), GANT 61 (b) after a 24h period of incubation. Results were obtained using the mean of 2 independent experiments performed in triplicate ± SD.

Concerning the nutraceutical compounds, our results demonstrated that proliferation is not affected by Scutellarein tetramethylether in either HT-29 and LS174T cell lines (Figure 4.8 a). Due to limitations in the amount of compound, tangeretin was exclusively tested in HT-29 cell line, where no effect on proliferation was shown (Figure 4.8 b). According to our results, SFN has potential to impair proliferation in both HT-29 and LS174T cell lines (Figure 4.6 c) at an estimated IC_{50} doses of 39,1±3,9μM and 51,9±22μM, respectively, which, regarding the dose dependent effect of SFN in CCD 841 CoN cell line, is estimated to affect proliferation in >40% in these cell line (Appendix G Figure 1-d).

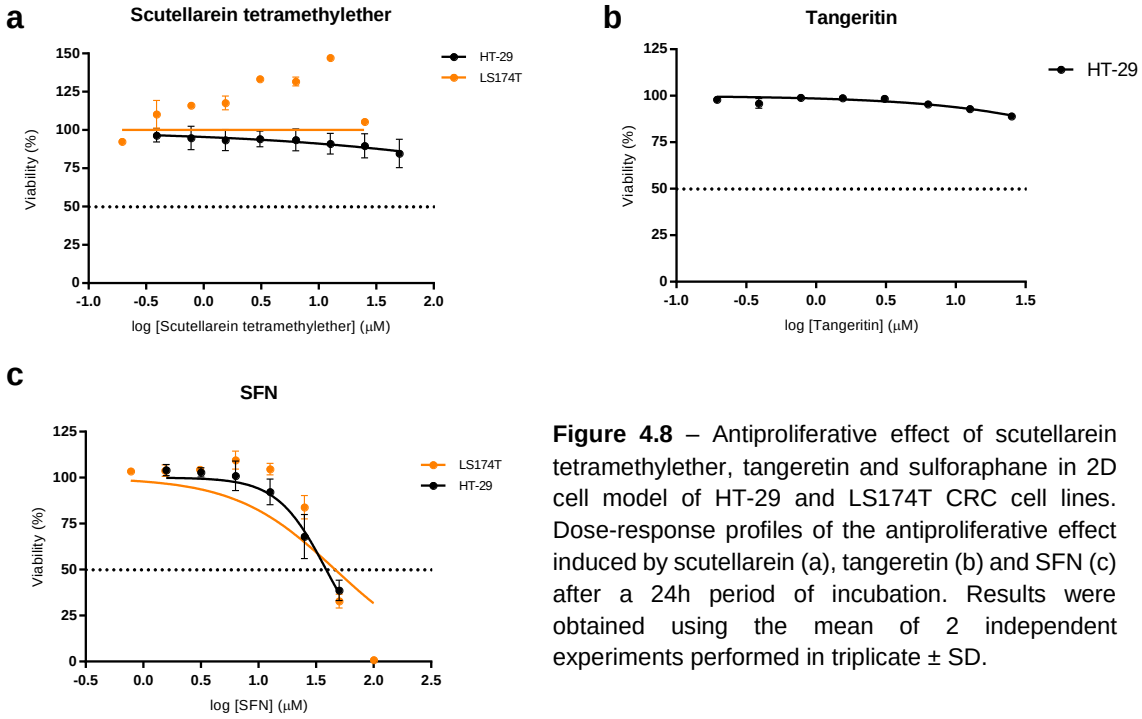

Figure 4.8 – Antiproliferative effect of scutellarein tetramethylether, tangeretin and sulforaphane in 2D cell model of HT-29 and LS174T CRC cell lines. Dose-response profiles of the antiproliferative effect induced by scutellarein (a), tangeretin (b) and SFN (c) after a 24h period of incubation. Results were obtained using the mean of 2 independent experiments performed in triplicate ± SD.

Taken together, these results suggest that HT-29 CRC cell line is, in terms of proliferation ability, more resistant than LS174T to all compounds tested in this panel, with the exception of irinotecan. In order to perform the selection of the most promising compounds to carry further in this work, we took

into account the significant effect of each isolated compound on the proliferation ability of the CRC cell lines and also its effect on the normal colon cell line.

In agreement, out of the 10 tested compounds, four were able to effectively reduce viability on HT-29 cells (irinotecan, oxaliplatin, GANT61 and SFN), however only irinotecan led to an IC_{50} dose that does not significantly impaired viability on CCD 841 CoN cells (Appendix G). Viability on LS174T cells was decreased by treatment with five out of the ten tested compounds (irinotecan, azacitidine, vorinostat, GANT61 and SFN), three of which (irinotecan, azacitidine and vorinostat) led to IC_{50} doses that do not significantly affect viability on CCD 841 CoN. Figures 4.9 a) and b) summarise the anti-proliferative results in both cell lines, showing the effect of all compounds that efficiently reduced viability in each cell line respectively on HT-29 (a) and LS174T (b).

Considering the higher resistance exhibited by HT-29, we selected this cell line for further studies in this project. Moreover, we selected promising compounds affecting viability on HT-29 cells for further analysis along this work. Irinotecan, GANT61 and SFN, were selected for expression analysis of cell cycle, stemness, EMT and specific signaling pathway markers, after treating HT-29 monolayer cells with the estimated IC_{50} doses for each agent, for 24h. This selection was based on the fact that these three agents were the most promising in reducing cell viability on this cell line. However, due to cytotoxic effects of the respective IC_{50} doses, observed in the CCD 841 CoN cell line, we aimed to explore different therapeutic strategies allowing a reduction of the used doses. Thus, we selected Irinotecan, GANT61 (to which HT-29 cell line appears to be more sensitive) and oxaliplatin (to which HT-29 cell line appears to be more resistant), as the basis of a series of combinations, especially with nutraceuticals, allowing to reduce treatment doses and explore the enhanced effect and eventual synergies between specific compounds.

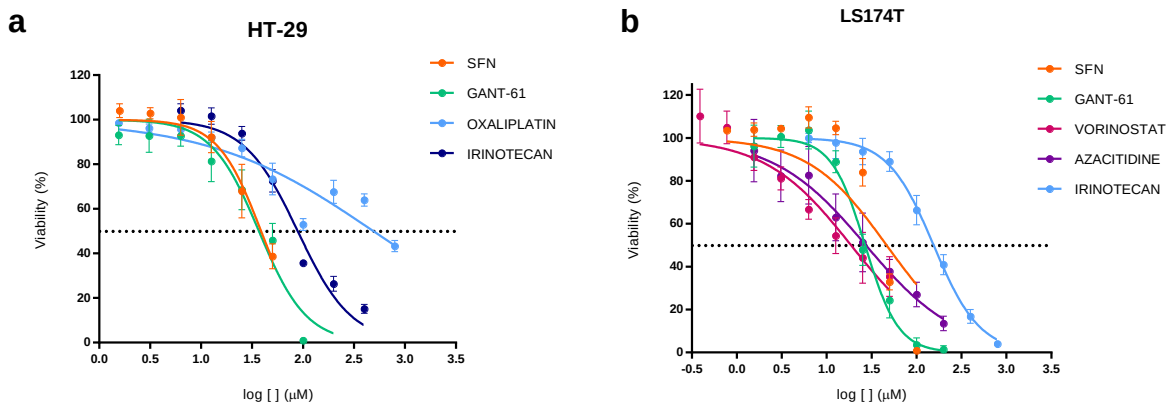

Figure 4.9 – Antiproliferative effect of promising agents in 2D cell model of HT-29 (a) and LS174T (b) CRC cell lines. Dose-response profiles of the antiproliferative effect induced by treatment in a 24h period of incubation. Results were obtained using the mean of 2 independent experiments performed in triplicate ± SD

4.3 Effect of selected compounds on the expression of cell cycle, proliferation, stemness, EMT, and specific signaling pathway markers in HT-29 CRC cell line

Taking into account the results obtained for the antiproliferative effect, we selected three most promising compounds affecting HT-29 CRC cell line and tested their effect on the expression of a series of cell cycle, proliferation, stemness, EMT, and Wnt/Shh signaling pathways markers. The analysis was performed using the 2D cell model of HT-29 cell line, exposed to the previously estimated IC_{50} doses of either irinotecan, GANT61 or SFN for 24h.

4.3.1 Effect of irinotecan, GANT61 and SFN in cell cycle of HT-29 CRC cell line.

To better understand the effect of irinotecan, GANT61 and SFN on cell cycle of HT-29 CRC cell line, we assessed the mRNA levels of *CDKN1A* (p21) and *CCNA2* (Cyclin-A2) in this cell line, after 24h treatment, at the estimated IC_{50} dose for each compound.

Cell cycle regulation is a key feature in cancer cells. The cell cycle is characterized by a series of organized and monitored events that guarantee the correct duplication and segregation of the genome, thus leading to proper cell division. Different from normal cells, which proliferate in response to growth stimuli and specific signals, cancer cells proliferate in an unregulated manner. Moreover, there has been a pronounced link between disrupted cell cycle and tumorigenesis and nearly all described molecules involved in cell cycle regulation have been related to tumor formation (Hartwell and Kastan, 1994; Xuereb and Blundell, 2008; Diaz-Moralli *et al.*, 2013). We here used *CDKN1A* (p21) and *CCNA2* (CyclinA2) as target genes for cell cycle analysis.

Exposing HT-29 cells to irinotecan led to an induction of *CDKN1A*, accompanied by maintained *CCNA2* mRNA levels, when compared to untreated (control) HT-29 cells (Figure 4.7 a and b). *CCNA2* is expressed in late G1, begins to accumulate in S-phase and is rapidly destroyed at the onset of mitosis (Yam *et al.*, 2002). The overexpression of *CDKN1A*, an inhibitor of cyclin-dependent kinases (CDKs) activity, usually leads to G1 or G2 arrest by inhibiting CDK activity, though *CDKN1A* can also directly inhibit DNA synthesis by binding to proliferating cell nuclear antigen (PCNA) (Waga *et al.*, 1994; Chen *et al.*, 1995). Overexpression of *CDKN1A* has also been reported to result in S-phase arrest (Ogryzko *et al.*, 1997). Moreover, several studies have reported S-phase arrest in HT-29 cells, after treatment with irinotecan, for 24h, resulting from the induction of *CDKN1A* (Arnould *et al.*, 2002; Abal *et al.*, 2004). Although additional experiments (e.g. cell cycle arrest analysis by flow cytometry) would be necessary to confirm cell cycle phase, our results suggest a late-G1/S blockage or delay, due to the increase in *CDKN1A* mRNA , suggestive of cell cycle arrest, accompanied by maintained levels of *CCNA2* mRNA levels, which is indicative that cells are beyond G1 and before G2/M. *CDKN1A* is the major target of p53 activity, however, HT-29 cell line is mutant for the *TP53* gene (Appendix B, table B.2), suggesting that *CDKN1A* induction in response to irinotecan is p53-independent, which comes in agreement with studies reporting S phase arrest with *CDKN1A* induction in a p53-independent manner (Abal *et al.*, 2004).

Regarding GANT61, exposing HT-29 cells to this compound, at the estimated IC_{50} dose, for 24h, led to an increase in *CDKN1A* mRNA levels accompanied by an apparent decrease in *CCNA2* mRNA levels (Figure 4.10 a-b). These results suggest a G1/S arrest, consistent with other studies that report

transient accumulation of HT-29 cells at the G1/S boundary and in early S-phase (Mazumdar *et al.*, 2011c). Additionally, cDNA microarray gene profiling previously demonstrated upregulated expression of *CDKN1A* mRNA and downregulated expression of genes involved in the G1/S transition (CyclinE, CyclinA, CDK2, CDC25A) in HT-29 cell line treated with GANT61 for 24h (Shi *et al.*, 2010). This maximization effect in cell cycle arrest achieved by the increase in *CDKN1A* mRNA levels accompanied by a decrease in *CCNA2* mRNA levels is in agreement with the anti-proliferative effect of GANT-61, in comparison with the other compounds, observed in figure 4.9-a.

Considering the treatment of HT-29 cells with SFN, for 24h, with estimated IC_{50} dose, results show slight induction in *CDKN1A* expression accompanied by maintained expression levels of *CCNA2* (Figure 4.10 a-b). It is known that SFN induces time and dose-dependent cell cycle arrest on HT-29 cells (Gamet-Payrastre *et al.*, 2000; Parnaud *et al.*, 2004; Shen *et al.*, 2006). In 2006, Shen and colleagues reported *CCNA2* expression levels to decrease in HT-29 cells after treatment with high doses (> 50 µM) of SFN, in contrast to *CDKN1A* expression levels, that were induced with 25µM dose and strongly induced with 50µM treatment. Moreover, the authors report the G_1 phase arrest after treatment with >50µM of SFN, associated to strongly induced expression levels of *CDKN1A* and significant decrease of cyclin-A2 expression levels (Shen *et al.*, 2006). Our results show that 39µM dose, is enough to cause an increase of *CDKN1A* expression levels, however, it seems not enough to cause a significant decrease in *CCNA2* expression, which can be associated to a late G1 phase, however, it is not in total agreement with G1 cell cycle arrest. Additional experiments as flow cytometry on treated synchronized cells should be performed in order to assess cell cycle phase.

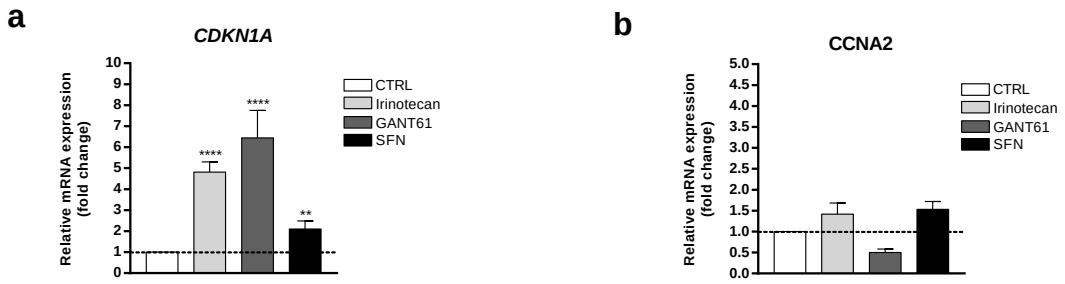

Figure 4.10 – Effect of irinotecan, GANT61 and SFN on the expression of genes involved in the cell cycle. Relative mRNA expression, in fold change, of p21 (a) and cyclin-A2 (b) in HT-29 cells, exposed to estimated IC_{50} doses of irinotecan (89.1µM), GANT61 (37,1µM) or SFN (39,1µM), for 24h. Normalized to GAPDH and β-actin. Results are expressed as mean of at least one experiment performed in triplicate ± SD. *p-value<0.05, **p-value<0.01, ***p-value<0.001 and ****p-value<0.0001 are relative to control.

4.3.2 Effect of irinotecan, GANT61 and SFN in stemness of HT-29 CRC cell line.

To determine whether irinotecan, GANT61 and SFN modulate CRC stemness in HT-29 cells, we examined the effect of these compounds on the expression of *CD44*, *PROM1* (CD133) and *LGR5* genes in treated HT-29 cells, using the IC_{50} estimated dose, for 24h. The effect of SFN in stemness of HT-29 cells was also assessed, however regarding the expression of the *LGR5* gene only.

Our results point out to a significant effect of irinotecan in stemness, associated to a significant decrease on the expression levels of *CD44*, *PROM1* and *LGR5* (Figure 4.11 a-c). GANT61 leads to a significant decrease of *PROM1* and *LGR5*, however the expression level of *CD44* seems to remain

unaltered after treatment (Figure 4.11 a).These results suggest that irinotecan and GANT61 affect stemness in HT-29 cells. In line with these results, it has been reported that GANT61 leads to significantly decrease cell viability of $CD133^+$ cells in pancreatic cancer (Miyazaki *et al.*, 2016). Moreover, irinotecan has been shown to induce transition of *LGR5*$^+$ CRC cells to *LGR5*$^-$ *in vivo*, however this transition was associated to retained expression of *CD44* and *PROM1*, which is not in agreement with our results (Kobayashi *et al.*, 2012). Nevertheless, irinotecan appears to be more effective in reducing cancer stemness than GANT61, although the latter showed a higher anti-proliferative effect. Treatment with SFN leads to a significant decrease of *LGR5* expression (Figure 4.11 c), suggesting it affects cancer stemness however, assessment of other markers is essential to complement this result.

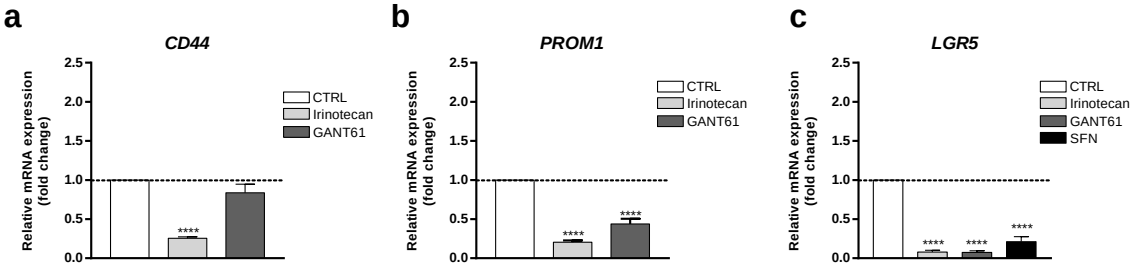

Figure 4.11 – Effect of irinotecan, GANT61 and SFN on the expression of genes involved in cancer stemness. Relative mRNA expression, in fold change, of *CD44* (a), *PROM1* (b) and *LGR5* (c) in HT-29 cells, exposed to estimated IC_{50} doses of irinotecan (89.1µM), GANT61 (37,1µM) or sulforaphane (39,1µM) for 24h. Normalized to *GAPDH* and β-actin. Results are expressed as mean of at least one experiment performed in triplicate ± SD. *p-value<0.05, **p-value<0.01, ***p- value<0.001 and ****p-value<0.0001 are relative to control.

4.3.3 Effect of irinotecan, GANT61 and SFN on EMT in HT-29 CRC cell line.

EMT is a very well described mechanism, thought to play a critical role on the invasive and metastatic behaviour of cancer cells, already mention in section 1.8 (Kalluri and Weinberg, 2009; Busch et al., 2014). Among the great variety of described EMT markers, we here analysed the expression of *VIM* (Vimentin), *ZEB1*, *CDH1* (E-cadherin) and *SNAI1* on our 2D cell model of HT-29 cell line, after treatment. E-cadherin is involved in cell adhesion, i.e., its overexpression refers to an epithelial rather than a mesenchymal state. The other three markers are representative of either an established mesenchymal state (*VIM*) or EMT-inducers (*SNAI1* and *ZEB1*). Therefore, for a compound to effectively prevent or counteract a mesenchymal state, we expect to observe a reduction of mesenchymal markers and eventual increase of epithelial markers.

Our results, illustrated in figure 4.12 a-d, show that treatment with the estimated IC_{50} dose of irinotecan, for 24h, leads to an increased expression of *SNAI1*, however, it seems to have no effect on *VIM* expression and lead to a reduction on the expression of both *CDH1* and *ZEB1*. GANT61 led to an increase in *SNAI1* and *VIM* expression and had no effect on the expression of *CDH1* and *ZEB1*. Additionally, treating cells with SFN led to an increase in *SNAI1*, *VIM* and *ZEB1* expression and a reduction in *CDH1*.

Overall these results point to the fact that none of the three tested compounds effectively reduced EMT, due to general increased or maintained levels of EMT inducers and/or mesenchymal marker, associated to decreased or maintained expression of the epithelial marker E-cadherin.

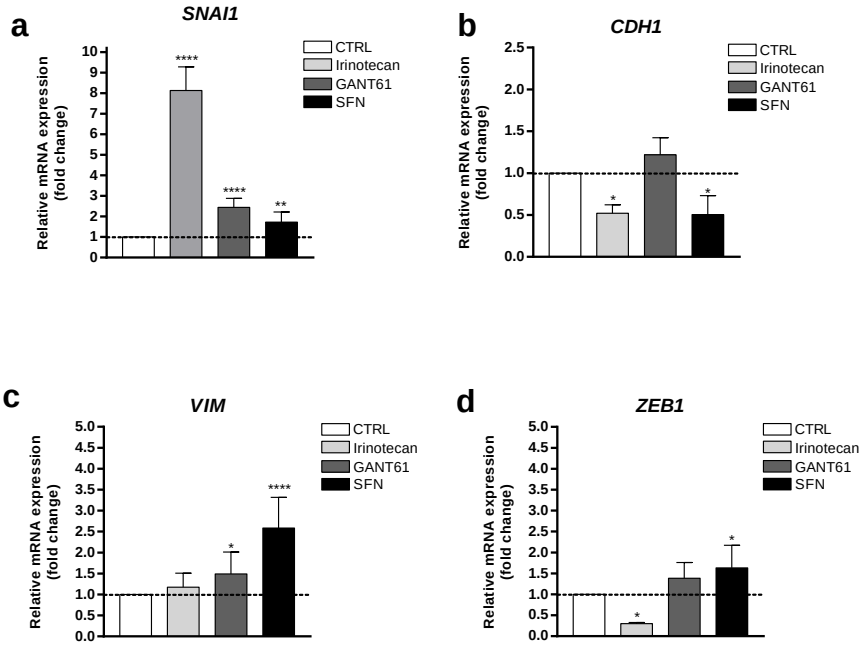

Figure 4.12 – Effect of irinotecan, GANT61 and SFN on the expression of genes involved in EMT. Relative mRNA expression, in fold change, of *SNAI1* (a), *CDH1* (b), *VIM* (c) and *ZEB1* (d) in HT-29 cells, exposed to estimated IC_{50} doses of irinotecan (89.1µM), GANT61 (37,1µM) or SFN (39,1µM) for 24h. Normalized to GAPDH and β-actin. Results are expressed as mean of at least one experiment performed in triplicate ± SD. *p-value<0.05, **p-value<0.01, ***p-value<0.001 and ****p-value<0.0001 are relative to control.

4.3.4 Effect of irinotecan, GANT61 and sulforaphane on WNT and SHH signaling pathways in HT-29 CRC cell line.

We next analysed the effect of irinotecan, GANT61 and SFN on the expression of Wnt/β-catenin and Shh/Gli signaling pathway markers. Thus, we assessed the expression of *CTNNB1*(β-catenin*)*, *TCF7L2* (TCF7L2), *TCF7L2[1-6]* (TCF7L2[1-6]), *AXIN2* (Axin2), *ABCB1* (P-gp) and *GLI1* (Gli1), 24h after treatment, at the previously estimated IC_{50} dose*. ABCB1* gene encodes an efflux pump (P-gp), transcriptionally regulated by a series of factors involved in different signaling pathways including Wnt/β-catenin.*ABCB1* overexpression is known to contribute to multiple drug resistance in human cancer cells, including specific resistance to chemotherapeutic agents in CRC (Sui *et al.*, 2012; Jensen *et al.*, 2015). Axin2 binds several components of the canonical Wnt signal transduction promoting β-catenin stabilization and further degradation in the cytoplasm, acting as a negative regulator of this signaling pathway. This component is transcriptionally induced following activation of Wnt/β-catenin signaling, generating a negative feedback loop to silence the signaling pathway. Moreover, transcriptional activation of *AXIN2* was also shown upon interaction of CDX2 intestinal transcription factor with its putative enhancer, related to decreased Wnt/β-catenin signal in CRC cells (Jho *et al.*, 2002; Olsen *et al.*, 2013). *TCF7L2[1-6]* marker is representative of *TCF7L2* (encoding TCF4 transcription factor) isoforms that exclude proximal exons (1 to 3-6). This region is of great interest in our study for including at least 4 described polymorphisms in *TCF7L2* gene, associated to increased susceptibility for CRC or other pathologies (Grant *et al.*, 2006; Mayans *et al.*, 2007; Duarte, 2015). Additionally, this marker also detects the expression of an isoform resembling a dominant-negative form of this transcription factor (*dnTCF7L2)*. *dnTCF7L2* represents a N-terminal truncated isoform that is unable to bind β-catenin in the nucleus, thus acting as a transcriptional repressor of Wnt/βcatenin target genes. The expression of this isoform is induced by *VAX2,* and possibly other transcription factors, through a possible activation

of a promoter region of *TCF7L2* intron 5 (Grove, 2011; Vacik *et al.*, 2011). Hence, reduced levels of *TCF7L2[1-6]*, allied to increased or unaffected levels of full-length *TCF7L2* may indicate unbalanced repressor/activator isoforms expression ratio.

Results, shown in figure 4.13 point irinotecan and SFN as promising agents in inhibiting Shh/Gli signaling pathway activation by reducing *GLI1* expression (Figure 4.13 f) Moreover, *ABCB1* was also reduced (Figure 4.13 e). These compounds also decreased the expression of *TCF7L2,* in the case of irinotecan, especially the *TCF7L2[1-6]* isoform that may act as dominant negative, and increased the Wnt target gene *AXIN2* (Figure 4.13 e), which may suggest an activation of the Wnt signalling pathway and would be in agreement with a consequent inhibition of the SHH pathway. Conversely, GANT61 appears to induce the expression of *ABCB1* and also of the *TCF7L2[1-6]* isoform (Figure 4.13 c and e). The latter, by a dominant negative effect, may trigger the SHH pathway. In agreement, GANT61 led to significant activation of *GLI1* expression. Mazumdar and colleagues have predicted, through analysis of the GLI1-DNA complex crystal structure, the docking of GANT61 to the GLI1 protein, the Gli1-DNA complex or to DNA itself, inhibiting Gli-induced transcription (Agyeman *et al.*, 2015) Thus, overexpression of *GLI1* after GANT61 treatment for 24h at our defined dose may not correlate with pathway activation, instead, the induced expression of *GLI1* may result of positive feedback mechanisms associated to downregulation of target genes. According with this hypothesis, SHH inhibition by GANT61, is also able to reduce dominant negative isoforms and thus might explain the decrease of *TCF7L2[1-6]* isoform. Analysis of other markers, such as Shh/Gli signaling direct targets, complemented with signaling activity assays (luciferase assay, for example), would be crucial to confirm these results and analyse pathway activation after treatment with GANT61.

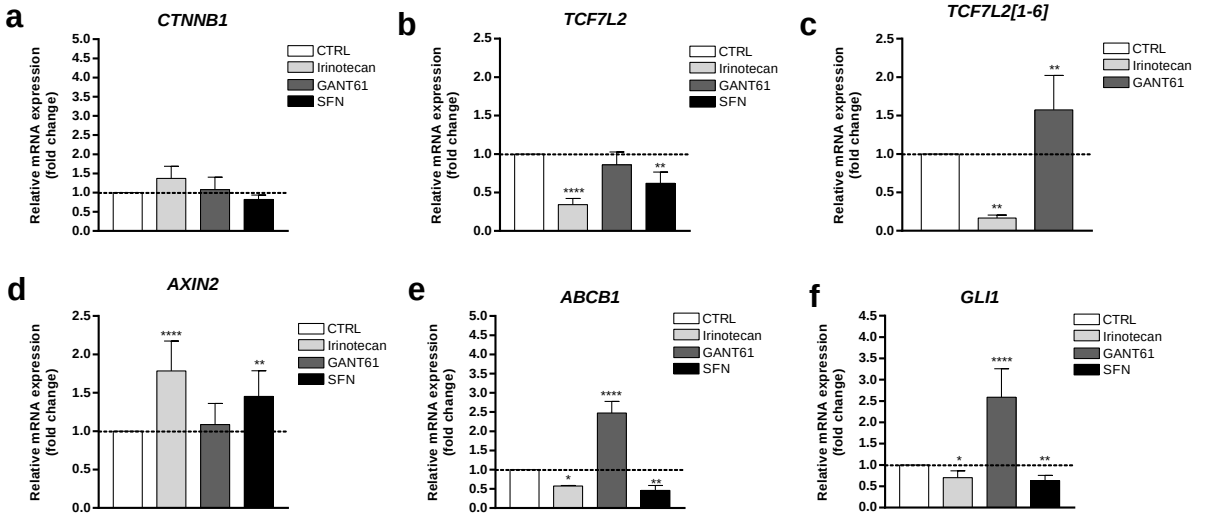

Figure 4.13 – Effect of irinotecan, GANT61 and SFN on the expression of genes involved on Wnt/β-catenin and Shh/Gli signaling pathways. Relative mRNA expression, in fold change, of *CTNNB1* (A), *TCF7L2* (B), *TCF7L2[1-6]* (C), *AXIN2* (D), *ABCB1* (E) and *GLI1* (F), in HT-29 cells, exposed to estimated IC_{50} doses of irinotecan (89.1µM), GANT61 (37,1µM) or SFN (39,1µM) for 24h. Normalized to GAPDH and β-actin. Results are expressed as mean of at least one experiment performed in triplicate ± SD. *p-value<0.05, **p-value<0.01, ***p- value<0.001 and ****p-value<0.0001 are relative to control.

4.4 Effect of a selection of compounds on the migratory ability of HT-29 CRC cell line

Migratory ability was tested using a 2D model of HT-29 cell line, exposed to irinotecan, GANT61 and SFN, selected by their promising anti-proliferative activity on this cell line, as well as to 5-FU and azacitidine to better understand the resistance of this cell line to these compounds. Treatment doses were selected based on our previously determined IC_{50} doses, selecting a dose related to high viability rates (≤ 80% viability), to guarantee we would have good viability rates 24h after treatment and therefore, evaluate migration.

The migratory ability of HT-29 seemed to be reduced after treatment with irinotecan for 24h (Figure 4.14 a). A 50µM dose seems to significantly reduce migration as soon as 24h after treatment and to maintain its effect until at least 72h after treatment. Reducing the dose for 25µM leads to significant reduction in migratory ability, however, this lower dose appears to have attenuated effect as the reduction on migration is lower, especially at 24 and 72h suggesting this dose may be effective in a shorter time window, compared to the higher dose. 5-FU did not show reduction on the migratory ability of HT-29 cells, on the contrary, a 50µM dose appears to induce a significant improvement of the migratory ability at 24 and 48h after treatment (Figure 4.14 b). These results, together with the poor anti-proliferative effect of isolated 5-FU in this cell line, highlight the relevance of complementing 5-FU with other cytostatic agents, such as irinotecan or oxaliplatin in conventional treatment of metastatic CRC.

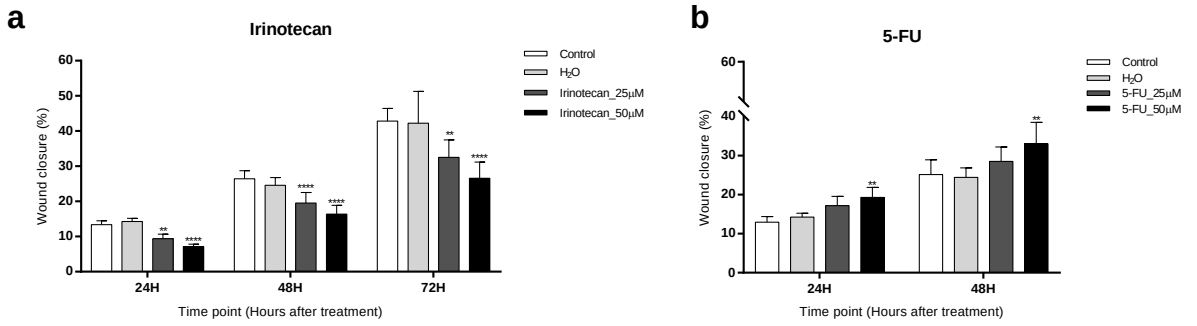

Figure 4.14 – Effect of irinotecan and 5-FU in the migratory ability of HT-29 CRC cell line. Wound closure represented as the percentage of the original wound area, at 24h, 48h and 72h. Results from cells exposed to individual doses (25µM and 50µM) of irinotecan (a) and 5-FU (b) as well as to solvent only (H_2O), were compared to non-treated cells (control) using analysis of variance (2way ANOVA). Results were obtained using the mean of 2 independent experiments performed in triplicate ± SD. $p < 0.05$ was considered as statistically significant. * $p < 0.05$, ** $p < 0.01$, *** $p < 0.001$ and **** $p < 0.0001$, relative to control;

HT-29 cells treated with azacitidine for a period of 24 hours show a significantly decrease in migration ability at 72h after treatment, suggesting a delayed effect of this agent, as illustrated in figure 4.15. Moreover, this effect was seen for doses ≥25µM. Thus, suggesting that azacitidine, in addition to its ineffectiveness in preventing HT-29 cells proliferation (Figure 4.6 a), using these doses it has also no relevant effects on migration ability of these cells.

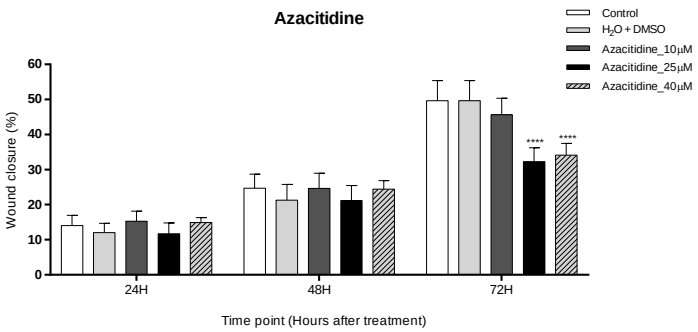

Figure 4.15 – Effect of azacitidine in the migratory ability of HT-29 CRC cell line. Wound closure represented as the percentage of the original wound area, at 24h, 48h and 72h after treatment. Results from cells exposed to individual doses (10, 25 and 50µM) of azacitidine as well as to solvent only (H_2O+DMSO), were compared to non-treated cells (control) using analysis of variance (2way ANOVA). Results were obtained using the mean of 2 independent experiments performed in triplicate ± SD. $p < 0.05$ was considered as statistically significant. * $p < 0.05$, ** $p < 0.01$, *** $p < 0.001$ and **** $p < 0.0001$, relative to control.

GANT61 appears to effectively reduce migration on HT-29 cell line (Figure 4.16). Cells treated with 15µM of GANT61 for 24h, show significant reduction of the migration rate as soon as 24h after treatment and maintained this reduction 48h after treatment. A lower dose (10µM) induces a significant reduction of migration rate at 48h after treatment, suggesting a delayed effect upon exposure to lower doses of this compound. Despite it has not been assessed in CRC, reduced motility it has been reported in GANT61-treated pancreatic CSCs (Fu *et al.*, 2013).

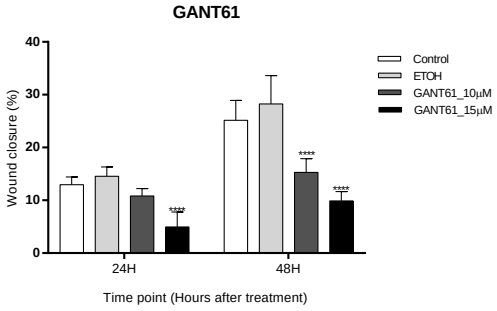

Figure 4.16 – Effect of GANT61 in the migratory ability of HT-29 CRC cell line. Wound closure represented as the percentage of the original wound area, at 24h and 48h after treatment. Results from cells exposed to individual doses (10 and 15µM) of GANT61 as well as to solvent only (ETOH), were compared to non-treated cells (control) using analysis of variance (2way ANOVA). Results were obtain using the mean of 2 independent experiments performed in triplicate ± SD. $p < 0.05$ was considered as statistically significant. * $p < 0.05$, ** $p < 0.01$, *** $p < 0.001$ and **** $p < 0.0001$, relative to control.

Lastly, our results suggest that SFN has the ability of promoting migration during the first 72h after treatment when administrated in low doses (7.5µM) to HT-29 cells. Higher doses of SFN (10 and 15µM) seem to have no influence on the migratory ability of HT-29 cells (Figure 4.17). These results suggest that, despite SFN being effective in reducing cell viability, if used in very low doses, it appears to slightly facilitate migration on HT-29 CRC cell line.

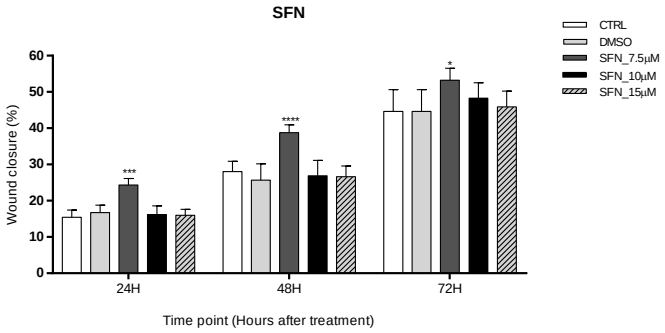

Figure 4.17 – Effect of SFN in the migratory ability of HT-29 CRC cell line. Wound closure represented as the percentage of the original wound area, at 24h, 48h and 72h after treatment. Results from cells exposed to individual doses (7,5, 10 and 15µM) of SFN as well as to solvent only (DMSO), were compared to non-treated cells (control) using analysis of variance (2way ANOVA). Results were obtained using the mean of 2 independent experiments performed in triplicate ± SD. $p < 0.05$ was considered as statistically significant. * $p < 0.05$, ** $p < 0.01$, *** $p < 0.001$ and **** $p < 0.0001$, relative to control;

Taken together, these results show that irinotecan and GANT61 are promising agents for impairing migratory ability of HT-29 cells, suggesting their high potential even at low doses.

4.5 Antiproliferative effect of selected combinations of promising compounds for treatment of HT-29 CRC cell line

Along this work, taking together both anti-proliferative and anti-migratory activities as well as their effect in gene expression markers of cell-cycle, stemness, EMT and specific signalling pathways, the results have pointed irinotecan and GANT61 as promising compounds leading to impairment of homeostasis in HT-29 cells. Additionally, most estimated IC_{50} estimated doses, have a negative impact on viability of normal colon CCD 841 CoN cell line (Appendix G, Figure G.1 a-d). In order to explore the potential synergic effect between other compounds and irinotecan/GANT61 , to reduce doses therefore reducing cytotoxicity in normal colon cells, herein we used low doses of these two promising compounds combined to oxaliplatin, SFN and tangeretin. As a primary approach, aiming to achieve a specific dose for each combination, we assessed the antiproliferative effect, through dose-response profiles, of oxaliplatin, SFN and tangeretin combined with defined doses of either irinotecan (50µM) or GANT61 (15µM). These doses corresponded to the IC_{25} and IC_{20}, respectively and were selected based on two rationales: 1) induce some anti-proliferative effect in the HT-29 cell line without inducing cytotoxicity in the normal colon CCD 841 CoN cell line; 2) had anti-migratory capacity in the HT-29 cell line.

The results suggest a potential synergic anti-proliferative effect of the combination of 50µM of irinotecan with oxaliplatin, SFN or tangeretin, as shown in figure 4.18 a-c, on HT-29 cells. For all dose-response profiles obtained, we observed an improvement on the effect of the specific 50µM dose of irinotecan, as the percentage of viability decreased in combination with increased doses oxaliplatin (Figure 4.18 a), SFN (Figure 4.18 b) and tangeretin (Figure 4.18 c). Regarding the combination of 15µM of GANT61 with oxaliplatin, SFN or tangeretin (Figure 4.19 a-c), the results also suggest a potential synergic anti-proliferative effect, as we observed a decrease on the percentage of viability after combination of the specific dose of GANT61 with different doses of oxaliplatin (Figure 4.19 a), SFN (Figure 4.19 b) and tangeretin (Figure 4.19 c). In response to oxaliplatin, either isolated or in

combination, HT-29 cells' viability decreased until a specific dose, however, after this point, increasing doses led to a viability recover. This effect, as previously mentioned, may be due to cellular efflux mechanisms associated to Oxaliplatin (Martinez-Balibrea *et al.*, 2015). Additionally, it is suggested by our results a higher anti-proliferative effect by combining oxaliplatin or SFN with either irinotecan or GANT61, than by combining them to tangeretin. Thus, it is suggested that this latter nutraceutical has lower impact on HT-29 cells' viability, however, it enhanced the effect of 50µM irinotecan.

Concerning these results, we selected a panel of promising compound combinations in order to assess their effect on the expression of a series of markers implicated in CRC carcinogenesis, in the HT-29 cells. Thus, based on the dose-response profiles, we selected specific doses that did not necessarily inflict highly reduced viability, but revealed promising synergic outcomes, by enhancing the effect of either GANT61 or irinotecan on isolated treatment allied to a reduced cytotoxic effect (≤20%) on CCD 842 CoN normal colon cells. Therefore, the following combinations were selected: irinotecan (50µM) + tangeretin (25µM); irinotecan (50µM) + SFN (25µM); irinotecan (50µM) + oxaliplatin (100µM); GANT61 (15µM) + SFN (25µM); GANT61 (15µM) + oxaliplatin (100µM), to explore the synergic effect between these compounds, reducing cytotoxicity in normal colon cells.

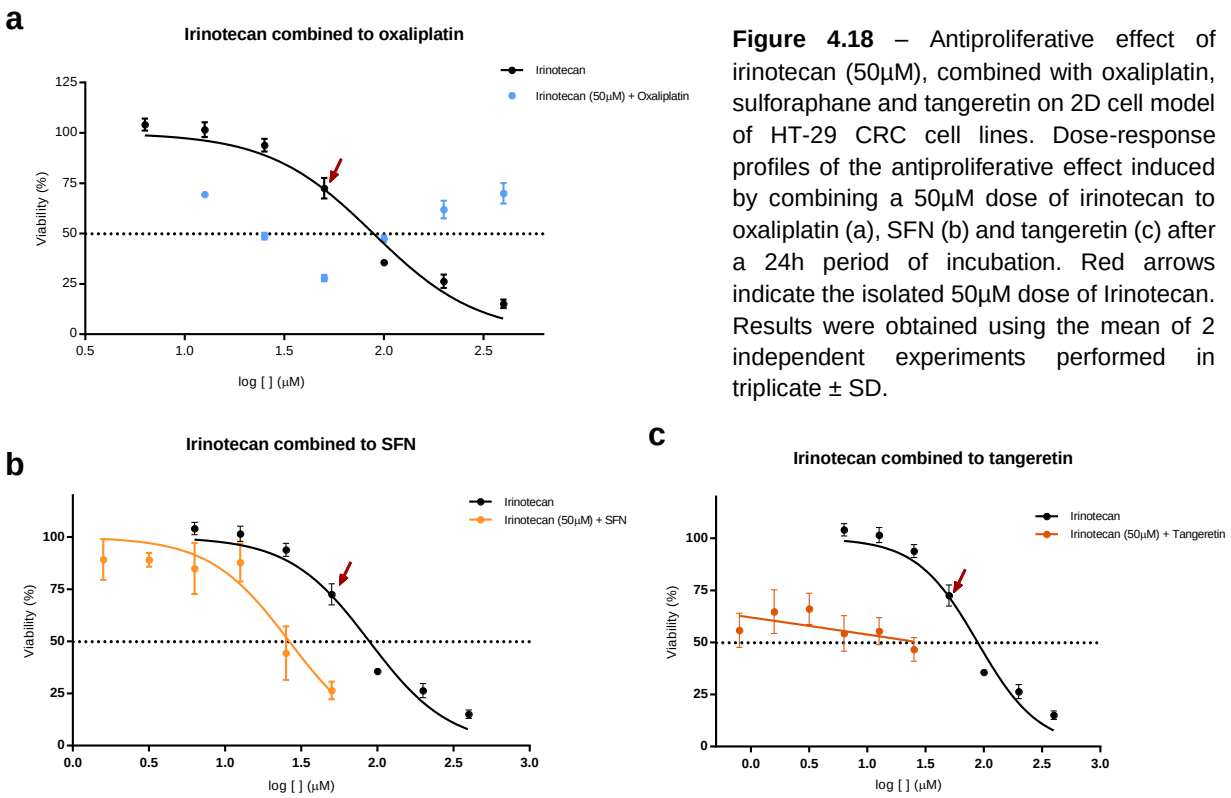

Figure 4.18 – Antiproliferative effect of irinotecan (50µM), combined with oxaliplatin, sulforaphane and tangeretin on 2D cell model of HT-29 CRC cell lines. Dose-response profiles of the antiproliferative effect induced by combining a 50µM dose of irinotecan to oxaliplatin (a), SFN (b) and tangeretin (c) after a 24h period of incubation. Red arrows indicate the isolated 50µM dose of Irinotecan. Results were obtained using the mean of 2 independent experiments performed in triplicate ± SD.

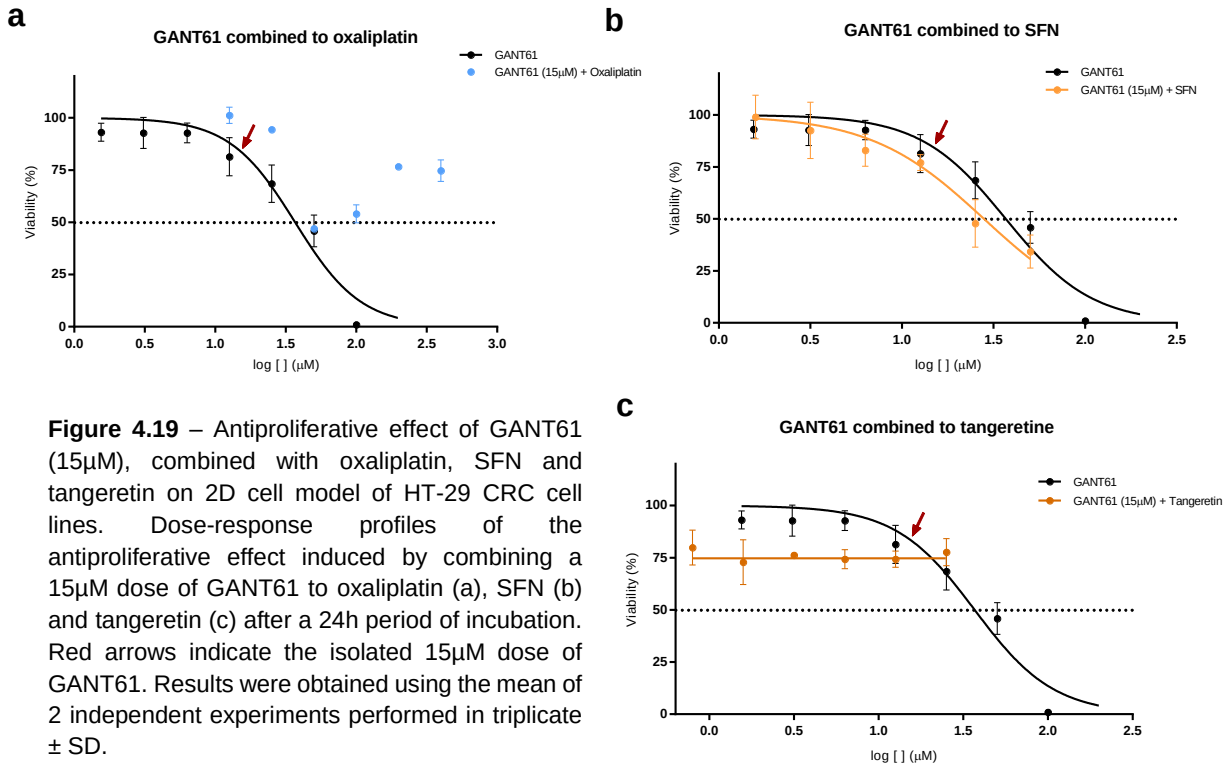

Figure 4.19 – Antiproliferative effect of GANT61 (15µM), combined with oxaliplatin, SFN and tangeretin on 2D cell model of HT-29 CRC cell lines. Dose-response profiles of the antiproliferative effect induced by combining a 15µM dose of GANT61 to oxaliplatin (a), SFN (b) and tangeretin (c) after a 24h period of incubation. Red arrows indicate the isolated 15µM dose of GANT61. Results were obtained using the mean of 2 independent experiments performed in triplicate ± SD.

4.6 Effect of selected combinations of compounds on the expression of cell cycle, proliferation, stemness, EMT, and signaling pathway markers in the HT-29 CRC cell line.

In order to evaluate the putative effect of a selected panel of compound combinations in CRC tumorigenesis and metastasizing processes of CRC, we assessed the expression of a series of molecular targets involved in cell cycle, stemness, EMT, Wnt/β-catenin and Shh/GI1 signaling pathways. This analysis was performed using two different cell models of HT-29 CRC cell line – monolayer (2D) and aggregate (3D) cell models. The molecular markers, compounds and combinations used in this section are listed in table 3.5 and 3.6, respectively. The compound doses used in this experiment were previously established (sections 4.2 and 4.5) according to the most promising results obtained in cell viability assays.

Three dimensional cell models are complex but more effective for studying tumor biology. The 3D cell model allowed the formation of cell aggregates, better mimetizing the arrangement of cells in the tumor context and potentially mimetizing the behaviour of circulating cell aggregates. It is known that gene expression may vary between these two models (Weiswald *et al.*, 2015). Treatments including oxaliplatin were tested regarding the expression of a reduced panel of marker and combinations. Thus for these treatments, the data presented in this section is represented in individual graphs, facilitating visual interpretation for the reader.

4.6.1. Effect of combined compounds in the expression of cell cycle markers on 2D and 3D cell culture models of HT-29 CRC cell line

Figures 4.20 and 4.21 illustrate the results regarding the expression of the mentioned cell cycle markers after treating HT-29 cells in a 2D (a) and 3D (b) cell models, for 24h.

Treating HT-29 monolayer cells with the combinations of irinotecan with tangeretin, SFN (Figure 4.20 a) or oxaliplatin (Figure 4.21 a), led to significantly increased expression of *CDKN1A* and maintained expression of *CCNA2*, compared to control. These results are compatible with late-G1/S-phase cell cycle arrest, as previously discussed in section 4.3.1. Tangeretin and oxaliplatin appear to enhance the effect of irinotecan on impairing cell cycle by significantly increasing the relative mRNA expression of *CDKN1A* when compared to treatment with the two tested doses of isolated irinotecan - 50µM and 89,1µM (the latter shown in section 4.3.1). Additionally, these combinations, as well as irinotecan-SFN, had no effect on the expression of *CCNA2*, suggestive of a late-G1/S-phase arrest rather than the apparent late G2/M arrest. Isolated irinotecan, at 50µM dose, led to increased expression of *CCNA2*, which differs from the results obtained in section 4.3.1, where unaffected levels of *CCNA2* were observed upon treatment with a 89,1µM dose. This difference may be due to the different doses used, however, these results are in agreement with previous studies showing an S-phase blockage, before accumulation at G2/M, of HT-29 cells after treatment with irinotecan at lower doses (Abal *et al.*, 2004; Harris *et al.*, 2005). It is interesting to note that isolated tangeretin had no effect on the expression of either marker, however, it significantly enhanced the effect of irinotecan on the expression of *CDKN1A*, inducing higher expression levels of this marker than those observed for treatment with a higher dose of irinotecan, in section 4.3.1.

Treating HT-29 monolayer cells with the combinations of GANT61 with SFN (Figure 4.20 a) or oxaliplatin (Figure 4.21 a), led to significantly increased levels of *CDKN1A* and maintained levels of *CCNA2* suggestive of a late-G1/S-phase arrest. Furthermore, results are suggestive of an enhancement of GANT61 effects on the expression of *CDKNA1* by SFN and oxaliplatin, which increased the mRNA expression relative to control, of this marker, after treatment with isolated GANT61 toward similar levels to those observed in section 4.3.1, where a highly cytotoxic dose of GANT61 was used.

Overall, these results suggest that all combinations were effective on impairing cell cycle on the HT-29 monolayer cell model. Furthermore, tangeretin and oxaliplatin are suggested to enhance the effect of isolated irinotecan while SFN and oxaliplatin seem to enhance the effect of GANT61 in this cell model.

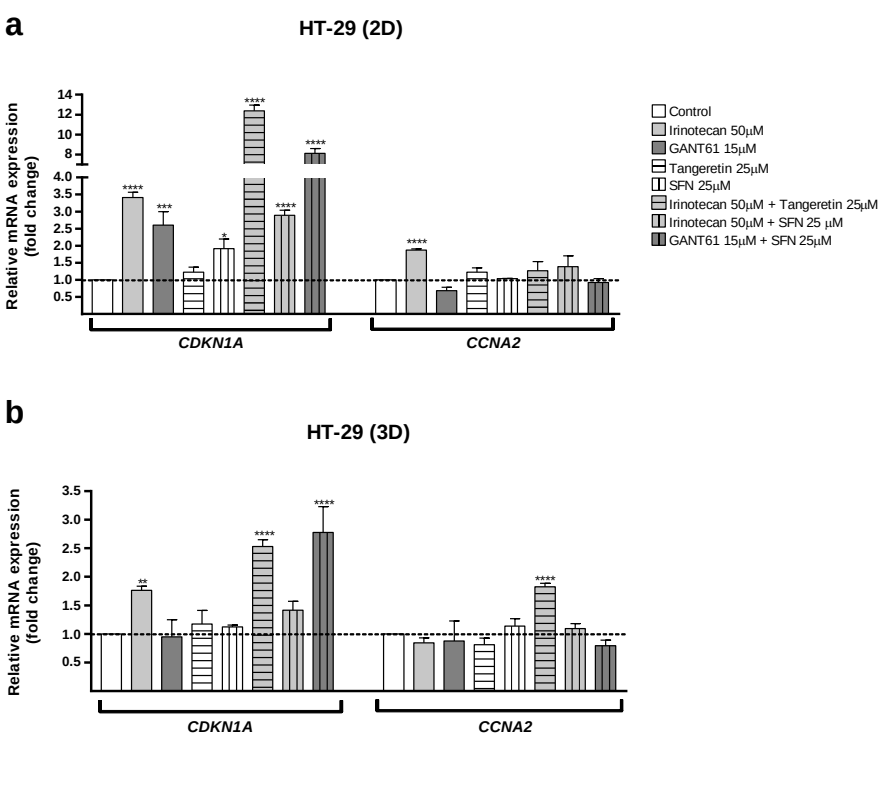

Figure 4.20 – Expression of cell cycle markers *CDKN1A* (P21) and *CCNA2* (CyclinA2) in HT-29 cells in monolayer (a) and aggregate (b) models. Relative mRNA expression, in fold change, in HT-29 cells, exposed to defined doses of selected agents and combinations of agents for 24h. Normalized to GAPDH and β-actin. Results are expressed as mean of at least one experiment performed in triplicate ± SD. *p-value <0.05, **p-value <0.01, ***p- value <0.001 and ****p-value <0.0001 are relative to control. Legend is common to all graphs.

Concerning the aggregate cell model, irinotecan combined with tangeretin (Figures 4.20 b) led to over expression of both markers, *CDKN1A* and *CCNA2*, suggestive of a late S-phase/G2/M arrest. Additionally, it appears that tangeretin enhanced the effect of irinotecan on the overexpression of *CDKN1A* and delay cell cycle blockage due to the increased levels of *CCNA2*, when compared to isolated irinotecan. The combination irinotecan-SFN (Figures 4.20 b) had no effect on the expression of either cell cycle marker, suggesting that SFN inhibited the effect of isolated irinotecan on the overexpression of *CDKN1A* and apparently preventing cell cycle arrest on HT-29 cell aggregates. Nevertheless, the doses used for this combination to evaluate gene expression were the same corresponding to IC50 in cell viability assays using this combination, therefore other markers need to be studied to understand this effect.

GANT61 combined with SFN (Figures 4.20 b) significantly induced the expression of *CDKN1A*, compatible with a late-G1/S-phase blockage and strongly suggesting a synergic effect, regarding that neither isolated GANT61 or SFN had effect on the expression of *CDKN1A*. The same results were obtained after combining GANT61 with oxaliplatin (Figures 4.21 b). Significantly increased *CDKN1A* mRNA levels were also observed with isolated oxaliplatin, after treating HT-29 cell aggregates, while GANT61 had no effect on the expression of this marker on this cell model.

Thus, our results suggest that irinotecan-tangeretin, GANT61-SFN and GANT61-oxaliplatin were able to impair cell cycle on our HT-29 aggregate cell model. Moreover, these combinations reveal great synergic potential, by the enhanced effect of isolated irinotecan and GANT61.

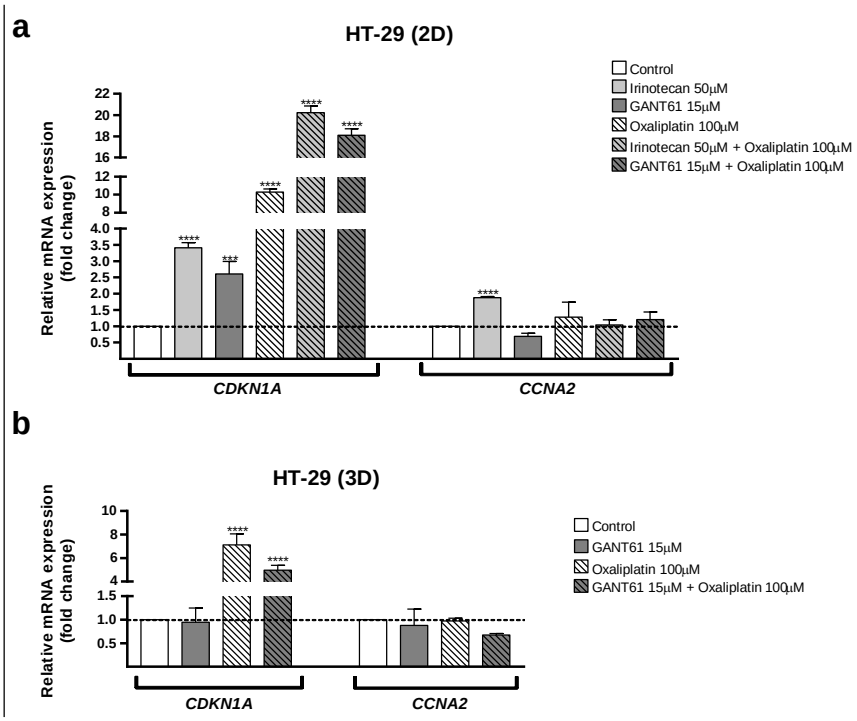

Figure 4.21 – Expression of cell cycle markers in HT-29 cells in monolayer (a) and aggregate (b) models. Relative mRNA expression, in fold change, in HT-29 cells, exposed to defined doses of selected agents and combinations of agents for 24h. Normalized to GAPDH and β-actin. Results are expressed as mean of at least one experiment performed in triplicate ± SD. *p-value<0.05, **p-value<0.01, ***p- value<0.001 and ****p-value<0.0001 are relative to control.

4.6.2. Effect of combined compounds in the expression of stemness markers on 2D and 3D cell culture models of the HT-29 CRC cell line

As mentioned in section 1.9, CSCs represent a major player in cancer tumorigenesis and metastasizing. Thus, we next analysed the effect of treating HT-29 cells with either isolated or combined agents, on the expression of CRC stem cells markers *LGR5* (Lgr5), *PROM1* (CD133), *CD44* and *EPCAM*. These markers, described in section 4.3.2, have been extremely associated to CRC stem cells in literature. (Merlos-Suárez *et al.*, 2011; Aguilar-Gallardo and Simón, 2013; Liu *et al.*, 2014; Wahab *et al.*, 2017)

Treating HT-29 cells in a monolayer cell model with irinotecan combined with tangeretin or SFN (Figures 4.22 a), led to a significantly reduced expression of the tested stemness markers. SFN appears to enhance the effect of isolated irinotecan through the accentuated reduction of *PROM1* expression to similar levels to those observed in section 4.3.2 after treating HT-29 cells with a higher dose of irinotecan (89,1μM). Moreover, SFN and tangeretin appear to enhance the effect of irinotecan on the expression of *EPCAM*, which was not affected after treatment with the isolated compound. It is also interesting to note that treatment with isolated tangeretin did not lead to promising effects on reducing stemness, on the contrary, it led to overexpression of *PROM1* and *EPCAM* markers. In combination with oxaliplatin (Figure 4.23 a), irinotecan led to reduced expression of both tested markers, *LGR5* and *PROM1*, with an apparent accentuated reduction of *PROM1* levels comparing to treatment with isolated irinotecan. It is interesting to highlight that isolated oxaliplatin resulted in overexpression of *LGR5* and had no effect on the expression of *PROM1*, suggesting a strong synergic effect of this combination.

Combining GANT61 with SFN (Figure 4.22 a) resulted in a reduced expression of all the tested markers with the exception of *EPCAM*, significantly enhancing the effects of treatment with isolated GANT61, which led to overexpression of *PROM1* and *EPCAM.* Moreover, this combination also

improved the effects of a higher dose of isolated GANT61 (37,1μM), discussed in section 4.3.2, especially regarding the expression of *CD44*, which was significantly reduced upon treatment with GANT61-SFN. Combined with oxaliplatin, GANT61 led to decreased expression of both *LGR5* and *PROM1*, achieving similar results to those regarding the expression of stemness marker after treatment with a higher dose of GANT61 (37,1 μM), from section 4.3.2 (Figure 4.23 a). Moreover, the synergic effect of this combination is also suggested by the overexpression of *LGR5* and unaffected levels of *PROM1* after treatment with isolated oxaliplatin.

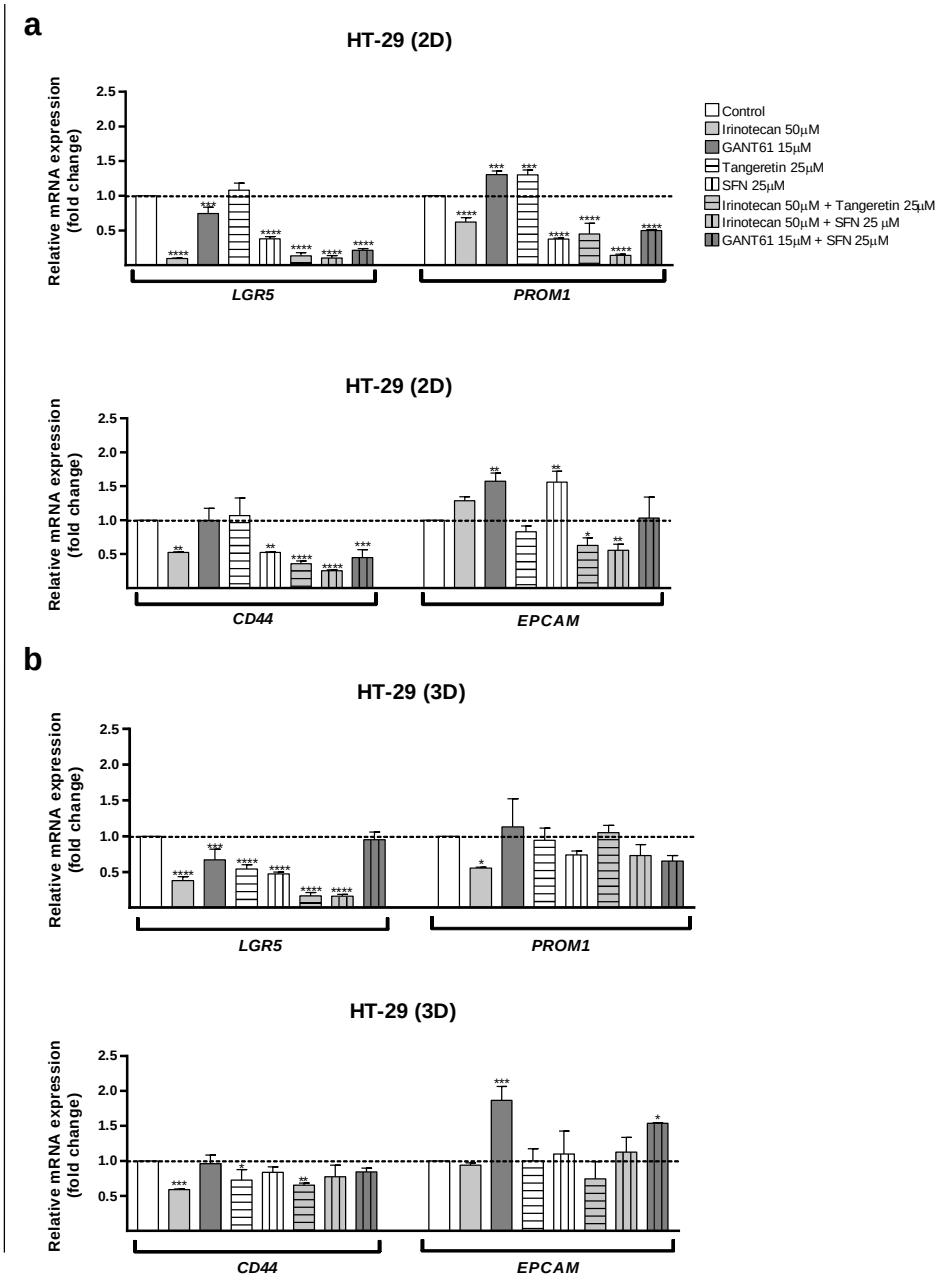

Figure 4.22 – Expression of stemness markers Lgr5 (*LGR5*), CD133 (*PROM1*), CD44 (*CD44*) and EpCAM (*EPCAM*) in HT-29 cells in monolayer (a) and spheroid (b) models. Relative mRNA expression, in fold change, in HT-29 cells, exposed to defined doses of selected agents and combinations of agents for 24h. Normalized to GAPDH and β-actin. Results are expressed as mean of at least one experiment performed in triplicate ± SD. *p-value <0.05, **p-value <0.01, ***p- value <0.001 and ****p-value <0.0001 are relative to control. Legend is common to all graphs

Overall, these results suggest that all five combinations tested are apparently able to reduce the presence of CSCs on HT-29 cells in a monolayer model. Moreover, it appears that combinations including irinotecan are more effective than those including GANT61, similar to what is suggested by our results from section 4.3.2.

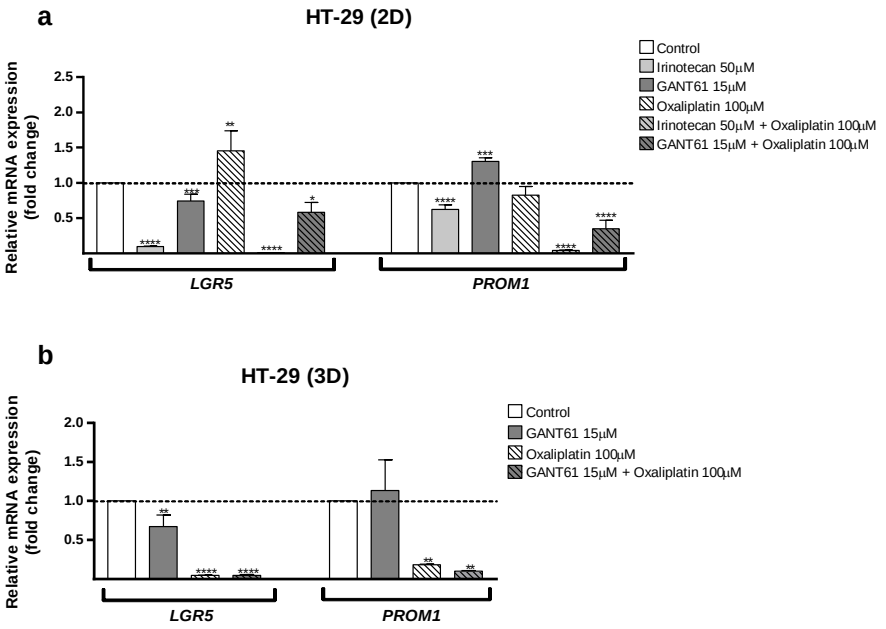

Figure 4.23 – Expression of stemness markers, Lgr5 (*LGR5*), CD133 (*PROM1*), CD44 (*CD44*) and EpCAM (*EPCAM*) in HT-29 cells in monolayer (a) and aggregate (b) models. Relative mRNA expression, in fold change, in HT-29 cells, exposed to defined doses of selected agents and combinations of agents for 24h. Normalized to GAPDH and β-actin. Results are expressed as mean of at least one experiment performed in triplicate ± SD. *p-value <0.05, **p-value <0.01, ***p- value <0.001 and ****p-value <0.0001 are relative to control.

The same treatment panel on HT-29 cells, in an aggregate model (Figures 4.22 b and 4.23 b), led to considerably different results. Here, we observe the most promising effect after treating cells with GANT61 combined with oxaliplatin (Figure 4.23 b), which led to a significant reduction of *LGR5* and *PROM1*, however, assessing the expression of additional marker would be crucial to confirm these results. Interestingly, oxaliplatin induced significantly decreased levels of both markers on this cell model and appears to significantly enhance the effects of isolated GANT61 suggesting that circulating CSC aggregates may be sensitive to oxaliplatin. Isolated irinotecan, led to significant decrease on *LGR5*, *PROM1* and *CD44* and unaffected levels of *EPCAM*. It is interesting to note that this results were similar to those obtained in section 4.3.2, even though we here used a lower dose of 50μM compared to the 89,1μM used in the latter assay. Different from the observed in the monolayer model, combining either SFN or tangeretin with irinotecan seems to have no effect on the expression of *PROM1* and *EPCAM*. Despite the accentuated decrease of *LGR5*, it seems that none of these combinations was as effective in HT-29 aggregate model, as it was for the monolayer model. Additionally, combining GANT61 to SFN also revealed no effect on reducing stemness markers, on the contrary, it seems to induce slight increase on *EPCAM* levels. Together, these results suggest that oxaliplatin, either isolated or in combination with GANT61 is the most promising treatment preventing the presence of CSCs, regarding our aggregate model. Nevertheless, irinotecan-tangeretin and irinotecan-SFN combinations do not significantly reduce the effect of isolated irinotecan, suggesting these combinations are yet to be considered for treatment, regarding their effect on the expression of other markers.

4.6.3. Effect of combined compounds in the expression of EMT markers on 2D and 3D cell culture models of HT-29 CRC cell line

EMT has been implicated in the invasive and metastatic behaviour of cancer cells, already mention in sections 1.8 (Kalluri and Weinberg, 2009; Busch et al., 2014). Among the great variety of described EMT markers, we here analyse the expression of *VIM*, *ZEB1*, *CDH1* and *SNAI1* (detailed in section and 4.3.3) on HT-29 monolayer (Figures 4.24 a and 4.25 a) and aggregate (Figures 4.24 b and 4.25 b) cell models, 24h after treatment.

In line with the results obtained in section 4.3.3, after treatment with the estimatedIC_{50} doses of isolated irinotecan, GANT61 and SFN, none of the treatments tested in this section was promising for impairing EMT on the HT-29 monolayer cell model. Combining irinotecan to SFN (Figure 4.24 a) led to increased expression of *SNAI1* and maintained levels of *CDH1*, *VIM* and *ZEB1*, eventually compatible with partial EMT. Nevertheless, irinotecan-SFN was able to counteract the significant overexpression of *VIM* of isolated irinotecan treatment. It is also interesting to highlight that isolated SFN led to downregulation of *VIM* and that this effect was lost after combined treatment. Combining irinotecan with tangeretin (Figure 4.24 a), despite leading to slightly increased *CDH1* levels, led to overexpression of both *VIM* and *SNAI1*, suggestive of a mesenchymal phenotype, rather than epithelial. The combination irinotecan-oxaliplatin (Figure 4.25 a) led to reduced expression of *ZEB1* and *CDH1* and unaffected expression of *VIM*, not suggestive of EMT reduction. However, this combination enhanced the effect of both compounds on the expression of *VIM*, which was significantly overexpressed after treatment with either of the isolated compound. GANT61, in combination to SFN (Figure 4.24 a) had no improvement on the effects of either of the isolated compounds, on the contrary it seems that combined treatment abolished the effect of isolated SFN on reducing *VIM* expression and improved the effect of GANT61 on the overexpression of *ZEB1*. Combining GANT61 with oxaliplatin (Figure 4.25 a) revealed no promising effect on impairing EMT, on the contrary, it led to significant over expression of *VIM* and unaltered expression of both *ZEB1* and *CDH1*.

Treating HT-29 aggregates with irinotecan combined with tangeretin (Figure 4.24 b) showed no promising results on EMT reduction. On the contrary, this combination maintained the significant overexpression of *SNAI1* obtained after treating these cells with isolated irinotecan and showed no improvements regarding the expression of other EMT markers. Irinotecan together with SFN (Figure 4.24 b), led to a downregulation of *ZEB1* but had no effect on the expression of other EMT markers. Thus, even though a generalized synergic effect was not achieved, this combination did not worsen the general effect of isolated irinotecan on EMT, suggesting it shall yet be considered regarding its effect on other markers. GANT61 combined with SFN (Figure 4.24 b) led to overexpression of *CDH1*, however, it also promoted the overexpression of EMT inducer markers *SNAI1* and *ZEB1*, suggestive of an EMT inducing signature. This combination led to a loss of isolated GANT61 effect, which led to decreased *SNAI1* levels and maintained expression of *ZEB1*. Oxaliplatin also did not enhance the effects of GANT61 on reducing EMT (Figure 4.25 b), since in combination, these compounds led to significant decreased expression of *CDH1* and *ZEB1*, allied to maintained expression of *VIM*. The assessment of other markers, such as *SNAI1* would be necessary to better understand the effects regarding combinations including oxaliplatin.

Overall, these results suggest that none of the tested compounds or combinations of compounds were able to efficiently reduce EMT induction, associated to increased epithelial signature on our monolayer and aggregate models of HT-29 cell line.

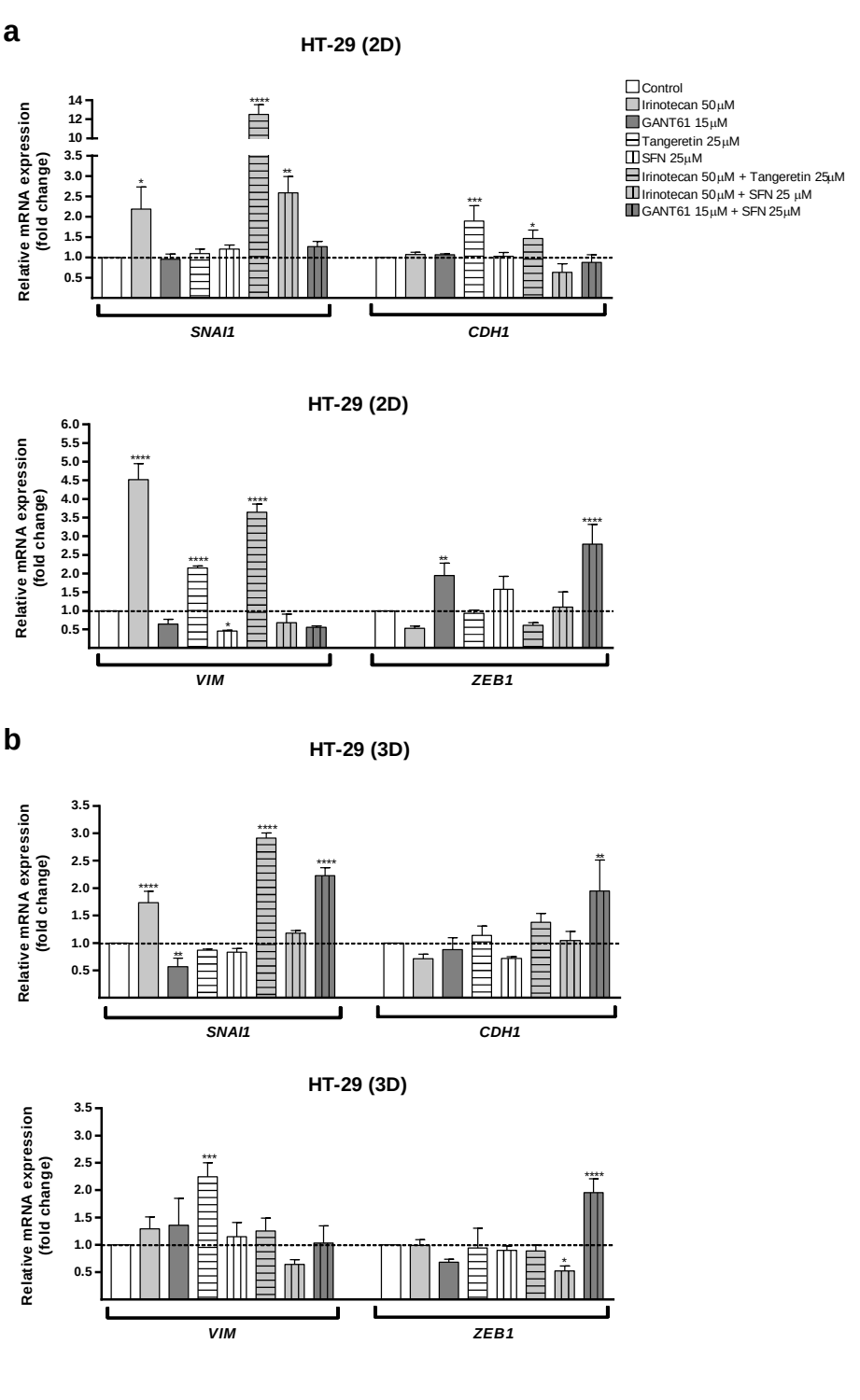

Figure 4.24 – Expression of EMT markers *SNAI1* (Snail), *CDH1* (E-cadherin), *VIM* (vimentin) and *ZEB1* (Zeb1) in HT-29 cells in monolayer (a) and aggregate (b) models. Relative mRNA expression, in fold change, in HT-29 cells, exposed to defined doses of selected agents and combinations of agents for 24h. Normalized to GAPDH and β-actin. Results are expressed as mean of at least one experiment performed in triplicate ± SD. *p-value <0.05, **p-value <0.01, ***p-value <0.001 and ****p-value <0.0001 are relative to control. Legend is common to all graphs.

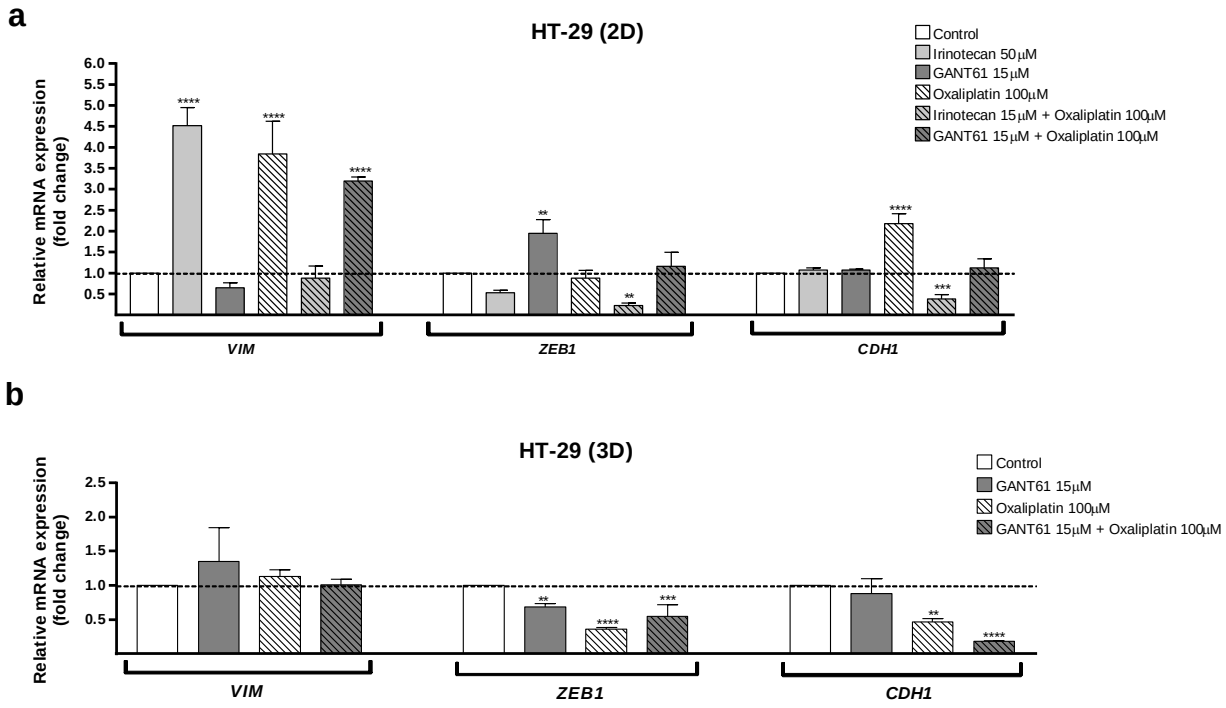

Figure 4.25 – Expression of EMT markers, *CDH1* (E-cadherin), *VIM* (vimentin) and *ZEB1* (Zeb1)in HT-29 cells in monolayer (a) and aggregate (b) models. Relative mRNA expression, in fold change, in HT-29 cells, exposed to defined doses of selected agents and combinations of agents for 24h. Normalized to GAPDH and β-actin. Results are expressed as mean of at least one experiment performed in triplicate ± SD. *p-value<0.05, **p-value<0.01, ***p-value<0.001 and ****p-value<0.0001 are relative to control.

4.6.4. Effect of combined compounds in the expression of Wnt/β-catenin signaling pathway markers on 2D and 3D cell culture models of HT-29 CRC cell line

Wnt signaling pathway aberrant activation has been implicated in tumor initiation and progression in CRC, as mentioned in section 1.6 (Brabletz *et al.*, 2002). We here assessed the expression of a series of Wnt/β-catenin signaling pathway markers on HT-29 monolayer (Figure 4.26) and aggregate (Figure 4.27) cell models, 24h after treatment. These markers include specific genes involved in signaling transduction and target genes (*CTNNB, AXIN2, TCF7L2*, *TCF7L2[1-6], ABCB1* and *MMP7*). In addition to the markers used and described in section 4.3.4, herein we used *MMP7,* encoding a matrix metalloproteinase (Matrilysin) regulated by Wnt/β-catenin signaling pathway which overexpression has been associated to invasion in CRC cells (Brabletz *et al.*, 1999; Kostova *et al.*, 2014).

Irinotecan, either isolated or combined with tangeretin or SFN led to overexpression of *AXIN2*, which would be suggestive of activation of WNT target genes. These results are suggestive that irinotecan, either isolated or in a combination context, does not reduce Wnt/β-catenin signaling. Additionally, it appears that these treatments do not overcome resistance mechanisms associated to increased expression of *ABCB1*. In fact, it seems that irinotecan prevents the effect of isolated SFN and tangeretin in reducing the expression of *ABCB1*, suggesting that irinotecan may be responsible for the triggering resistance mechanisms associated to the increased expression of the mentioned marker.

Combining GANT61 to SFN resulted in increased levels of *AXIN2*, *MMP7* and *ABCB1*, which, despite the unaffected expression of *CTNNB1* and *TCF7L2*, is suggestive of WNT signaling activation.

Moreover, no general beneficial effect is observed by GANT61-SFN treatment, compared to either of the isolated compounds.

Overall, these results suggest that none of the combinations are effective in reducing Wnt/β-catenin signaling and also that no combination generally enhanced the effect of isolated compound treatments.

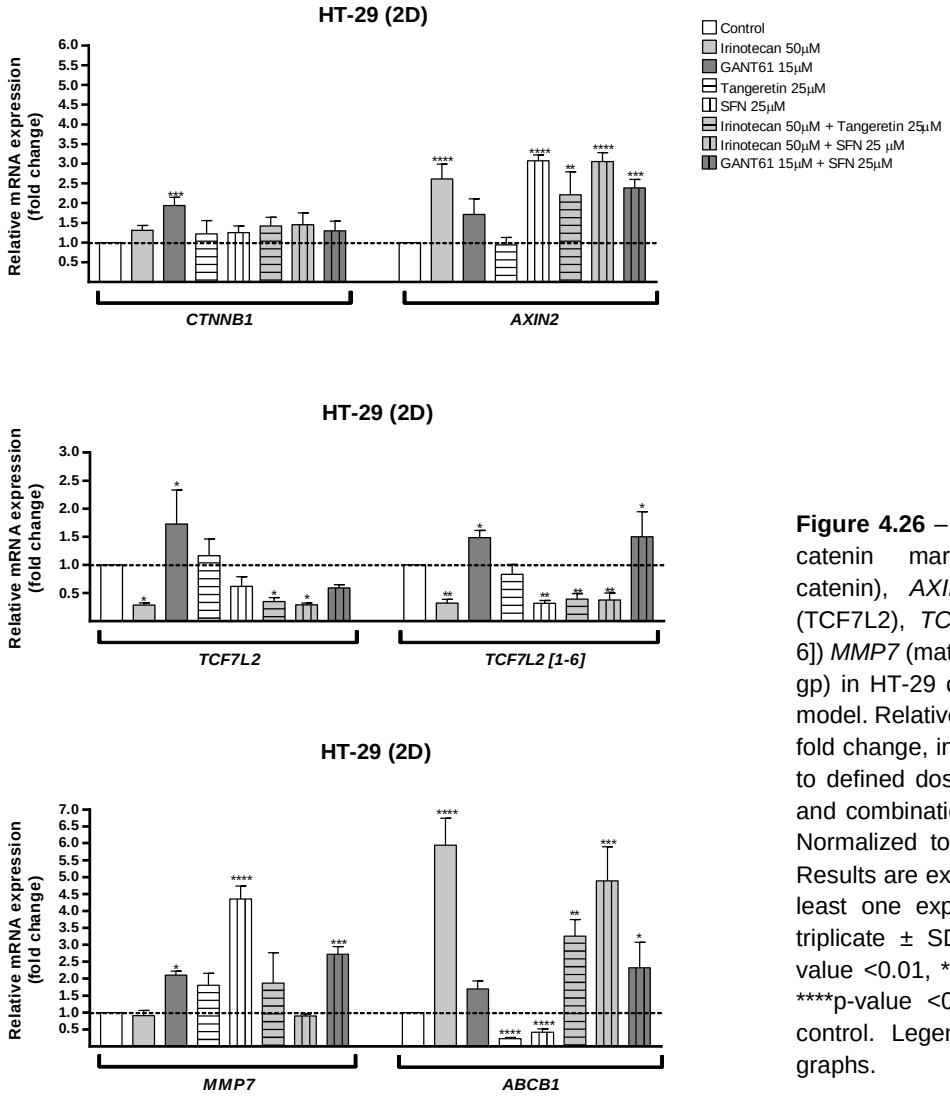

Figure 4.26 – Expression of Wnt/ β-catenin markers *CTNNB1* (β-catenin), *AXIN2* (Axin2), *TCF7L2* (TCF7L2), *TCF7L2[1-6]* (TCF7L2[1-6]) *MMP7* (matrilysin) and *ABCB1* (P-gp) in HT-29 cells in monolayer cell model. Relative mRNA expression, in fold change, in HT-29 cells, exposed to defined doses of selected agents and combinations of agents for 24h. Normalized to GAPDH and β-actin. Results are expressed as mean of at least one experiment performed in triplicate ± SD. *p-value<0.05, **p-value <0.01, ***p- value <0.001 and ****p-value <0.0001 are relative to control. Legend is common to all graphs.

Our aggregate cell model (Figure 4.27), revealed significantly different expression patterns. For instance, combining irinotecan with tangeretin led to decreased levels of *TCF7L2*, *MMP7* and *ABCB1*, allied with unaffected expression of the other markers. These results are in line with the hypothesis of either maintained or slightly reduced Wnt/β-catenin signaling by the reduced expression of the main transcription factor of this pathway and target genes. Moreover, tangeretin, improved the effect of irinotecan by a significant reduction of *ABCB1* levels, which was overexpressed after treatment with the isolated compound, suggestive of a promising synergic effect of this compounds in reducing WNT signaling. Combined with SFN, irinotecan led to overexpression of *AXIN2* and reduced expression of *TCF7L2[1-6]*, sorting no effect on the expression of other markers, suggestive of signaling activation.

However, it should be taken into account that *AXIN2* represents a Wnt/β-catenin target gene but also a promoter of β-catenin stabilization in the cytoplasm (Said *et al.*, 2014; Choi *et al.*, 2015; El Khoury *et al.*, 2016). Additionally, SFN seems to prevent the overexpression of *ABCB1* observed as an effect of treatment with isolated irinotecan. On the other hand, combining GANT61 with SFN resulted in increased expression of *AXIN2* and *MMP7*, allied to unaffected expression of other marker, which may be suggestive of WNT/β-catenin signaling activation. Regarding this aggregate model and its potential similarities to circulating cell aggregates, also taking into account that WNT signaling overactivation has been reported in association to tumor initiation and progression (Krishnamurthy and Kurzrock, 2018), it is suggested by our results that the combinations of irinotecan with tangeretin or SFN could be effective for treating initial stages of tumorigenesis, potentially preventing metastasis (Albuquerque and Pereira, 2018).

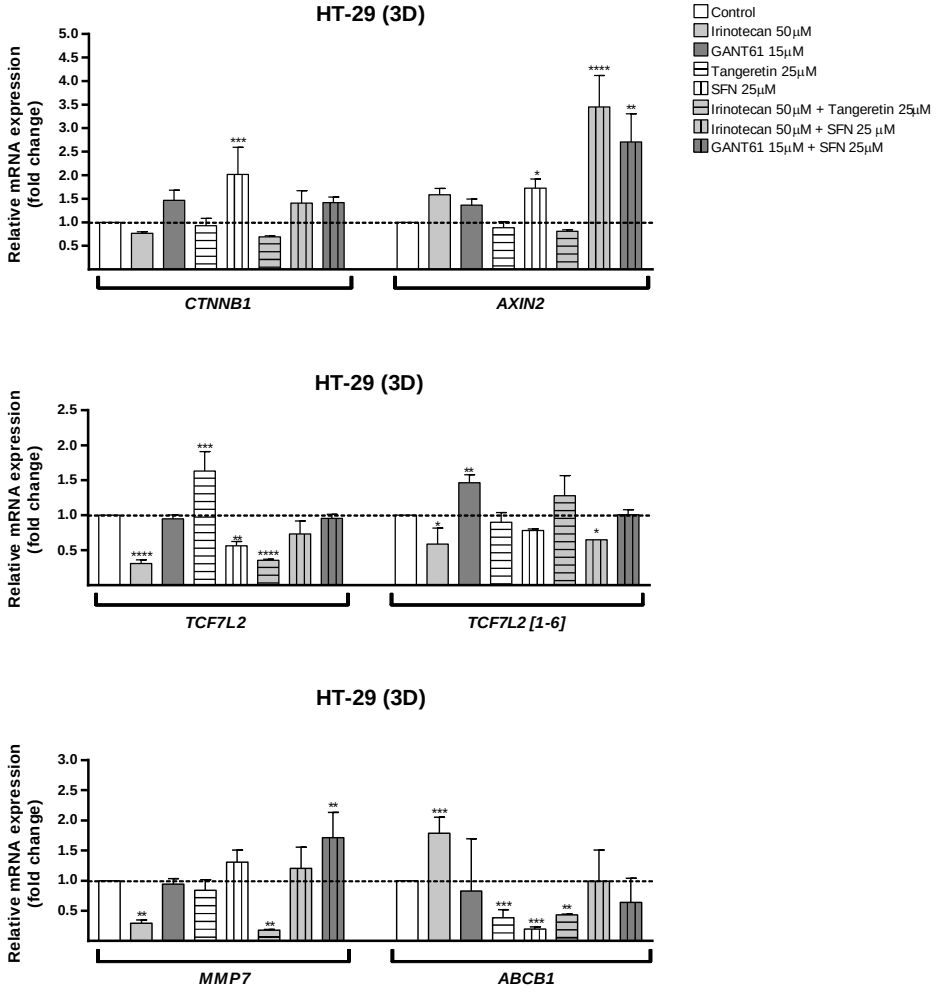

Figure 4.27 – Expression of Wnt/ β-catenin signaling pathway markers *CTNNB1* (β-catenin), *AXIN2* (Axin2), *TCF7L2* (TCF7L2), *TCF7L2[1-6]* (TCF7L2[1-6]) *MMP7* (matrilysin) and *ABCB1* (P-gp) in HT-29 cells in aggregate cell model. Relative mRNA expression, in fold change, in HT-29 cells, exposed to defined doses of selected agents and combinations of agents for 24h. Normalized to GAPDH and β-actin. Results are expressed as mean of at least one experiment performed in triplicate ± SD. *p-value <0.05, **p-value <0.01, ***p- value <0.001 and ****p-value <0.0001 are relative to control. Legend is common to all graphs.

4.6.5. Effect of combined compounds in the expression of Shh/Gli signaling pathway markers on 2D and 3D cell culture models of HT-29 CRC cell line

As a final point, we tested the effect of our treatment panel on the expression of a series of Shh/Gli signaling pathway markers after treating HT-29 cells in monolayer (Figure 4.22 a) and aggregate (Figure 4.22 b) cell models. These markers include *GLI1*, as the main activator of this pathway, which expression is activated upon Shh signaling activation; *VAX2,* a direct target gene of Shh/Gli known to regulate the expression of Wnt/β-catenin signaling antagonists including that of *dnTCF7L2*, a truncated form of *TCF7L2* unable to bind b-catenin in the nucleus (Kim and Lemke, 2006; Vacik *et al.*, 2011); *TGFB1*, a factor previously shown to induce Gli1 expression through direct activation of Gli2, independent from the PTCH/SMO axis (Mauviel *et al.*, 2011; Javelaud *et al.*, 2012); *PTCH1*, the transmembrane receptor Patched1, activated by specific ligands, which controls the downstream modification of Gli transcriptional effectors, being also a transcriptional target of Gli factors (Kogerman *et al.*, 2004; Cohen *et al.*, 2015).

Concerning treatment of HT-29 monolayer cells, shown in figures 4.28-a and 4.29-a, our results suggest that combining irinotecan with SFN maintains or slightly reduces SHH signaling, by not affecting the expression off *GLI1*, *VAX2* and *TGFB1* and leading to decreased expression of *PTCH1*. The downregulation of *PTCH1* together with maintained expression of the other tested markers does not provide accurate information regarding Shh/Gli signaling activation, since this marker represents a direct target of the SHH pathway yet, it plays an inhibitory role by inhibiting SMO in the absence of HH ligand, hence inhibiting downstream signaling. Thus, these results may be suggestive of either reduced or maintained Shh/Gli signaling, respectively. Interestingly, SFN appears to improve the effects of isolated irinotecan, which treatment had led to significant overexpression of *VAX2* and *TGFB1*. In the presence of tangeretin, irinotecan appears to induce SHH signaling, suggested by the overexpression of *GLI1*, *VAX2* and *TGFB1*, allied to maintained expression of *PTCH1*. Combining irinotecan and oxaliplatin seems promising in reducing SHH signaling in this HT-29 monolayer cell model. This combination led to decreased expression of both target genes *VAX2* and *PTCH1*, suggesting signaling reduction. Moreover, the strong synergic effect of this combination is shown, regarding the fact that in isolated treatment, oxaliplatin led to increased expression of *GLI1* and, as well as irinotecan, to significant increased levels of *VAX2*, both indicative of signaling activation.

GANT61 combined with SFN led to overexpression of *TGFB1* and *GLI1* and to a downregulation of *VAX2* and *PTCH1*. As mentioned in section 4.3.4, GANT61 acts as an active Shh/Gli pathway inhibitor, through binding Gli1 protein, Gli1-DNA complex or DNA itself, inhibiting Gli-induced transcription (Agyeman *et al.*, 2015). Thus, overexpression of GLI1 after GANT61 treatment for 24h may not indicate actual signaling activation, instead, the induced expression of *GLI1* may result of positive feedback mechanisms associated to downregulation of target genes, for instance, *GLI1* transcriptional activation by Gli2 through TGFβ (Javelaud *et al.*, 2012). Therefore, the synergic effect between GANT61 and SFN appears not sufficient to prevent positive feedback mechanisms, potentially through induction of *TGFB1* and therefore, increased *GLI1* mRNA levels. Regarding the nature of GANT61 and its mechanism of action, we would expect to obtain Shh/Gli signaling reduction or inactivation, which is not suggested in our results after treating HT-29 cells in a monolayer model. These results may instead

suggest that the used dose of 15µM and/or the exposure time of 24h is not sufficient to effectively suppress Shh/Gli signaling. In fact, most studies exploring the effect GANT61 treatment in cancer cells, refer to higher doses and/or higher time exposures than the ones used in this work, namely in this chapter using treatment combinations (Mazumdar *et al.*, 2011b; Srivastava *et al.*, 2014; Kurebayashi *et al.*, 2017). It is important to mention, however, that these lower doses were used in this work following results of cytotoxicity in the normal colon cell line. Therefore, higher GANT61 doses may me more effective but are not therapeutically useful. Targeting these and other markers, at the protein level and complement with signaling activity assays (luciferase assay, for example) would be essential to analyse pathway activation after treatment with GANT61. Moreover, as *PTCH1* functions also as a tumour suppressor upstream in SHH pathway, this may instead agree with a SHH activation suggested by increased *GLI1* and *TGFB1* mRNA levels. Another hypothesis is that Gli1 transcription is induced by Gli2 through TGFβ, generating a positive feedback mechanism. Once more, additional markers, such as Gli2 and complementary assays would be essential to understand the effect of our treatments in this pathway. Interestingly, combining GANT61 to oxaliplatin did not affect *GLI1* levels, even though the increased expression of *TGFB1*. Moreover, *GLI1* overexpression was observed after treatment with either isolated compound, suggesting that this combination, despite not suggestive of reducing SHH signaling, acts in synergy and seems to prevent Shh/Gli pathway overactivation.

Concerning treatment of HT-29 cell in an aggregate model (Figures 4.28 b and 4.29 b), our results point GANT61-oxaliplatin as the only combination with promising effects on reducing Shh/Gli signaling. This combination led to decreased expression of both *VAX2* and *PTCH1* target genes. As mentioned before in the present section, the binding of GANT61 at the protein, DNA-Gli complex and DNA levels (Agyeman *et al.*, 2015), inhibiting target gene activation, may trigger positive feedback mechanisms inducing *GLI1* expression. Thus, despite the significantly induced expression of *GLI1* by this combination, these results suggest a significant decrease in Shh/Gli signaling. Nevertheless, assessing protein levels by western blot and signaling activation through a luciferase assay, for example, is essential to confirm the obtained results. All the other tested compound combinations, either appear to induce or maintain SHH signaling and none showed no enhancing effect when compared to treatment with isolated compounds.

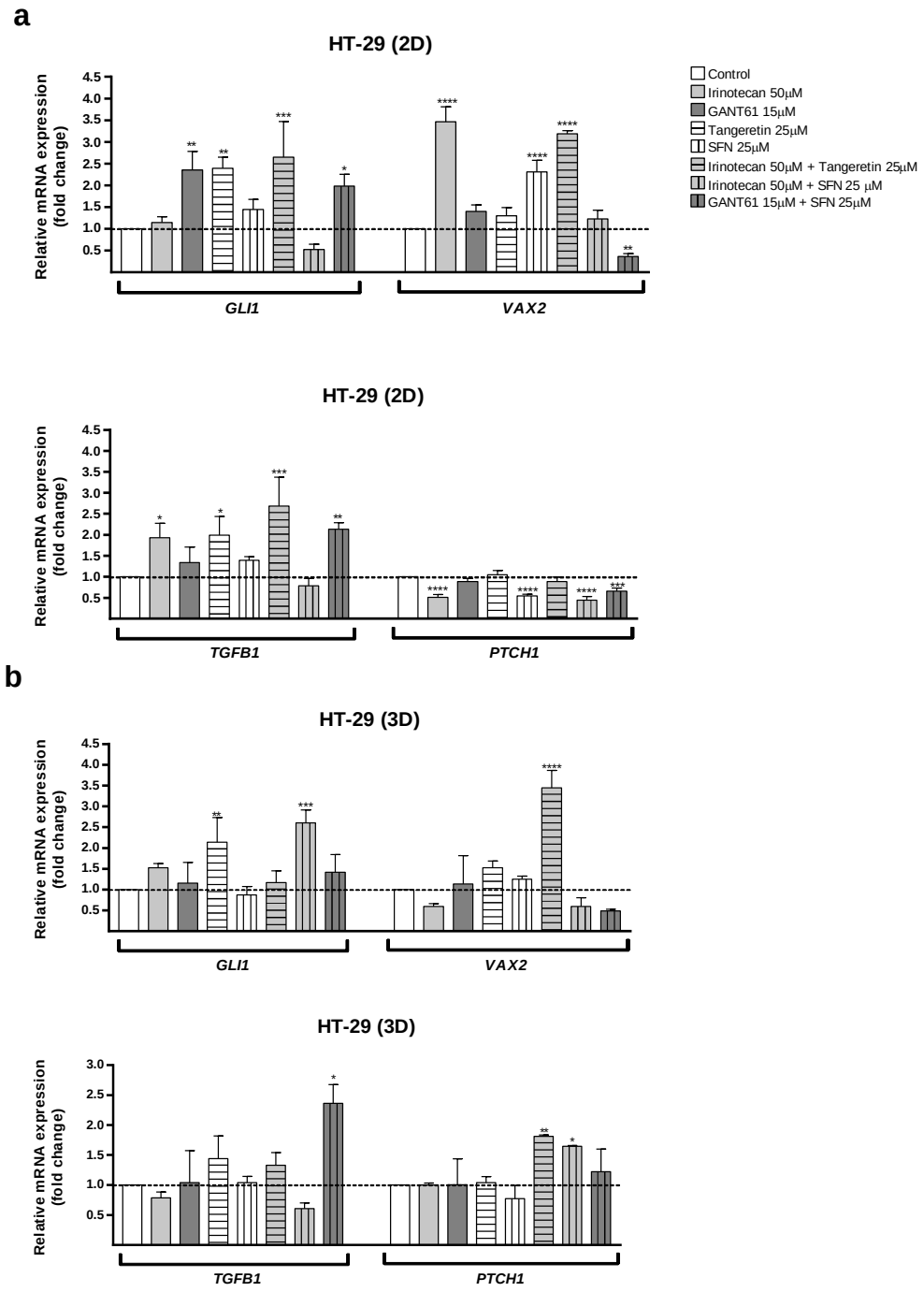

Figure 4.28 – Expression of Shh/Gli signaling pathway markers *GLI1* (Gli1), *VAX2* (Vax2), *TGFB1* (TGFβ1) and *PTCH1* (PTCH1*)* in HT-29 cells in monolayer (a) and aggregate (b) cell models. Relative mRNA expression, in fold change, in HT-29 cells, exposed to defined doses of selected agents and combinations of agents for 24h. Normalized to GAPDH and β-actin. Results are expressed as mean of at least one experiment performed in triplicate ± SD. *p-value <0.05, **p-value <0.01, ***p- value<0.001 and ****p-value<0.0001 are relative to control. Legend is common to all graphs.

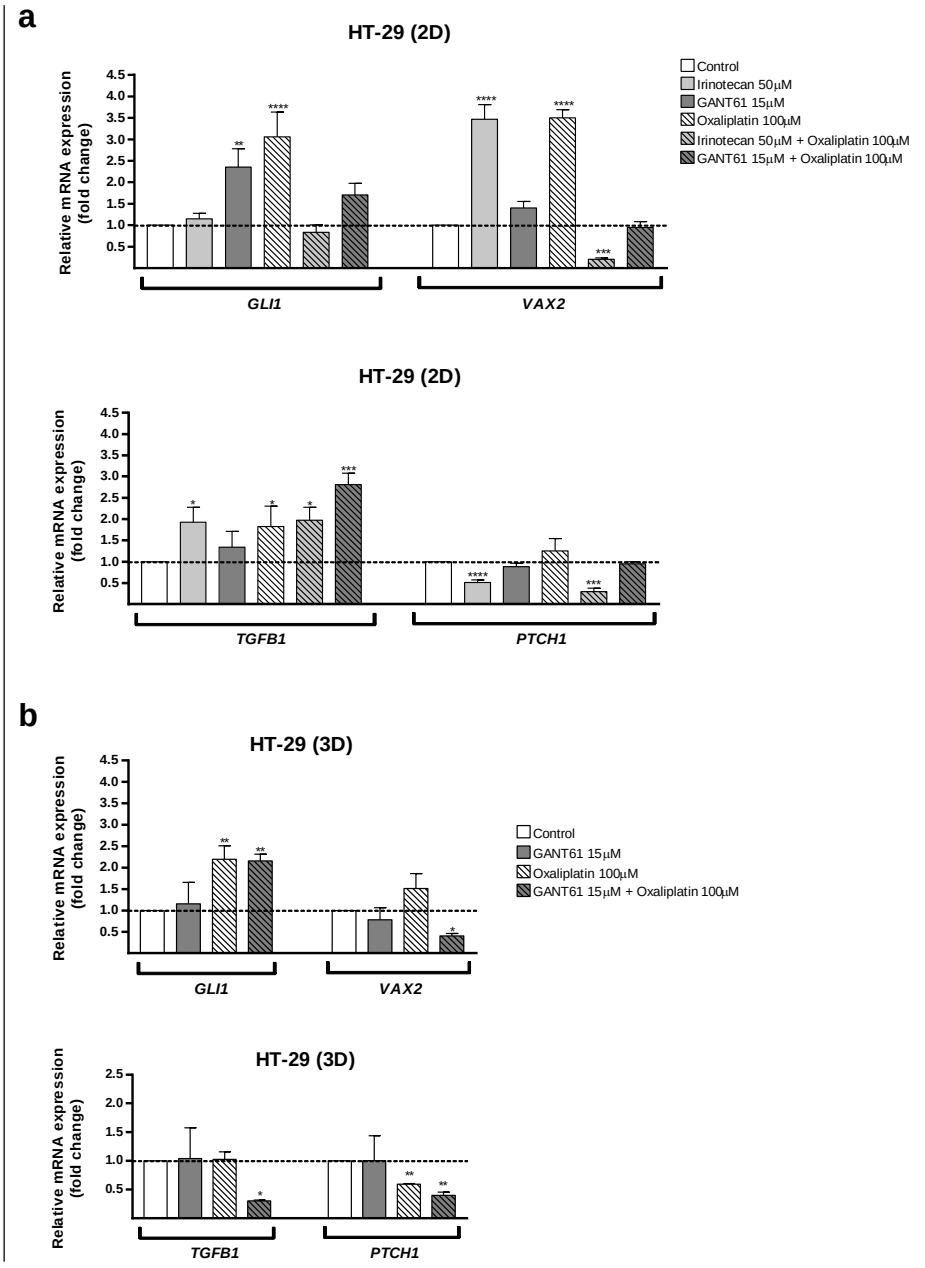

Figure 4.29 – Expression of Shh/Gli signaling pathway markers *GLI1* (Gli1), *VAX2* (Vax2), *TGFB1* (TGFβ1) and *PTCH1* (PTCH1*)* in HT-29 cells in monolayer (a) and aggregate (b) cell models. Relative mRNA expression, in fold change, in HT-29 cells, exposed to defined doses of selected agents and combinations of agents for 24h. Normalized to GAPDH and β-actin. Results are expressed as mean of at least one experiment performed in triplicate ± SD. *p-value <0.05, **p-value <0.01, ***p- value <0.001 and ****p-value <0.0001 are relative to control. Legends in panels a and b are common to all graphs in the respective panel.

4.7 Anti-cancer effect of combined compounds in 2D and 3D cell models of the HT-29 CRC cell line.

This section aims to summarise the results discussed in section 4.6 and present the most promising effect observed for each tested combination of agents. This analysis is of great relevance for understanding the effect of each of our selected combinations on the main pathways involved in tumorigenesis and metastasizing processes in CRC and define their potential as a complement for treating CRC patients.

4.7.1 Anti-cancer effect of irinotecan combined with Tangeretin or SFN in 2D and 3D cell models of HT-29 CRC cell line.

As illustrated in figure 4.30, treating HT-29 cells in a monolayer model, with a combination of irinotecan and tangeretin appears to induce impairment of cell cycle progression and reduce stemness, by significant overexpression of *CDKN1A*, related to G1/S arrest and significant decreased expression of stemness markers, respectively. However, the combination appears to significantly induce EMT and Shh/Gli signaling pathway. Regarding the effect of this combination in Wnt/β-catenin pathway, our results suggest signaling activation, through overexpression of *AXIN2* and maintained levels of *CTNNB1* and *MMP7*. Moreover, the increasing of *ABCB1* mRNA levels may suggest the activation of resistance mechanisms by these cells to the combined agents (Sui *et al.*, 2012; Jensen *et al.*, 2015). Interestingly, the expression patterns of Wnt/ β-catenin signaling pathway markers were similar to these, after treating HT-29 monolayer cells with a combination of irinotecan with SFN. This second combination, irinotecan/SFN (Figure 4.30), is also suggested by our results to induce cell cycle arrest, by inducing *CDKN1A* expression, and to effectively impair stemness through a significant reduction on the expression of the tested stemness markers. Despite increased *SNAI1* mRNA levels, the expression of the other EMT markers is not compatible with EMT induction since none of the markers was significantly increased. Moreover, the increase observed in *SNAI1* is much lower than in the combination with tangeretin. Shh/Gli signaling appears to be maintained or slightly reduced after treatment with this combination.

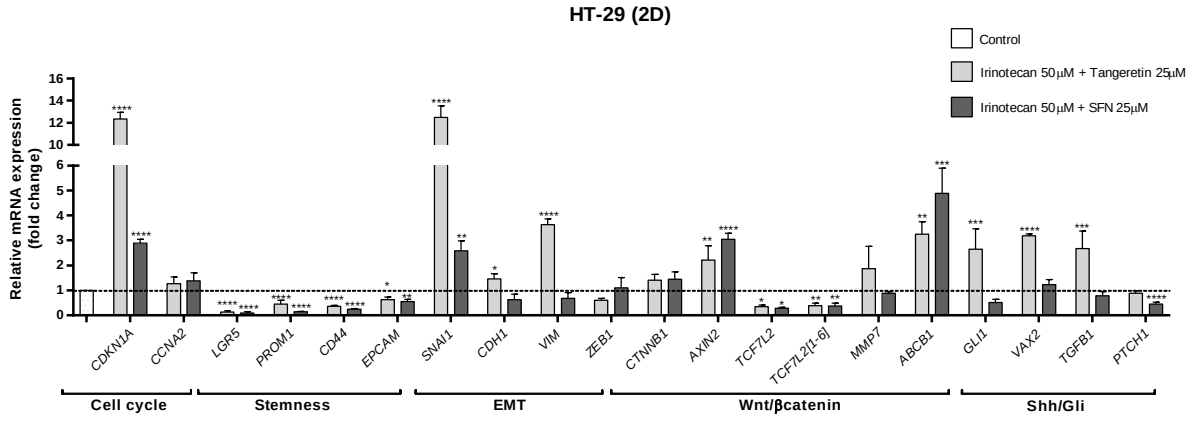

Figure 4.30 – Expression of markers involved in main pathways implicated in CRC tumorigenesis and metastasizing after treating HT-29 monolayer cells with irinotecan/tangeretin and irinotecan/SFN agent combinations. Relative mRNA expression, in fold change, in HT-29 monolayer cell model, exposed to defined doses of selected combinations of agents for 24h. Normalized to GAPDH and β-actin. Results are expressed as mean of at least one experiment performed in triplicate ± SD. *p-value<0.05, **p-value<0.01, ***p- value<0.001 and ****p-value<0.0001 are relative to control.

Results concerning combined treatments in an aggregate cell model of HT-29 cells, are illustrated in figure 4.31. These results suggest that combining irinotecan to tangeretin affects cell cycle, by overexpression of *CDKN1A*. Moreover, this combination appears to slightly reduce or maintain Wnt/β-catenin signaling by decreasing expression of *TCF7L2*, *MMP7* and *ABCB1* markers, allied to a maintained expression of *CTNNB1* and *AXIN2*. However, it was not able to induce reduced expression

of two out of the four tested stemness markers, suggesting that this combination may not be so effective in reducing stemness on HT-29 aggregates. Moreover, in the presence of tangeretin, irinotecan led to a significant increased expression of *SNAI1*, allied to unaffected expression of the other EMT markers, suggesting also some ineffectiveness impairing this mechanism. The significantly increased levels of *VAX2* and *PTCH1* after treatment are suggestive of overactivation of the Shh/Gli signaling pathway. Wnt/β-catenin and Shh/Gli appear to be the only pathways affected by treatment with the combination irinotecan/SFN on HT-29 aggregate cell model. This combination led to significant increased expression of *AXIN2* and decreased expression of *TCF7L2[1-6]*, suggestive WNT activation. Additionally, this treatment led to a significant overexpression of *GLI1* and *PTCH1*, together with unaltered expression levels of *VAX2* and *TGFB1*, suggesting pathway activation.

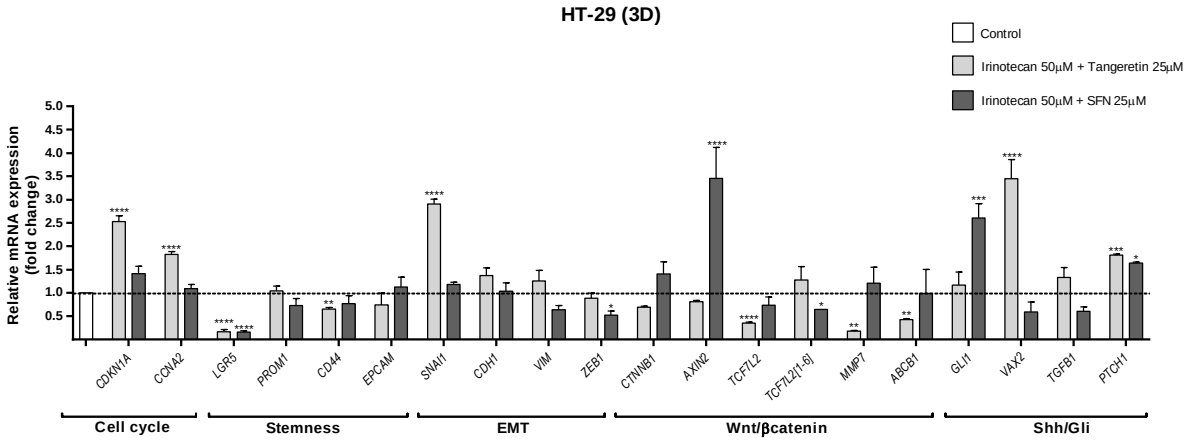

Figure 4.31 – Expression of markers involved in main pathways implicated in CRC tumorigenesis and metastasizing after treating HT-29 aggregate cell model with irinotecan/tangeretin and irinotecan/SFN agent combinations. Relative mRNA expression, in fold change, in HT-29 aggregate cell model, exposed to defined doses of selected combinations of agents for 24h. Normalized to GAPDH and β-actin. Results are expressed as mean of at least one experiment performed in triplicate ± SD. *p-value<0.05, **p-value<0.01, ***p- value<0.001 and ****p-value<0.0001 are relative to control.

4.7.2 Anti-cancer effect of GANT61 combined with SFN in 2D and 3D cell models of HT-29 CRC cell line.

In our HT-29 monolayer cell model (Figure 4.32), the combination GANT61/SFN appears to induce G1/S cell cycle arrest, through overexpression of *CDKN1A* and to prevent stemness through reduction of *LGR5*, *PROM1* and *CD44* mRNA levels. The effect of this combination on Shh/Gli signaling is unclear, regarding the possible feedback mechanisms discussed in section 4.6.5, thus, despite the reduced levels of Shh/Gli target genes, additional experiments are essential to analyse pathway activation after treatment with GANT61. Moreover, this combination appears to induce EMT on our cell model, through expression of *ZEB1*. In addition, results point to significant induction Wnt/β-catenin signaling, suggested by the overexpression of *MMP7*, *ABCB1* targets and *AXIN2.*

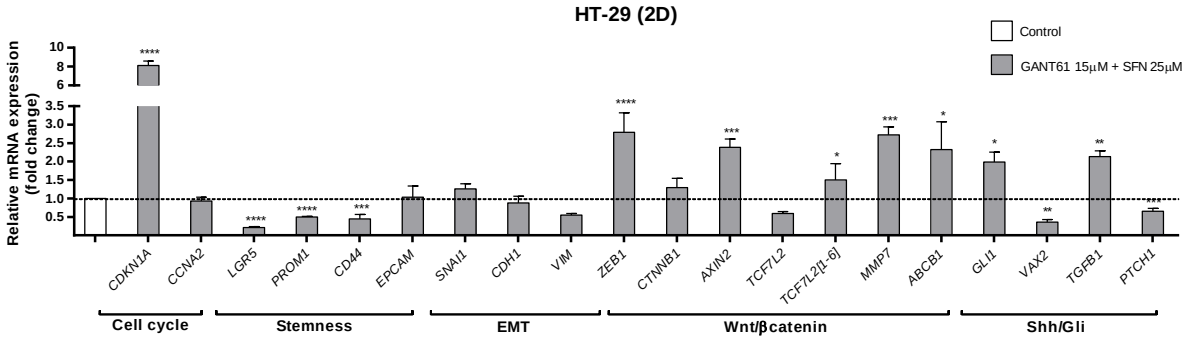

Figure 4.32 – Expression of markers involved in main pathways implicated in CRC tumorigenesis and metastasizing after treating HT-29 monolayer cell model with GANT61/SFN combination. Relative mRNA expression, in fold change, in HT-29 monolayer cell model, exposed to defined doses of selected combinations of agents for 24h. Normalized to GAPDH and β-actin. Results are expressed as mean of at least one experiment performed in triplicate ± SD. *p-value<0.05, **p-value<0.01, ***p- value<0.001 and ****p-value<0.0001 are relative to control.

Treating HT-29 cells in our aggregate cell model with the combination GANT61/SFN (Figure 4.33), led to significant increase of *CDKN1A* levels, suggesting cell cycle arrest, and appears to induce no effects regarding Shh/Gli signaling pathway. Moreover, this combination appears not to impair stemness and EMT, by the unaffected expression of CSC markers in general, and through significant increase of *SNAI1* and *ZEB1* EMT inducers mRNA levels, respectively. Moreover, these results are suggestive of a Wnt/β-catenin signaling overactivation, given the highly expressed *AXIN2* and *MMP7* target genes, allied to unaffected expression of other markers of this pathway.

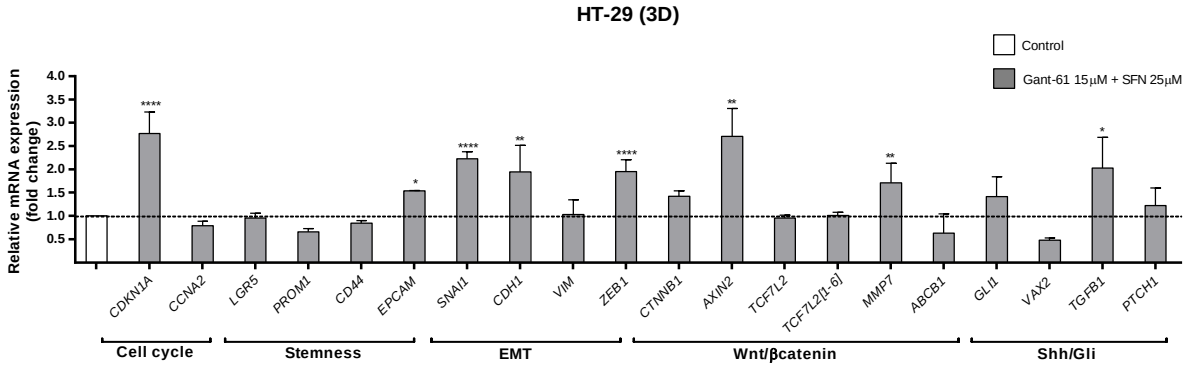

Figure 4.33 – Expression of markers involved in main pathways implicated in CRC tumorigenesis and metastasizing after treating HT-29 aggregate cell model with GANT61/SFN combination. Relative mRNA expression, in fold change, in HT-29 aggregate cell model, exposed to defined doses of selected combinations of agents for 24h. Normalized to GAPDH and β-actin. Results are expressed as mean of at least one experiment performed in triplicate ± SD. *p-value<0.05, **p-value<0.01, ***p- value<0.001 and ****p-value<0.0001 are relative to control.

4.7.3 Anti-cancer effect of irinotecan or GANT61 combined with oxaliplatin in 2D and 3D cell models of HT-29 CRC cell line.

HT-29 cells in a monolayer cell model exposed to the combination irinotecan/oxaliplatin (Figure 4.34), appear to undergo a G1/S cell cycle arrest, induced by increased levels of *CDKN1A* and to significantly reduce stemness through decrease on stemness markers *LGR5* and *PROM1* mRNA levels. Additionally, *ZEB1* expression was reduced by the treatment, however, we cannot assume EMT reduction, considering the reduced levels of *CDH1*, an epithelial marker, induced by this treatment, suggestive of partial EMT. Shh/Gli signaling appear to be reduced after this treatment, regarding the significantly decreased levels of *VAX2* and *PTCH1* targets, allied to unaffected *GLI1* expression. On the other hand, treating this cell model with the GANT61/oxaliplatin combination, led to promising results regarding cell cycle and stemness, through overexpressed *CDKN1A* and significant reduction of *LGR5* and *PROM1* markers, respectively, but not on any of the other tested pathways.

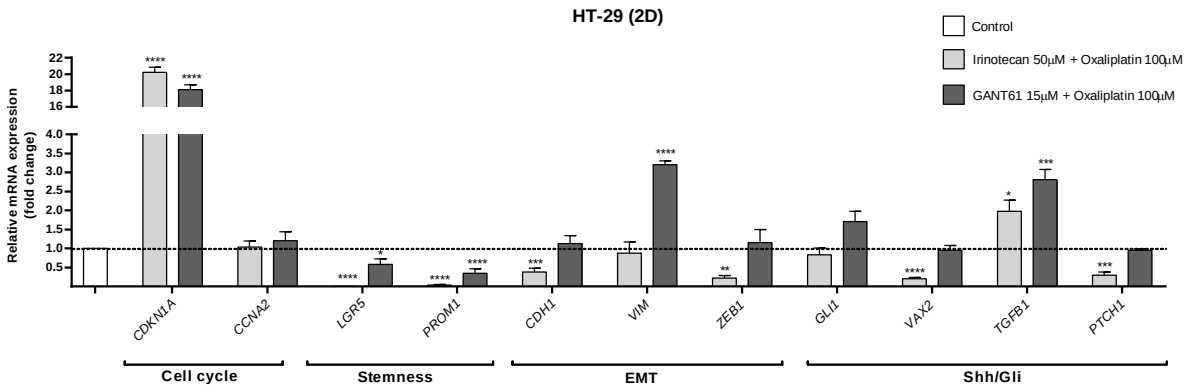

Figure 4.34 – Expression of markers involved in main pathways implicated in CRC tumorigenesis and metastasizing after treating HT-29 monolayer cell model with irinotecan/oxaliplatin and GANT61/oxaliplatin combinations. Relative mRNA expression, in fold change, in HT-29 monolayer cell model, exposed to defined doses of selected combinations of agents for 24h. Normalized to GAPDH and β-actin. Results are expressed as mean of at least one experiment performed in triplicate ± SD. *p-value<0.05, **p-value<0.01, ***p- value<0.001 and ****p-value<0.0001 are relative to control.

Finally, treating HT-29 cells in an aggregate cell model with the combination GANT61/oxaliplatin (Figure 4.35), led to increased expression of *CDKN1A*, suggesting a G1/S cell cycle arrest, to significant reduction on stemness markers *LGR5* and *PROM1*, suggesting its potential for reducing stemness in these cell model and also to an apparent reduction of Shh/Gli signaling, through significantly decreased expression of *VAX2*, *TGFB1* and *PTCH1* markers. However, this combination was unable to induce an epithelial signature on these cells. On the contrary, it led to a significant reduction of the epithelial marker *CDH1* mRNA levels, despite also leading to significant reduction of the EMT inducer *ZEB1,* suggestive of partial EMT. Additional marker implicated in stemness, EMT and Wnt/β-catenin signaling, would need to be assessed in order to better understand the potential of combinations including oxaliplatin.

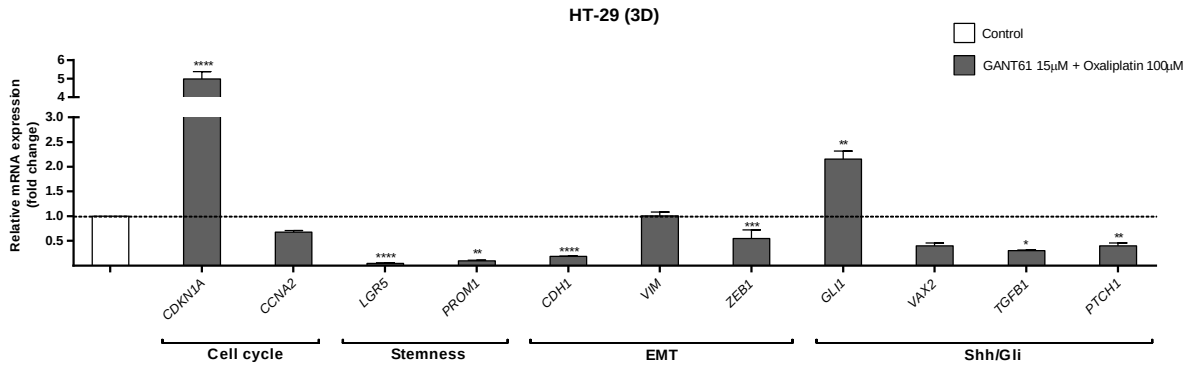

Figure 4.35 – Expression of markers involved in main pathways implicated in CRC tumorigenesis and metastasizing after treating HT-29 aggregate cell model with irinotecan/oxaliplatin and GANT61/oxaliplatin combinations. Relative mRNA expression, in fold change, in HT-29 aggregate cell model, exposed to defined doses of selected combinations of agents for 24h. Normalized to GAPDH and β-actin. Results are expressed as mean of at least one experiment performed in triplicate ± SD. *p-value<0.05, **p-value<0.01, ***p- value<0.001 and ****p-value<0.0001 are relative to control.

5. CONCLUSION

This work has brought innovative data regarding the knowledge of the molecular mechanisms underlying CRC tumorigenesis.

Assessing the expression profiles of *TCF7L2* isoforms comprised in two main fragments (exons 1-5 and exons 12-17), which contain most of the described splicing regions of this gene, is of great relevance for understanding the regulation of the expression of defined isoforms in a specific tumor context and eventually the regulation of this complex gene. Herein, we show the expression of different isoforms, comprised in these two fragments, in CRC patients and CRC cell lines. Moreover, we identified, by RT-PCR followed by Sanger sequencing, 8 of these isoforms, and we concluded that they are differential expressed among patients' samples. Inclusively, some of these isoforms appear to be differentially expressed between CRC and normal tissue (blood leukocytes and normal colon cell line). We hypothesize that different patterns of expressed isoforms may contribute to increased CRC risk and eventually to tumor progression.

Moreover, we showed that, from a panel of 10 tested compounds (cytostatic drugs used in conventional CRC treatment, epigenetic modulators, targeted therapies of specific signaling pathways and nutraceuticals), only five were able to impair proliferation in the LS174T CRC cell line and four in the HT-29 CRC cell line, with only 1/4 in this latter cell line showing a strong impairment. Among these compounds, two appeared to be more efficient. In agreement, at the estimated IC_{50} dose, GANT61 was able to prevent cell cycle progression and stemness, as well as irinotecan, which additionally appears to reduce of Wnt/β-catenin signaling on HT-29 cells. However, most of the IC50 doses also significantly affected proliferation in CCD 841 CoN normal colon cells. Therefore, the understanding of the molecular mechanisms implicated in CRC tumorigenesis and metastasizing process is crucial to find new therapeutic targets, enabling the use of innovative therapeutic strategies that overcome the resistance mechanisms, faced by conventional therapy, and allows the administration of non-cytotoxic doses. Metastatic cells acquire different characteristics, along the EMT process, allowing them to escape the original tumor and establish elsewhere in the body, through their migratory ability. Results presented in this work, showed that irinotecan and GANT61 appear to be promising agents on the impairment of migration in HT-29 CRC cells at non-cytotoxic doses.

Following the line of results, pointing GANT61 and irinotecan as promising agents, we used low doses of these compounds, without cytotoxic effect in normal colon cells and presenting anti-migratory effect, as a basis of a series of compound combinations with low doses of two nutraceuticals and a cytostatic agent: tangeretin, SFN and a oxaliplatin, the latter two affecting HT-29 cells proliferation at cytotoxic doses. As a results of this work, we suggest four promising compound combinations affecting the HT-29 CRC cell line. Combining irinotecan with either oxaliplatin, tangeretin or SFN, appears to induce significant impairment of cell cycle progression, stemness, Shh/Gli signaling (Irinotecan/oxaliplatin) in our 2D cell model. Moreover, for our 3D cell model, we suggest that combining GANT61 with oxaliplatin significantly inhibits cell cycle progression, stemness and Shh/Gli signaling. Further evidence concerning cell cycle, signaling pathways activation, expression of additional markers and assessment of protein levels is crucial for supporting these results.

These results are also for great interest for the different effects caused by treatments on 2D and 3D cell models, which elucidates to the importance of exploring different therapeutic strategies targeting primary tumors and circulating cell aggregates. Effective treatments on the aggregate cell model represent potential treatments targeting circulating cell aggregates, allowing a re-direction of future studies towards different cell models with different potential therapies.

The present study brings a new therapeutic perspective in using the synergic behaviour of different compound combinations on CRC tumors. Moreover, this study opens the door for further investigation regarding these and other agent combinations for finding promising therapeutic strategies capable of impairing the main pathways implicated in CRC tumorigenesis and, simultaneously, overcome the greatest barriers in conventional therapeutics such as resistance mechanisms and cytotoxicity.

6. REFERENCES

Abal, M., Bras-Goncalves, R., Judde, J. G., *et al.* 2004. Enhanced sensitivity to irinotecan by Cdk1 inhibition in the p53-deficient HT29 human colon cancer cell line. Oncogene 23(9), 1737–1744.

Aguilar-Gallardo, C., and Simón, C. 2013. Cells, Stem Cells, and Cancer Stem Cells. Seminars in Reproductive Medicine 31(01), 005-013.

Agyeman, A., Jha, B. K., Mazumdar, T., *et al.* 2015. Mode and specificity of binding of the small molecule GANT61 to GLI determines inhibition of GLI-DNA binding. Oncotarget 5(12).

Al-Sohaily, S., Biankin, A., Leong, R., *et al.* 2012. Molecular pathways in colorectal cancer. Journal of Gastroenterology and Hepatology 27(9), 1423–1431.

Albuquerque, C., Breukel, C., van der Luijt, R., *et al.* 2002. The 'just-right' signaling model: APC somatic mutations are selected based on a specific level of activation of the beta-catenin signaling cascade. Human molecular genetics 11(13), 1549–1560.

Albuquerque, C., and Pereira, L. 2018. Wnt Signalling-Targeted Therapy in the CMS2 Tumour Subtype: A New Paradigm in CRC Treatment? pp 75–100, Springer.

Androutsopoulos, V. P., Ruparelia, K., Arroo, R. R. J., *et al.* 2009. CYP1-mediated antiproliferative activity of dietary flavonoids in MDA-MB-468 breast cancer cells. Toxicology 264(3), 162–170.

Angus-Hill, M. L., Elbert, K. M., Hidalgo, J., *et al.* 2011. T-cell factor 4 functions as a tumor suppressor whose disruption modulates colon cell proliferation and tumorigenesis. Proceedings of the National Academy of Sciences of the United States of America 108(12), 4914–4919.

Armaghany, T., Wilson, J. D., Chu, Q., *et al.* 2012. Genetic alterations in colorectal cancer. Gastrointestinal cancer research : GCR 5(1), 19–27.

Arnould, S., Guichard, S., Hennebelle, I., *et al.* 2002. Contribution of apoptosis in the cytotoxicity of the oxaliplatin-irinotecan combination in the HT29 human colon adenocarcinoma cell line. Biochemical Pharmacology 64(8), 1215–1226.

Atcha, F. A., Syed, A., Wu, B., *et al.* 2007. A Unique DNA Binding Domain Converts T-Cell Factors into Strong Wnt Effectors. Molecular and Cellular Biology 27(23), 8352–8363.

Bae, J. M., Kim, J. H., and Kang, G. H. 2016. Molecular Subtypes of Colorectal Cancer and Their Clinicopathologic Features, With an Emphasis on the Serrated Neoplasia Pathway. Archives of Pathology & Laboratory Medicine 140(5), 406–412.

Baecker, V. 2012. ImageJ Macro Tool Sets for Biological Image Analysis.Page 919941 in ImageJ User and Developer Conference. Luxembourg: Centre de Recherche Public Henri Tudor.

Baker, A.-M., Graham, T. A., Elia, G., *et al.* 2015. Characterization of LGR5 stem cells in colorectal adenomas and carcinomas. Scientific Reports 5(1), 8654.

Binefa, G., Rodríguez-Moranta, F., Teule, À., *et al.* 2014. Colorectal cancer: From prevention to personalized medicine. World Journal of Gastroenterology 20(22), 6786–6808.

Boland, R. C., and Goel, A. 2010. Microsatellite Instability in Colorectal Cancer. Gastroenterology 138(6), 2073–2087.

Brabletz, T., Jung, A., Dag, S., *et al.* 1999. B-Catenin Regulates the Expression of the Matrix Metalloproteinase-7 in Human Colorectal Cancer. American Journal of Pathology 155(4), 1033–1038.

Brabletz, T., Jung, A., and Kirchner, T. 2002. β-Catenin and the morphogenesis of colorectal cancer. Virchows Archiv 441(1), 1–11.

Burrell, R. A., McGranahan, N., Bartek, J., *et al.* 2013. The causes and consequences of genetic heterogeneity in cancer evolution. Nature 501(7467), 338–345.

Busch, E. L., McGraw, K. A., and Sandler, R. S. 2014. The Potential for Markers of Epithelial-Mesenchymal Transition to Improve Colorectal Cancer Outcomes: A Systematic Review. Cancer Epidemiology Biomarkers & Prevention 23(7), 1164–1175.

Carballal, S., Leoz, M. L., Moreira, L., *et al.* 2014. Hereditary colorectal cancer syndromes. Colorectal Cancer 3(1), 57–76.

Carrato, A. 2008. Adjuvant treatment of colorectal cancer. Gastrointestinal cancer research 2(4 Suppl), S42-6.

Chaffer, C. L., Brennan, J. P., Slavin, J. L., *et al.* 2006. Mesenchymal-to-epithelial transition facilitates bladder cancer metastasis: Role of fibroblast growth factor receptor-2. Cancer Research 66(23), 11271–11278.

Chambers, A. F., Groom, A. C., and MacDonald, I. C. 2002. Dissemination and growth of cancer cells in metastatic sites. Nature Reviews Cancer 2(8), 563–572.

Chen, J., Jackson, P. K., Kirschner, M. W., *et al.* 1995. Separate domains of p21 involved in the inhibition of Cdk kinase and PCNA. Nature 374(6520), 386–388.
Chen, K. H., Weng, M. S., and Lin, J. K. 2007. Tangeretin suppresses IL-1β-induced cyclooxygenase (COX)-2 expression through inhibition of p38 MAPK, JNK, and AKT activation in human lung carcinoma cells. Biochemical Pharmacology 73(2), 215–227.
Chen, Y., Lu, X., Montoya-Durango, D. E., *et al.* 2017. ZEB1 regulates multiple oncogenic components involved in uveal melanoma progression. Scientific Reports 7(1), 1–14.
Choi, S. H., Hong, H. K., Cho, Y. B., *et al.* 2015. Identification of sestrin3 involved in the in vitro resistance of colorectal cancer cells to irinotecan. PLoS ONE 10(5), 1–14.
Chu, P., Clanton, D. J., Snipas, T. S., *et al.* 2009. Characterization of a subpopulation of colon cancer cells with stem cell-like properties. International Journal of Cancer 124(6), 1312–1321.
Clarke, J. D., Dashwood, R. H., and Ho, E. 2008. Multi-targeted prevention of cancer by sulforaphane. Cancer Letters 269(2), 291–304.
Cohen, M., Kicheva, A., Ribeiro, A., *et al.* 2015. Ptch1 and Gli regulate Shh signalling dynamics via multiple mechanisms. Nature Communications 6, 1–12.
Colussi, D., Brandi, G., Bazzoli, F., *et al.* 2013. Molecular pathways involved in colorectal cancer: implications for disease behavior and prevention. International journal of molecular sciences 14(8), 16365–16385.
Conteduca, V., Sansonno, D., Russi, S., *et al.* 2013. Precancerous colorectal lesions (Review). International Journal of Oncology 43(4), 973–984.
Cunningham, J. M., Christensen, E. R., Tester, D. J., *et al.* 1998. Hypermethylation of the hMLHl Promoter in Colon Cancer with Microsatellite Instability. Cancer Research 58, 3455–3460.
Cunningham, D., Maroun, J., Vanhoefer, U., *et al.* 2001. Optimizing the use of irinotecan in colorectal cancer. The oncologist 6 Suppl 4(suppl 4), 17–23.
Dalerba, P., Cho, R. W., and Clarke, M. F. 2007. Cancer Stem Cells: Models and Concepts. Annual Review of Medicine 58(1), 267–284.
Deming, D. A., Ninan, J., Bailey, H. H., *et al.* 2014. A Phase i study of intermittently dosed vorinostat in combination with bortezomib in patients with advanced solid tumors. Investigational New Drugs 32(2), 323–329.
Diaz-Moralli, S., Tarrado-Castellarnau, M., Miranda, A., *et al.* 2013. Targeting cell cycle regulation in cancer therapy. Pharmacology and Therapeutics 138(2), 255–271.
van Dop, W. A., Uhmann, A., Wijgerde, M., *et al.* 2009. Depletion of the Colonic Epithelial Precursor Cell Compartment Upon Conditional Activation of the Hedgehog Pathway. Gastroenterology 136(7), 2195–2203.e7.
Du, L., Wang, H., He, L., *et al.* 2008. CD44 is of Functional Importance for Colorectal Cancer Stem Cells. Clinical Cancer Research 14(21), 6751–6760.
Duarte, M. 2015. Envolvimento de variantes genéticas específicas na suscetibilidade para o risco de cancro do cólon e reto e na agressividade tumoral. Dissertação de Mestrado. Universidade Egas Moniz
Fearon, E. F., and Vogelstein, B. 1990. A genetic model for Colorectal Tumorigenesis. Cell 61, 759–767.
Ferlay, J., Soerjomataram, I., Dikshit, R., *et al.* 2015. Cancer incidence and mortality worldwide: Sources, methods and major patterns in GLOBOCAN 2012. International Journal of Cancer 136(5), E359–E386.
Fevr, T., Robine, S., Louvard, D., *et al.* 2007. Wnt / β -Catenin Is Essential for Intestinal Homeostasis and Maintenance of Intestinal Stem Cells Wnt. 27(21), 7551–7559.
Fimognari, C., and Hrelia, P. 2007. Sulforaphane as a promising molecule for fighting cancer. Mutation Research/Reviews in Mutation Research 635(2–3), 90–104.
Fu, J., Rodova, M., Roy, S. K., *et al.* 2013. GANT-61 inhibits pancreatic cancer stem cell growth in vitro and in NOD/SCID/IL2R gamma null mice xenograft. Cancer Letters 330(1), 22–32.
Gala, M., and Chung, D. C. 2011. Hereditary colon cancer syndromes. Seminars in Oncology 38(4), 490–499.
Gamet-Payrastre, L., Li, P., Lumeau, S., *et al.* 2000. Sulforaphane, a naturally occurring isothiocyanate, induces cell cycle arrest and apoptosis in HT29 human colon cancer cells. Cancer research 60(5), 1426–33.
Gang, A. O., Frøsig, T. M., Brimnes, M. K., *et al.* 2014. 5-Azacytidine treatment sensitizes tumor cells to T-cell mediated cytotoxicity and modulates NK cells in patients with myeloid malignancies. Blood Cancer Journal 4(3), e197–e197.

Gelsomino, F., Barbolini, M., Spallanzani, A., *et al.* 2016. The evolving role of microsatellite instability in colorectal cancer: A review. Cancer Treatment Reviews 51, 19–26.
Gherman, C., Pileczki, V., Petric, R. C., *et al.* 2012. Molecular mechanisms of action and prediction of response to oxaliplatin in colorectal cancer cells. Annals of the Romanian Society for Cell Biology 17(1), 194–200.
Grant, S. F. A., Thorleifsson, G., Reynisdottir, I., *et al.* 2006. Variant of transcription factor 7-like 2 (TCF7L2) gene confers risk of type 2 diabetes. Nature Genetics 38(3), 320–323.
Grove, E. A. 2011. Wnt signaling meets internal dissent. Genes & Development 25(17), 1759–1762.
Guinney, J., Dienstmann, R., Wang, X., *et al.* 2015. The consensus molecular subtypes of colorectal cancer. Nature Medicine 21(11).
Haggar, F. a, Boushey, R. P., and Ph, D. 2009. Colorectal Cancer Epidemiology : Incidence , Mortality , Survival , and Risk Factors. Clinics in colon and rectal surgery 6(212), 191–197.
Hagland, H. R., Berg, M., Jolma, I. W., *et al.* 2013. Molecular pathways and cellular metabolism in colorectal cancer. Digestive Surgery 30(1), 12–25.
Half, E., Bercovich, D., and Rozen, P. 2009. Familial adenomatous polyposis. Orphanet Journal of Rare Diseases 4(1), 1–23.
Harris, S. M., Mistry, P., Freathy, C., *et al.* 2005. Antitumour activity of XR5944 in vitro and in vivo in combination with 5-fluorouracil and irinotecan in colon cancer cell lines. British Journal of Cancer 92(4), 722–728.
Hartwell, L. H., and Kastan, M. B. 1994. Cell Cycle Control and Cancer. Science 266(December), 1821–1828.
He, G., Guan, X., Chen, X., *et al.* 2015. Expression and splice variant analysis of human TCF4 transcription factor in esophageal cancer. Journal of Cancer 6(4), 333–341.
Herbst, A., Jurinovic, V., Krebs, S., *et al.* 2014. Comprehensive analysis of beta-catenin target genes in colorectal carcinoma cell lines with deregulated Wnt/beta-catenin signaling. BMC genomics 15, 74.
Hinoue, T., Weisenberger, D. J., Lange, C. P. E., *et al.* 2012. Genome-scale analysis of aberrant DNA methylation in colorectal cancer. Cancer Research 22(2), 271–282.
Hrckulak, D., Kolar, M., Strnad, H., *et al.* 2016. TCF/LEF transcription factors: An update from the internet resources. Cancers 8(7).
Huber, M. A., Kraut, N., and Beug, H. 2005. Molecular requirements for epithelial-mesenchymal transition during tumor progression. Current Opinion in Cell Biology 17(5 SPEC. ISS.), 548–558.
Jasperson, K. W., Tuohy, T. M., Neklason, D. W., *et al.* 2010. Hereditary and Familial Colon Cancer. Gastroenterology 138(6), 2044–2058.
Javelaud, D., Pierrat, M.-J., and Mauviel, A. 2012. Crosstalk between TGF-β and hedgehog signaling in cancer. FEBS Letters 586(14), 2016–2025.
Jensen, N. F., Stenvang, J., Beck, M. K., *et al.* 2015. Establishment and characterization of models of chemotherapy resistance in colorectal cancer: Towards a predictive signature of chemoresistance. Molecular Oncology 9(6), 1169–1185.
Jho, E. -h., Zhang, T., Domon, C., *et al.* 2002. Wnt/ -Catenin/Tcf Signaling Induces the Transcription of Axin2, a Negative Regulator of the Signaling Pathway. Molecular and Cellular Biology 22(4), 1172–1183.
Johnson, C. M., Wei, C., Ensor, J. E., *et al.* 2013. Meta-Analyses of colorectal cancer risk factors. Cancer Causes and Control 24(6), 1207–1222.
Kalluri, R., and Weinberg, R. A. 2009. The basics of epithelial-mesenchymal transition. Journal of Clinical Investigation 119(6), 1420–1428.
Kang, Y., and Massagué, J. 2004. Epithelial-Mesenchymal Transitions. Cell 118(3), 277–279.
Keyvani-Ghamsari, S., Rabbani-Chadegani, A., Sargolzaei, J., *et al.* 2017. Effect of irinotecan on HMGB1, MMP9 expression, cell cycle, and cell growth in breast cancer (MCF-7) cells. Tumor Biology 39(4), 1–10.
El Khoury, F., Corcos, L., Durand, S., *et al.* 2016. Acquisition of anticancer drug resistance is partially associated with cancer stemness in human colon cancer cells. International Journal of Oncology 49(6), 2558–2568.
Kim, S.-J., Kim, H.-J., Kim, H.-R., *et al.* 2012. Antitumor actions of baicalein and wogonin in HT-29 human colorectal cancer cells. Molecular Medicine Reports 6(6), 1443–1449.
Kim, J. G., Bae, J. H., Kim, J. A., *et al.* 2014. Combination effect of epigenetic regulation and ionizing radiation in colorectal cancer cells. PLoS ONE 9(8), 1–10.
Kim, J. W., and Lemke, G. 2006. Hedgehog-regulated localization of Vax2 controls eye development.

Genes & Development 20(20), 2833–2847.
Kinnersley, B., Chubb, D., Dobbins, S. E., *et al.* 2016. Correspondence: SEMA4A variation and risk of colorectal cancer. Nature Communications 7, 3–5.
Kobayashi, S., Yamada-Okabe, H., Suzuki, M., *et al.* 2012. LGR5-Positive Colon Cancer Stem Cells Interconvert with Drug-Resistant LGR5-Negative cells and are Capable of Tumor Reconstitution. STEM CELLS 30(12), 2631–2644.
Kogerman, P., Kleman, M. I., Wessling, M., *et al.* 2004. Expression of the PTCH1 tumor suppressor gene is regulated by alternative promoters and a single functional Gli-binding site. Gene 330, 101–114.
Komiya, Y., and Habas, R. 2008. Wnt signal transduction pathways. Organogenesis 4(2), 68–75.
Kostova, E., Slaninka-Miceska, M., Labacevski, N., *et al.* 2014. Expression of matrix metalloproteinases 2, 7 and 9 in patients with colorectal cancer. Vojnosanitetski pregled 71(1), 52–59.
Krausova, M., and Korinek, V. 2014. Wnt signaling in adult intestinal stem cells and cancer. Cellular Signalling 26(3), 570–579.
Krishnamurthy, N., and Kurzrock, R. 2018. Targeting the Wnt/beta-catenin pathway in cancer: Update on effectors and inhibitors. Cancer Treatment Reviews 62(14), 50–60.
Kroepil, F., Fluegen, G., Totikov, Z., *et al.* 2012. Down-Regulation of CDH1 Is Associated with Expression of SNAI1 in Colorectal Adenomas. PLoS ONE 7(9), 1–9.
Kurebayashi, J., Koike, Y., Ohta, Y., *et al.* 2017. Anti-cancer stem cell activity of a hedgehog inhibitor GANT61 in estrogen receptor-positive breast cancer cells. Cancer Science 108(5), 918–930.
Larue, L., and Bellacosa, A. 2005. Epithelial-mesenchymal transition in development and cancer: Role of phosphatidylinositol 3′ kinase/AKT pathways. Oncogene 24(50), 7443–7454.
Lauth, M., Bergstrom, A., Shimokawa, T., *et al.* 2007. Inhibition of GLI-mediated transcription and tumor cell growth by small-molecule antagonists. Proceedings of the National Academy of Sciences 104(20), 8455–8460.
Lee, M. S., Menter, D. G., and Kopetz, S. 2017a. Right versus left colon cancer biology: Integrating the consensus molecular subtypes. Journal of the National Comprehensive Cancer Network 15(3), 411–419.
Lee, D.-H., Lee, S., and Oh, S. C. 2017b. Hedgehog signaling pathway as a potential target in the treatment of advanced gastric cancer. Tumor Biology 39(6), 1 –10.
Leung, J. Y., Kolligs, F. T., Wu, R., *et al.* 2002. Activation of AXIN2 expression by β-catenin-T cell factor: A feedback repressor pathway regulating Wnt signaling. Journal of Biological Chemistry 277(24), 21657–21665.
Lin, N., Sato, T., Takayama, Y., *et al.* 2003. Novel anti-inflammatory actions of nobiletin, a citrus polymethoxy flavonoid, on human synovial fibroblasts and mouse macrophages. Biochemical Pharmacology 65(12), 2065–2071.
Lindor, N. M., Rabe, K., Petersen, G. M., *et al.* 2005. Lower Cancer Incidence in Amsterdam-I Criteria Families Without Mismatch Repair Deficiency: Familial Colorectal Cancer Type X. JAMA 293(16), 1979–1985.
Lindor, N. M. 2009. Hereditary colorectal cancer: MYH-associated polyposis and other newly identified disorders. Best practice & research. Clinical gastroenterology 23, 75–87.
Linnekamp, J. F., Van Hooff, S. R., Prasetyanti, P. R., *et al.* 2018. Consensus molecular subtypes of colorectal cancer are recapitulated in in vitro and in vivo models. Cell Death and Differentiation 25, 616–633.
Liu, X., Wang, Q., Yang, G., *et al.* 2011. A novel kinase inhibitor, INCB28060, blocks c-MET-dependent signaling, neoplastic activities, and cross-talk with EGFR and HER-3. Clinical Cancer Research 17(22), 7127–7138.
Liu, D., Sun, J., Zhu, J., *et al.* 2014. Expression and clinical significance of colorectal cancer stem cell marker EpCAMhigh/CD44+ in colorectal cancer. Oncology Letters 7(5), 1544–1548.
Liu, C.-Y., Lin, H.-H., Tang, M.-J., *et al.* 2015. Vimentin contributes to epithelial-mesenchymal transition cancer cell mechanics by mediating cytoskeletal organization and focal adhesion maturation. Oncotarget 6(18).
Llor, X., Pons, E., Xicola, R. M., *et al.* 2005. Differential features of colorectal cancers fulfilling Amsterdam criteria without involvement of the mutator pathway. Clinical Cancer Research 11(20), 7304–7310.
Longley, D. B., Harkin, D. P., and Johnston, P. G. 2003. 5-Fluorouracil: Mechanisms of action and clinical strategies. Nature Reviews Cancer 3(5), 330–338.
Ma, Z. 2005. Baicalein, a component of Scutellaria radix from Huang-Lian-Jie-Du-Tang (HLJDT), leads

to suppression of proliferation and induction of apoptosis in human myeloma cells. Blood 105(8), 3312–3318.
Ma, J., Cheng, J., Gong, Y., *et al.* 2015. Downregulation of Wnt signaling by sonic hedgehog activation promotes repopulation of human tumor cell lines. Disease Models & Mechanisms 8(4), 385–391.
Ma, I., and Allan, A. L. 2011. The Role of Human Aldehyde Dehydrogenase in Normal and Cancer Stem Cells. Stem Cell Reviews and Reports 7(2), 292–306.
MacDonald, B. T., Tamai, K., and He, X. 2009. Wnt/β-Catenin Signaling: Components, Mechanisms, and Diseases. Developmental Cell 17(1), 9–26.
Manthey, J. A., and Guthrie, N. 2002. Antiproliferative activities of citrus flavonoids against six human cancer cell lines. Journal of Agricultural and Food Chemistry 50(21), 5837–5843.
Marques, R. P., Duarte, G. S., Sterrantino, C., *et al.* 2017. Triplet (FOLFOXIRI) versus doublet (FOLFOX or FOLFIRI) backbone chemotherapy as first-line treatment of metastatic colorectal cancer: A systematic review and meta-analysis. Critical Reviews in Oncology/Hematology 118(October 2016), 54–62.
Martinez-Balibrea, E., Martinez-Cardus, A., Gines, A., *et al.* 2015. Tumor-Related Molecular Mechanisms of Oxaliplatin Resistance. Molecular Cancer Therapeutics 14(8), 1767–1776.
Martínez-Maqueda, D., Miralles, B., and Recio, I. 2015. HT29 Cell Line.Pages 113–124 in The Impact of Food Bioactives on Health: in vitro and ex vivo models. Verhoeckx, K., Cotter, P., López-Expósito, I., Kleiveland, C., Lea, T., Mackie, A., Requena, T., Swiatecka, D., Wichers, H., eds. Springer International Publishing, Cham.
Mauviel, A., Dennler, S., Alexaki, V. I., *et al.* 2011. TGF- /SMAD/GLI2 Signaling Axis in Cancer Progression and Metastasis. Cancer Research 71(17), 5606–5610.
Mayans, S., Lackovic, K., Lindgren, P., *et al.* 2007. TCF7L2 polymorphisms are associated with type 2 diabetes in northern Sweden. European Journal of Human Genetics 15(3), 342–346.
Mazumdar, T., Devecchio, J., Agyeman, A., *et al.* 2011a. The GLI genes as the molecular switch in disrupting Hedgehog signaling in colon cancer AbstrAct : Oncotarget 2(8), 638–645.
Mazumdar, T., DeVecchio, J., Shi, T., *et al.* 2011b. Hedgehog Signaling Drives Cellular Survival in Human Colon Carcinoma Cells. Cancer Research 71(3), 1092–1102.
Mazumdar, T., DeVecchio, J., Agyeman, A., *et al.* 2011c. Blocking Hedgehog Survival Signaling at the Level of the GLI Genes Induces DNA Damage and Extensive Cell Death in Human Colon Carcinoma Cells. Cancer Research 71(17), 5904–5914.
Merlos-Suárez, A., Barriga, F. M., Jung, P., *et al.* 2011. The Intestinal Stem Cell Signature Identifies Colorectal Cancer Stem Cells and Predicts Disease Relapse. Cell Stem Cell 8(5), 511–524.
Miyazaki, Y., Matsubara, S., Ding, Q., *et al.* 2016. Efficient elimination of pancreatic cancer stem cells by hedgehog/GLI inhibitor GANT61 in combination with mTOR inhibition. Molecular Cancer 15(1), 49.
Morley, K. L., Ferguson, P. J., and Koropatnick, J. 2007. Tangeretin and nobiletin induce G1 cell cycle arrest but not apoptosis in human breast and colon cancer cells. Cancer Letters 251(1), 168–178.
Mothersill, C., and Seymour, C. B. 2004. Radiation-induced bystander effects — implications for cancer. Nature reviews. Cancer 4(2), 153–158.
Mundade, R., Imperiale, T. F., Prabhu, L., *et al.* 2014. Genetic pathways, prevention, and treatment of sporadic colorectal cancer. Oncoscience 1(6), 400.
Nieminen, T. T., Abdelrahman, W. M., Ristimki, A., *et al.* 2011. BMPR1A mutations in hereditary nonpolyposis colorectal cancer without mismatch repair deficiency. Gastroenterology 141(1), 23–26.
Nieminen, T. T., O'Donohue, M. F., Wu, Y., *et al.* 2014. Germline mutation of RPS20, encoding a ribosomal protein, causes predisposition to hereditary nonpolyposis colorectal carcinoma without DNA mismatch repair deficiency. Gastroenterology 147(3), 595–598.e5.
O'Brien, C. A., Pollett, A., Gallinger, S., *et al.* 2007. A human colon cancer cell capable of initiating tumour growth in immunodeficient mice. Nature 445(7123), 106–110.
Ogryzko, V. V, Wong, P., and Howard, B. H. 1997. WAF1 Retards S-Phase Progression Primarily by Inhibition of Cyclin-Dependent Kinases. 17(8), 4877–4882.
Olsen, A. K., Coskun, M., Bzorek, M., *et al.* 2013. Regulation of APC and AXIN2 expression by intestinal tumor suppressor CDX2 in colon cancer cells. Carcinogenesis 34(6), 1361–1369.
Otte, J.-M., Schmitz, F., Kiehne, K., *et al.* 2000. Functional Expression of HGF and Its Receptor in Human Colorectal Cancer. Digestion 61(4), 237–246.
Pan, M.-H., Chen, W.-J., Lin-Shiau, S.-Y., *et al.* 2002. Tangeretin induces cell-cycle G1 arrest through inhibiting cyclin-dependent kinases 2 and 4 activities as well as elevating Cdk inhibitors p21 and

p27 in human colorectal carcinoma cells. Carcinogenesis 23(10), 1677–1684.
Pancione, M., Remo, A., and Colantuoni, V. 2012. Genetic and epigenetic events generate multiple pathways in colorectal cancer progression. Pathology Research International 2012, 1–11.
Pantel, K., and Brakenhoff, R. H. 2004. Dissecting the metastatic cascade. Nature Reviews Cancer 4(6), 448–456.
Papadopoulos, V., Tsapakidis, K., Riobo Del Galdo, N. A., *et al.* 2016. The prognostic significance of the Hedgehog signaling pathway in colorectal cancer. Clinical Colorectal Cancer 15(2), 116–127.
Parajuli, P., Joshee, N., Rimando, A., *et al.* 2009. In vitro Antitumor Mechanisms of Various Scutellaria Extracts and Constituent Flavonoids. Planta Medica 75(01), 41–48.
Parnaud, G., Li, P., Cassar, G., *et al.* 2004. Mechanism of Sulforaphane-Induced Cell Cycle Arrest and Apoptosis in Human Colon Cancer Cells. Nutrition and Cancer 48(2), 198–206.
Peinado, H., Olmeda, D., and Cano, A. 2007. Snail, ZEB and bHLH factors in tumour progression: An alliance against the epithelial phenotype? Nature Reviews Cancer 7(6), 415–428.
Pereira, L. P., Silva, P., Duarte, M., *et al.* 2017. Targeting colorectal cancer proliferation, stemness and metastatic potential using Brassicaceae extracts enriched in isothiocyanates: A 3D cell model-based study. Nutrients 9(4), 1–26.
Pino, M. S., and Chung, D. C. 2010. The chromosomal instability pathway in colon cancer. Gastroenterology 138(6), 2059–2072.
Regan, J. L., Schumacher, D., Staudte, S., *et al.* 2017. Non-Canonical Hedgehog Signaling Is a Positive Regulator of the WNT Pathway and Is Required for the Survival of Colon Cancer Stem Cells. Cell Reports 21(10), 2813–2828.
Reya, T., Morrison, S. J., Clarke, M. F., *et al.* 2001. Stem cells, cancer and cancer stem cells. Nature 414(6859), 105–111.
Richon, V. M. 2006. Cancer biology: Mechanism of antitumour action of vorinostat (suberoylanilide hydroxamic acid), a novel histone deacetylase inhibitor. British Journal of Cancer 95(SUPPL. 1), 2–6.
Ruiz i Altaba, A., Sánchez, P., and Dahmane, N. 2002. Gli and hedgehog in cancer: tumours, embryos and stem cells. Nature Reviews Cancer 2(5), 361–372.
Ruiz i Altaba, A. 2007. The Gli code: an information nexus regulating cell fate, stemness and cancer. Trends Cell Biol. 17(9), 438–447.
Rustgi, A. K. 2007. The genetics of hereditary colon cancer. Genes & Development 21, 2525–2538.
Safaie Qamsari, E., Safaei Ghaderi, S., Zarei, B., *et al.* 2017. The c-Met receptor: Implication for targeted therapies in colorectal cancer. Tumor Biology 39(5), 101042831769911.
Said, A. H., Raufman, J. P., and Xie, G. 2014. The role of matrix metalloproteinases in colorectal cancer. Cancers 6(1), 366–375.
Saigusa, S., Inoue, Y., Tanaka, K., *et al.* 2012a. Clinical significance of LGR5 and CD44 expression in locally advanced rectal cancer after preoperative chemoradiotherapy. International Journal of Oncology 41(5), 1643–1652.
Saigusa, S., Toiyama, Y., Tanaka, K., *et al.* 2012b. Inhibition of HGF/cMET expression prevents distant recurrence of rectal cancer after preoperative chemoradiotherapy. International Journal of Oncology 40(2), 583–591.
Sarkar, S., Horn, G., Moulton, K., *et al.* 2013. Cancer development, progression, and therapy: An epigenetic overview. International Journal of Molecular Sciences 14(10), 21087–21113.
Sartore-Bianchi, A., Loupakis, F., Argilés, G., *et al.* 2016. Challenging chemoresistant metastatic colorectal cancer: therapeutic strategies from the clinic and from the laboratory. Annals of Oncology 27(8), 1456–1466.
Satelli, A., and Li, S. 2011. Vimentin as a potential molecular target in cancer therapy Or Vimentin, an overview and its potential as a molecular target for cancer therapy. Cell Mol Life Sci. 68(18), 3033–3046.
Schulz, E., Klampfl, P., Holzapfel, S., *et al.* 2014. Germline variants in the SEMA4A gene predispose to familial colorectal cancer type X. Nature Communications 5(May 2014).
Shen, G., Xu, C., Chen, C., *et al.* 2006. p53-independent G1 cell cycle arrest of human colon carcinoma cells HT-29 by sulforaphane is associated with induction of p21CIP1 and inhibition of expression of cyclin D1. Cancer chemotherapy and pharmacology 57(3), 317–327.
Shi, T., Mazumdar, T., DeVecchio, J., *et al.* 2010. cDNA Microarray Gene Expression Profiling of Hedgehog Signaling Pathway Inhibition in Human Colon Cancer Cells (T Lee, Ed.). PLoS ONE 5(10), e13054.
Shiina, H., Igawa, M., Breault, J., *et al.* 2003. The human T-cell factor-4 gene splicing isoforms, Wnt

signal pathway, and apoptosis in renal cell carcinoma. Clinical cancer research : an official journal of the American Association for Cancer Research 9(6), 2121–32.
Shiovitz, S., Copeland, W. K., Passarelli, M. N., *et al.* 2014. Characterisation of Familial Colorectal Cancer Type X, Lynch syndrome, and non-familial colorectal cancer. British Journal of Cancer 111(3), 598–602.
Silva, P., Albuquerque, C., Lage, P., *et al.* 2016. Serrated polyposis associated with a family history of colorectal cancer and/or polyps: The preferential location of polyps in the colon and rectum defines two molecular entities. International Journal of Molecular Medicine 38(3), 687–702.
Song, L., Li, Z. Y., Liu, W. P., *et al.* 2015. Crosstalk between Wnt/β-catenin and Hedgehog/Gli signaling pathways in colon cancer and implications for therapy. Cancer biology & therapy 16(1), 1–7.
Srivastava, R. K., Kaylani, S. Z., Edrees, N., *et al.* 2014. GLI inhibitor GANT-61 diminishes embryonal and alveolar rhabdomyosarcoma growth by inhibiting Shh/AKT-mTOR axis. Oncotarget 5(23), 2.
Stoffel, E. M., and Kastrinos, F. 2014. Familial Colorectal Cancer, Beyond Lynch Syndrome. Clinical Gastroenterology and Hepatology 12(7), 1059–1068.
Subramaniam, V., Vincent, I. R., Gardner, H., *et al.* 2007. CD44 regulates cell migration in human colon cancer cells via Lyn kinase and AKT phosphorylation. Experimental and Molecular Pathology 83(2), 207–215.
Sui, H., Fan, Z.-Z., and Li, Q. 2012. Signal Transduction Pathways and Transcriptional Mechanisms of ABCB1 /Pgp-mediated Multiple Drug Resistance in Human Cancer Cells. Journal of International Medical Research 40(2), 426–435.
Tafakh, M. S., Saidijam, M., Ranjbarnejad, T., *et al.* 2018. Sulforaphane, a Chemopreventive Compound, Inhibits Cyclooxygenase-2 and Microsomal Prostaglandin E Synthase-1 Expression in Human HT-29 Colon Cancer Cells. Cells Tissues Organs, 1–8.
Tang, W., Dodge, M., Gundapaneni, D., *et al.* 2008. A genome-wide RNAi screen for Wnt/beta-catenin pathway components identifies unexpected roles for TCF transcription factors in cancer. Proceedings of the National Academy of Sciences of the United States of America 105(28), 9697–702.
Tang, K. H., Ma, S., Lee, T. K., *et al.* 2012. CD133 + liver tumor-initiating cells promote tumor angiogenesis, growth, and self-renewal through neurotensin/interleukin-8/CXCL1 signaling. Hepatology 55(3), 807–820.
Thiery, J. P. 2002. Epithelial–mesenchymal transitions in tumour progression. Nature Reviews Cancer 2(6), 442–454.
Ting, Y., Chiou, Y. S., Pan, M. H., *et al.* 2015. In vitro and in vivo anti-cancer activity of tangeretin against colorectal cancer was enhanced by emulsion-based delivery system. Journal of Functional Foods 15, 264–273.
Tom, B. H., Rutzky, L. P., Jakstys, M. M., *et al.* 1976. Human Colonic Adenocarcinoma Cells. I. Establishment and Description of a New Line. in vitro 12(3), 180–191.
Tomimaru, Y., Koga, H., Yano, H., *et al.* 2013. Upregulation of T-cell factor-4 isoform-responsive target genes in hepatocellular carcinoma. Liver International 33(7), 1100–1112.
Tsedensodnom, O., Koga, H., Rosenberg, S. A., *et al.* 2011. Identification of T-cell factor-4 isoforms that contribute to the malignant phenotype of hepatocellular carcinoma cells. Experimental Cell Research 317(7), 920–931.
Uchida, H., Yamazaki, K., Fukuma, M., *et al.* 2010. Overexpression of leucine-rich repeat-containing G protein-coupled receptor 5 in colorectal cancer. Cancer Science 101(7), 1731–1737.
Umar, A., Risinger, J. I., Hawk, E. T., *et al.* 2004. Testing guidelines for hereditary non-polyposis colorectal cancer. Nat.Rev.Cancer 4(February), 153–158.
Vacik, T., Stubbs, J. L., and Lemke, G. 2011. A novel mechanism for the transcriptional regulation of Wnt signaling in development. Genes & Development 25(17), 1783–1795.
Varnat, F., Siegl-Cachedenier, I., Malerba, M., *et al.* 2010. Loss of WNT-TCF addiction and enhancement of HH-GLI1 signalling define the metastatic transition of human colon carcinomas. EMBO Molecular Medicine 2(11), 440–457.
Vega, S., Morales, A. V., Ocaña, O. H., *et al.* 2004. Snail blocks the cell cycle and confers resistance to cell death. Genes and Development 18(10), 1131–1143.
Vilar, E., and Gruber, S. B. 2010. Microsatellite instability in colorectal cancerthe stable evidence. Nature Reviews Clinical Oncology 7(3), 153–162.
Waga, S., Hannon, G. J., Beach, D., *et al.* 1994. The p21 inhibitor of cyclin-dependent kinases controls DNA replication by interaction with PCNA. Nature 369(6481), 574–578.
Wahab, S. M. R., Islam, F., Gopalan, V., *et al.* 2017. The Identifications and Clinical Implications of

Cancer Stem Cells in Colorectal Cancer. Clinical Colorectal Cancer 16(2), 93–102.
Wang, Y., Shi, J., Chai, K., *et al.* 2013. The Role of Snail in EMT and Tumorigenesis. Current Cancer Drug Targets 13(9), 963–972.
Weise, A., Bruser, K., Elfert, S., *et al.* 2009. Alternative splicing of Tcf7l2 transcripts generates protein variants with differential promoter-binding and transcriptional activation properties at Wnt/β-catenin targets. Nucleic Acids Research 38, 1–18.
Weiswald, L. B., Bellet, D., and Dangles-Marie, V. 2015. Spherical Cancer Models in Tumor Biology. Neoplasia (United States) 17(1), 1–15.
Wells, K., and Wise, P. E. 2017. Hereditary Colorectal Cancer Syndromes. Surgical Clinics of North America 97(3), 605–625.
Van de Wetering, M., Sancho, E., Verweij, C., *et al.* 2002. The β-catenin/TCF-4 complex imposes a crypt progenitor phenotype on colorectal cancer cells. Cell 111(2), 241–250.
Wilson, P. M., Labonte, M. J., Martin, S. C., *et al.* 2013. Sustained inhibition of deacetylases is required for the antitumor activity of the histone deactylase inhibitors panobinostat and vorinostat in models of colorectal cancer. Investigational New Drugs 31(4), 845–857.
Xiang, C., Chen, J., and Fu, P. 2017. HGF/Met signaling in cancer invasion: The impact on cytoskeleton remodeling. Cancers 9(5), 1–12.
Xuereb, J., and Blundell, R. 2008. The Role of Cell Cycle Regulation in Cancer. Research Journal of Biological Sciences 3(2), 251–257.
Yam, C. H., Fung, T. K., and Poon, R. Y. C. 2002. Cyclin A in cell cycle control and cancer. Cellular and Molecular Life Sciences 59(8), 1317–1326.
Yamagishi, H., Kuroda, H., Imai, Y., *et al.* 2016. Molecular pathogenesis of sporadic colorectal cancers. Chinese Journal of Cancer 35(1), 1–8.
Yang, X., Han, H., DeCarvalho, D. D., *et al.* 2014. Gene body methylation can alter gene expression and is a therapeutic target in cancer. Cancer Cell 26(4), 577–590.
Yin, S., Li, J., Hu, C., *et al.* 2007. CD133 positive hepatocellular carcinoma cells possess high capacity for tumorigenicity. International Journal of Cancer 120(7), 1444–1450.
Yokoyama, K., Kamata, N., Fujimoto, R., *et al.* 2003. Increased invasion and matrix metalloproteinase-2 expression by Snail-induced mesenchymal transition in squamous cell carcinomas. International Journal of Oncology, 891–898.
Zambirinis, C. P., Theodoropoulos, G., and Gazouli, M. 2009. Undefined familial colorectal cancer. World journal of gastrointestinal oncology 1(1), 12–20.
Zeng, Z., Weiser, M. R., D'Alessio, M., *et al.* 2004. Immunoblot analysis of c-Met expression in human colorectal cancer: overexpression is associated with advanced stage cancer. Clinical & experimental metastasis 21(5), 409–17.
Zhang, J., Tian, X.-J., and Xing, J. 2016. Signal Transduction Pathways of EMT Induced by TGF-β, SHH, and WNT and Their Crosstalks. Journal of Clinical Medicine 5(4), 41.

7. APPENDICES

Appendix A – TNM classification of CRC

Table A.1 – TNM classification of CRC (Adapted from: Binefa *et al.*, 2014).

T = Primary tumor
- TX = Primary tumor cannot be assessed
- T0 = No evidence of primary tumor
- Tis = Carcinoma in situ: intraepithelial or invasion of lamina propria
- T1 = Tumor invades submucosa
- T2 = Tumor invades muscularis propria
- T3 = Tumor invades through the muscularis propia into subserosa or into nonperitonealized pericolic or perirectal tissues
- T4a = Tumor penetrates to the surface of the visceral peritoneum
- T4b = Tumor directly invades or is adherent to other organs or structures

N = Regional lymph nodes
- NX = Regional lymph nodes cannot be assessed
- N0 = No regional lymph node metastasis
- N1a = Metastasis in one regional lymph node
- N1b = Metastasis in two to three regional lymph nodes
- N1c = Tumor deposit(s) in the subserosa, mesentery, or nonperitonealized pericolic or perirectal tissues without regional nodal metastasis
- N2a = Metastasis in four to six regional lymph nodes
- N2b = Metastasis in seven or more regional lymph nodes

M = Distant metastasis
- MX = Distant metastasis cannot be assessed
- M0 = No distant metastasis
- M1a = Distant metastasis to one organ or site
- M1b = Distant metastasis to more than one organ/site or the peritoneum

Staging
- Stage Ⅰ (T1-T2, N0, M0)
- Stage ⅡA (T3, N0, M0)
- Stage ⅡB (T4a, N0, M0)
- Stage ⅡC (T4b, N0, M0)
- Stage ⅢA (T1-T2, N1, M0 and T1, N2a, M0)
- Stage ⅢB (T1-T2, N2b, M0; T2-T3, N2a, M0 and T3-T4a, N1, M0)
- Stage ⅢC (T3-T4a, N2b, M0 and T4b, N1-N2, M0 and T4a, N2a, M0)
- Stage ⅣA (any T, any N and M1a)
- Stage ⅣB (any T, any N and M1b)

Appendix B – Described relevant mutations and characterization regarding CRC carcinogenesis pathways of CRC cell lines.

Table B.1 – Molecular characteristics of cell lines used in this work.

	Chromosomic instability (CIN)	Microsatellite stability status (MS)	CpG islands methylator phenotype (CIMP)
HT-29	+	MSS	+
LS174T	-	MSI	-
Sw48	-	MSI	+
Sw480	+	MSS	-
Sw620	+	MSS	-
Lovo	-	MSI	-
HCT116	-	MSI	+

Data from: Ahmed *et al,* 2013

Table B.2 – HT-29 and LS174T mutation list

Gene \ Cell line	HT-29	LS174T
APC	c.2557T>G c.789T>C	-
AXIN2	-	c.2500A>G c.1994delG
BRAF	c.356C>G c.1799T>A	c.632C>T
CD44	-	c.1600T>C
CTNNB1	-	c.134T>C
KRAS	c.182A>T	c.35T>C
MMP9	c.2053C>T	-
MYH1	-	c.2942delA
MYH2	-	c.2327T>G
MYH6	c.3068C>T	-
MYH7	-	c.3634C>T
MYH9	-	c.2968T>G
MYH11	-	c.5798delC c.773G>A
MYH13	-	c.1525G>A
PIK3CA	c.1345A>C	c.3140G>A
PTCH1		c.801G>A
TCF7L2	-	c.1377delA
TGFB1	c.713-9delC	-
TP53	c.818T>C c.422T>C c.701T>C	-

Data from: http://colonatlas.org/ (visited on April 25, 2018)

Appendix C - Preparation of the reagents used in agarose gel electrophoresis

I. Preparation of the electrophoresis buffer (TBE 1x):

To obtain 1x TBE, a 10x TBE solution (0.89M Tris Borate pH8.3 + 20mM Na_2 EDTA, *National Diagnostics*) was diluted to a final volume of 2L in ddH_2O.

II. Preparation of 2% (w/v) agarose gel:

I. Weigh 5g of agarose (Seaken® LE Agarose, Lonza) in a 500ml Erlenmeyer;
II. Add 250ml of TBE 1x buffer;
III. Dissolve the solution in the microwave;
IV. Add 12.5µL of ethidium bromide (10 mg/ml, MP biomedicals) and stir for homogenization;
V. Place the solution in a polymerization base with 4 well molds and allow to cool until the gel solidifies

III. Preparation of 0.8 and 1.2% (w/v) agarose gel:

I. Weigh 1.2g for 0.8% or 1.8g for 1.2% of agarose (Seaken® LE Agarose, Lonza) in a 500ml Erlenmeyer;
II. Add 150ml of TBE 1x buffer;
III. Dissolve the solution in the microwave;
IV. Add 7.5µL of ethidium bromide (10mg/ml, MP biomedicals) and stir for homogenization;
V. Place the solution in a polymerization base with 1 well mold and allow to cool until the gel solidifies.

IV. Preparation of Orange G 5x and 1x:

Orange G 5x: Prepared from 12ml Ficoll (Sigma), 125g of Orange G (Sigma) and 50ml of ddH2O, under stirring. Store at -20 °C.

Orange G 1x: Diluted from Orange G 5x to a final volume of 1ml in ddH2O. Store at 4ºC.

V. Preparation of the molecular weight marker GeneRuler 50bp DNA Ladder (Thermofisher Scientific):

Add 50µL of GeneRuler 50bp DNA Ladder (Thermofisher Scientific), 250µL of Orange G 5x and 700µL of ddH2O.

VI. Preparation of the molecular weight marker Lambda/HindIII DNA Ladder (Fermentas):

Add 20µL of Lambda/HindIII DNA Ladder (Fermentas), 100µL of Orange G 5x and 280µL of ddH2O.

Appendix D – PCR and qPCR conditions used in this study

Table D.1 – PCR conditions used for the amplification of TCF7L2 isoforms by PCR.

***TCF7L2* isoform**	**Commercial kit**	**$MgCl^{2+}$ (µL)**	**Temperature (°C)**
1-5	Biotaq™ (Bioline)	1	61
12-17			

Table D.2 – PCR conditions used for the amplification of molecular markers for cancer stemness, EMT, apoptosis, cell cycle status and key signaling pathways, by RT-qPCR.

Molecular marker	**Commercial kit**	**Primer concentration (pmol/µL)**	**cDNA concentration (ng/µL)**	**Temperature (°C)**
GAPDH	1	5	5	60
β-ACTIN	1	3,5		
TCF7L2	1	5		
TCF7L2 (ISO 1-6)	1	5		
CDKN1A	1	5		
CCNA2	2	5		
β-CATENIN	1	5		
ABCB1	1	5		
MMP7	1	7,5		
MMP9	2	5		
AXIN2	1	3,5		
GLI1	2	3		
LGR5	1	7.5		
VIMENTIN	1	5		
CDH1	1	5		
CD44	2	5		
CD133	2	3		
SNAIL	1	5		
ZEB1	1	5		

1.Power SYBR® Green PCR, Master Mix kit (Applied Biosystems)
2. KAPA SYBR® FAST qPCR Kit Master Mix Universal (KapaBiosystems)

Appendix E - PCR amplification programs used in this study

Table E.1 – PCR amplification program used with the reagents from the Biotaq^{TM} kit (Bioline). PCR amplification was performed in a UNO96 thermocycler (VWR).

Step	Temperature (°C)	Time	Cycles
Initial denaturation	95	5 min	1
Denaturation	94	50 sec	40
Annealing	Variable	30 sec	
Elongation	72	50 sec	
Final elongation	72	7 min	1
Pause	15	∞	∞

Table E.2 – Program used for sequencing reaction of the studied genes.

Step	Temperature (°C)	Time	Cycles
Initial denaturation	96	5 min	1
Denaturation	95	10 sec	25
Annealing	59	5 sec	
Elongation	60	4 min	
Pause	4	∞	∞

Table E.3 – Reverse transcription program used for cDNA synthesis.

Step	Temperature (°C)	Time	Cycles
Denaturation and binding of hexamers	70	10 min	1
Pause	10	∞	
cDNA synthesis	42	60 min	
Elongation	70	15 min	
Pause	4	∞	∞

Table E.4 – qPCR program used for expression analysis of molecular markers.

Step	Temperature (°C)	Time	Cycles
Incubation	50	2 min	1
Polymerase activation	95	10 min	
Denaturation	95	15 sec	40
Hybridization and elongation	60	1 min	

Appendix F - Precipitation and purification protocol of DNA Ethanol / EDTA / Sodium acetate - BigDye® Terminator v1.1 Cycle Sequencing Kit (Applied Biosystems) – after sequencing reaction

1. Protocol:

I. In a 2ml eppendorf-like tube add 2µL of EDTA (125mM), 2µL sodium acetate (3M) and 50µL absolute ethanol, for each reaction;
II. Vortex and spin-down;
III. Transfer 54µL of the supernatant to new 1.5ml eppendorf-like tube, add the total volume of the sequencing reaction and homogenize;
IV. Incubate for 15 minutes at room temperature;
V. Centrifuge at 14000rpm for 30minutes at 4°C;
VI. Remove the supernatant completely with a micropipette;
VII. Add 100µL of 70% (v/v) ethanol and slightly vortex;
VIII. Centrifuge at 14000rpm for 15minutes at 4°C;
IX. Remove the supernatant completely with a micropipette;
X. Dry the pellet in a dry bath at 37°C for about 10 minutes;
XI. Store the pellet at 4ºC.

2. Solutions:

EDTA (125 mM, pH 8):

Dissolve 4.65g of EDTA in ddH2O and make up the volume to 100 mL, after pH adjustment with NaOH.

Sodium acetate (3M, pH 4.5):

Dissolve 24.8g of sodium acetate in ddH2O. Adjust the pH with acetic acid and make up the volume to 100 mL.

Ethanol 70%:

Add 30mL of ddH2O to 70mL of absolute ethanol and homogenize.

Appendix G – Cytotoxicity in CCD841CoN colon cell line

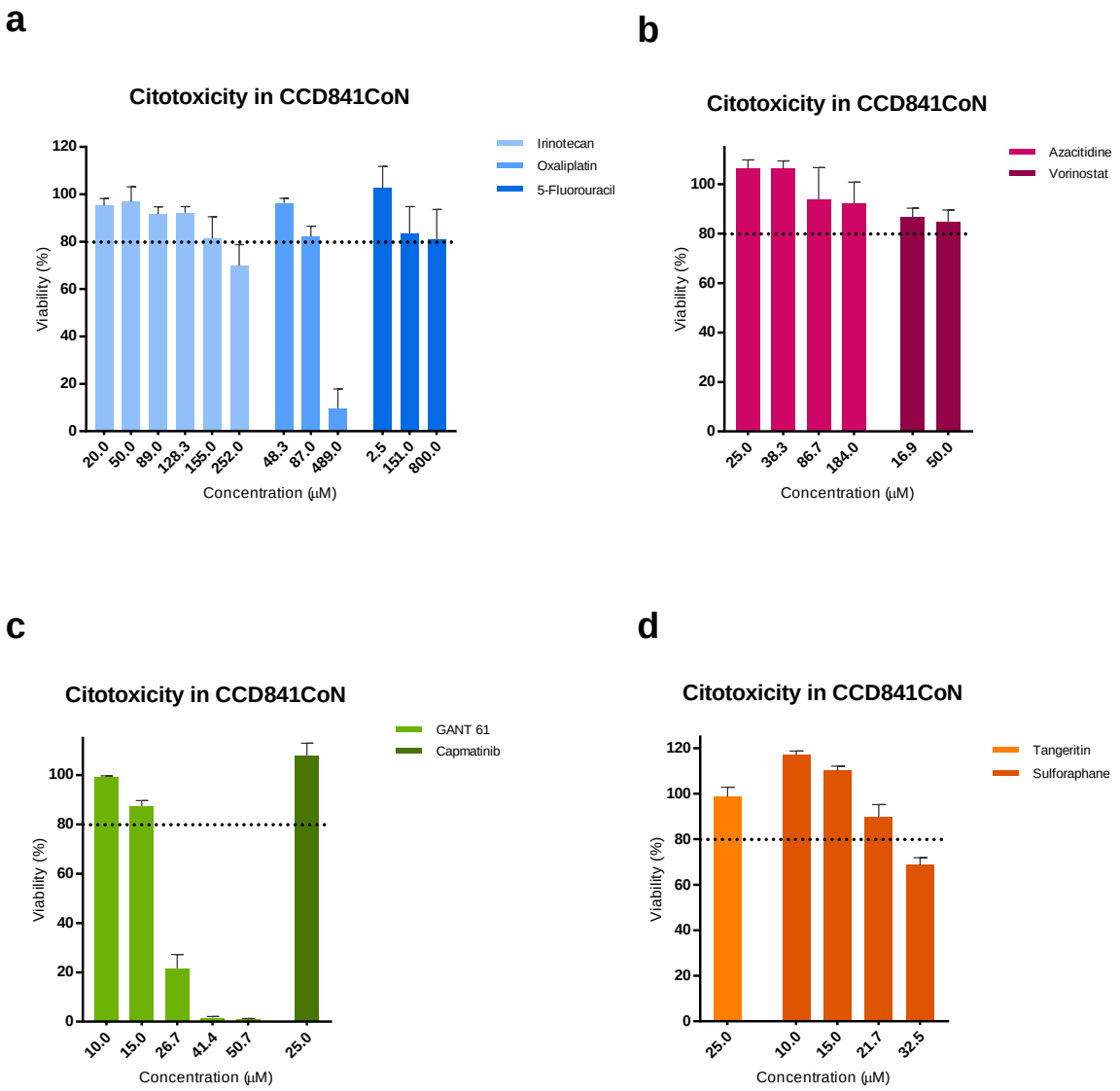

Figure G.1 – Effect of irinotecan, oxaliplatin, 5-Fluorouracil (a); azacitidine, vorinostat (b); GANT61, capmatinib (c); Tangeritin and sulforaphane (d) on the viability of CCD841CoN normal colon cell line. Assay previously performed in the lab. Dose-response profiles were obtained after a 24h period of incubation. Results were obtain using the mean of 2 independent experiments performed in triplicate ± SD.